



U.S. Department  
of Transportation  
**National Highway  
Traffic Safety  
Administration**



---

DOT HS 812 814

October 2019

# Development of Oblique Restraint Countermeasures

## DISCLAIMER

This publication is distributed by the U.S. Department of Transportation, National Highway Traffic Safety Administration, in the interest of information exchange. The opinions, findings, and conclusions expressed in this publication are those of the authors and not necessarily those of the Department of Transportation or the National Highway Traffic Safety Administration. The United States Government assumes no liability for its contents or use thereof. If trade or manufacturers' names or products are mentioned, it is because they are considered essential to the object of the publications and should not be construed as an endorsement. The United States Government does not endorse products or manufacturers.

Suggested APA Format Citation:

Hu, J., Fischer, K., Schroeder, A., Boyle, K., Adler, A., & Reed, M. (2019, October). *Development of oblique restraint countermeasures* (Report No. DOT HS 812 814). Washington, DC: National Highway Traffic Safety Administration.

## Technical Report Documentation Page

1. Report No. DOT HS 812 814	2. Government Accession No.	3. Recipient's Catalog No.	
4. Title and Subtitle Development of Oblique Restraint Countermeasures		5. Report Date October 2019	
		6. Performing Organization Code 081666	
7. Authors Jingwen Hu, Kurt Fischer, Alex Schroeder, Kyle Boyle, Angelo Adler, Matthew Reed		8. Performing Organization Report No.	
9. Performing Organization Name and Address University of Michigan Transportation Research Institute 2901 Baxter Road, Ann Arbor, MI 48109 ZF Active & Passive Safety Technology 4505 26 Mile Road, Washington, MI 48094		10. Work Unit No. (TRAIS)	
		11. Contract or Grant No. DTNH2215C00032	
12. Sponsoring Agency Name and Address National Highway Traffic Safety Administration 1200 New Jersey Avenue SE Washington, DC 20590		13. Type of Report and Period Covered Final, Oct. 2015-Nov. 2017	
		14. Sponsoring Agency Code	
15. Supplementary Notes			
16. Abstract The objective of this study was to develop and demonstrate modified restraint systems for front seat occupants that can help provide reduced injury potential for the 50th percentile male Test device for Human Occupant Restraint (THOR) in both left and right oblique frontal crashes. First, four baseline sled tests (i.e., driver near-side, driver far-side, passenger near-side, and passenger far-side) were conducted to set up the baseline restraint performance, which produced similar THOR kinematics and injury measures to those in the oblique moving deformable barrier (OMDB) full vehicle tests proposed by NHTSA. Second, a set of baseline Mathematical Dynamic Models (MADYMO) were developed and validated against the baseline sled tests as well as the Federal Motor Vehicle Safety Standards (FMVSS) No. 208 and the United States New Car Assessment Program (US-NCAP) frontal barrier tests. Third, a wide variety of seat belt and air bag designs were proposed to evaluate possible improvements in occupant protection in oblique crashes. Fourth, nearly 100 sled tests and hundreds of MADYMO simulations were conducted to systematically select and tune the proposed restraint designs to analyze the potential reduction of injury measures of THOR in four oblique crash conditions. Last, two types of modified restraint systems, one with a 3-point belt and relocated retractor, and one with a suspender 4-point belt, were identified and used in the final sled tests. Both modified restraint systems showed potential for reduced head lateral rotation, brain injury criterion (BrIC), maximal chest deflection, and the joint injury probabilities of THOR in all four testing conditions. To the extent that such systems can be feasibly integrated by vehicle manufactures into future models, these results demonstrated that a variety of modified restraint systems can be tuned to help reduce the injury measures of THOR in oblique frontal crashes.			
17. Key Word oblique crash test, crash simulation, restraint system, seat belt, air bag, head injury, chest injury, BrIC		18. Distribution Statement This document is available to the public through the National Technical Information Service, <a href="http://www.ntis.gov">www.ntis.gov</a> .	
19. Security Classif. (of this report)	20. Security Classif. (of this page)	21. No. of Pages 94	22. Price

Form DOT F 1700.7 (8-72)

Reproduction of completed page authorized

## **Acknowledgments**

This study was funded by NHTSA under Contract No: DTNH2215C00032. The opinions expressed herein are those of the authors and do not represent NHTSA. The authors would like to thank James Saunders, Stephen Summers, Dan Parent, and Matthew Craig from NHTSA for their tremendous support of this project.

# Table of Contents

Acknowledgments.....	ii
List of Figures.....	vi
List of Tables.....	viii
Executive Summary.....	1
1 Introduction.....	3
1.1 Significance of Oblique Crashes.....	3
1.2 NHTSA Oblique Moving Deformable Barrier Test.....	3
1.3 Potential Technologies for Improved Occupant Protection in Oblique Crashes.....	4
1.4 Restraint Design Optimizations.....	5
1.5 Objective and Research Tasks.....	5
2 Baseline Tests.....	7
2.1 Goal.....	7
2.2 Baseline Vehicle Selection.....	7
2.3 Baseline Sled Test Procedures.....	8
2.3.1 THOR positioning.....	8
2.3.2 Crash pulse and impact angle.....	9
2.3.3 Restraint firing time.....	11
2.3.4 Summary of baseline sled setup and targets.....	11
2.4 Baseline Sled Test Results.....	12
2.4.1 Driver near-side baseline sled test.....	13
2.4.2 Driver far-side baseline sled test.....	14
2.4.3 Passenger near-side baseline sled test.....	15
2.4.4 Passenger far-side baseline sled test.....	16
3 Baseline Model Validation.....	17
3.1 Goal.....	17
3.2 Baseline Model Development and Validation.....	17
3.3 Validation Against Baseline Oblique Sled Tests.....	18
3.4 Validation Against US-NCAP or FMVSS No. 208 Crash Tests.....	20
4 Modified Restraint Selection.....	23
4.1 Goals.....	23
4.2 Rationale.....	23
4.3 Countermeasures for Oblique Crashes.....	23

4.3.1	3-point belt with pretensioner, load limiting, and dynamic locking tongue .....	24
4.3.2	X-type 4-point belt .....	25
4.3.3	Suspender 4-point belt .....	25
4.3.4	Reversed 3-point belt .....	25
4.3.5	Rerouted 3-point belt .....	25
4.3.6	Cone driver air bag.....	25
4.3.7	SQS driver air bag.....	25
4.3.8	Driver support bag .....	25
4.3.9	V13 PAB .....	26
4.3.10	Clapper PAB.....	26
4.3.11	Parallel cell PAB.....	26
4.3.12	Kickstand PAB .....	26
4.3.13	Three-small-chamber CAB .....	26
4.3.14	Buckle curtain.....	26
4.3.15	Two-medium-chamber CAB .....	26
4.3.16	Single-large-chamber .....	26
5	Develop, Validate, and Tune Proposed Modified Restraint Systems .....	28
5.1	Goal.....	28
5.2	Design Optimization Method Overview .....	28
5.3	Relocated D-Ring/Retractor, Reversed, or Rerouted 3-Point Belts.....	30
5.3.1	Parametric simulations.....	31
5.3.2	Sled tests.....	33
5.4	Suspender 4-point Belt and X-type 4-point Belt .....	34
5.4.1	Sled tests.....	34
5.4.2	Parametric simulations .....	35
5.5	Various Driver Air Bags .....	37
5.6	Various Passenger Air Bags .....	39
5.7	Knee Air Bags.....	40
5.8	Curtain Air Bags .....	41
5.9	Air Bag and Seat Belt Optimization in Driver Far-Side Impact.....	44
5.9.1	SQS air bag parameter optimization .....	44
5.9.2	Combined Seat Belt and air bag design effects .....	46
5.10	Air Bag and Seat Belt Optimization in Passenger Far-Side Impact.....	48
5.10.1	Baseline air bag and suspender belt parameter optimization .....	48

5.10.2	V13 PAB and suspender belt parameter optimization.....	50
6	Final Series of Sled Tests With Modified restraints .....	52
6.1	Goal.....	52
6.2	Modified Restraints and Testing Matrix .....	52
6.3	Results .....	53
6.3.1	Final sled tests .....	53
6.3.2	Out-of-position Tests .....	57
6.3.3	FMVSS No. 208 simulations.....	59
7	Discussion.....	61
7.1	Challenges for Occupant Protection in Oblique Crashes .....	61
7.2	Chest Deflections of THOR .....	62
7.3	Abdomen Deflections of THOR.....	63
7.4	Limitations.....	63
8	Summary.....	64
8.1	Baseline Tests .....	64
8.2	Baseline Model Development and Validation.....	64
8.3	Propose Modified Prototype Restraint Systems .....	64
8.4	Design Optimizations.....	65
8.5	Final Sled Tests.....	65
	References .....	67
	Appendix A: Summary of NHTSA Oblique Crash Test Results .....	A-1
	Appendix B: Time Histories and CORA Ratings for Baseline Model Validations.....	B-1
	Appendix C: Examples of Model Validations Against Sled Tests With Modified Restraints....	C-1

## List of Figures

Figure 1: Illustration of NHTSA (left) OMDB test procedure (Saunders & Parent 2014).....	4
Figure 2: Method overview for developing modified, prototype restraint system in oblique crashes .....	6
Figure 3: THOR position relative to the driver interior in small/midsize passenger cars.....	8
Figure 4: THOR position relative to the passenger interior in small/midsize passenger cars.....	9
Figure 5: Vehicle kinematics for 8 vehicles in NHTSA oblique crash tests.....	10
Figure 6: Comparison of free flight head trajectories among different vehicles.....	10
Figure 7: Occupant kinematics in the driver near-side baseline sled test .....	13
Figure 8: Occupant kinematics in the driver far-side baseline sled test.....	14
Figure 9: Occupant kinematics in the passenger near-side baseline sled test .....	15
Figure 10: Occupant kinematics in the passenger far-side baseline sled test.....	16
Figure 11: Baseline MADYMO model.....	17
Figure 12: Model validation – Driver near-side baseline oblique .....	19
Figure 13: Model validation – Driver far-side baseline oblique.....	19
Figure 14: Model validation – Passenger near-side baseline oblique.....	19
Figure 15: Model validation – Passenger far-side baseline oblique .....	20
Figure 16: Model validation – US-NCAP driver 50th HIII .....	21
Figure 17: Model validation – US-NCAP passenger 5th HIII .....	21
Figure 18: Model validation – FMVSS No. 208 unbelted driver 5th HIII.....	21
Figure 19: Model validation – FMVSS No. 208 unbelted passenger 5th HIII.....	22
Figure 20: An overview of countermeasures for oblique crashes .....	24
Figure 21: Design optimization process.....	28
Figure 22: Simulated occupant kinematics between baseline and relocated D-ring locations.....	32
Figure 23: Occupant kinematics with different 3-point belt designs in driver far-side crash.....	33
Figure 24: Occupant kinematics with different 4-point belt designs in driver far-side crash.....	35
Figure 25: D-ring locations in the parametric simulation study .....	37
Figure 26: Occupant kinematics with different DAB designs in driver far-side crash.....	38
Figure 27: Occupant kinematics with different PAB designs in passenger far-side crash .....	39
Figure 28: Occupant kinematics with different KnAB designs in passenger far-side crash.....	41
Figure 29: Occupant kinematics with different CAB designs in driver near-side crash.....	42
Figure 30: Occupant kinematics with different CAB designs in passenger near-side crash.....	43

Figure 31: SQS DAB parameter effects on ATD injury measures with a 3-point belt.....	45
Figure 32: SQS DAB parameter effects on ATD injury measures with a suspender 4-point belt	46
Figure 33: Air bag and seat belt effects on ATD injury measures in driver far-side impacts.....	47
Figure 34: Air bag and seat belt effects on ATD injury measures in passenger far-side impacts.	49
Figure 35: ATD kinematics and head/neck injury measures with the baseline restraint and an alternate PAB and suspender belt in passenger far-side impact condition.....	50
Figure 36: ATD kinematics and head/neck injury measures with the baseline restraint and a V13 PAB and suspender belt in passenger far-side impact condition .....	51
Figure 37: Occupant kinematics in baseline and final sled tests for driver near-side impact .....	53
Figure 38: Occupant kinematics in baseline and final sled tests for driver far-side impact.....	54
Figure 39: Occupant kinematics in baseline and final sled tests for passenger near-side impact .	55
Figure 40: Occupant kinematics in baseline and final sled tests for passenger far-side impact....	56
Figure 41: Occupant kinematics in 6YO OOP tests for modified prototype passenger air bags ..	57
Figure 42: Occupant kinematics in H5 OOP tests for modified driver air bags.....	58
Figure 43: Example of chest deflection with suspender 4-point belt.....	62

## List of Tables

Table 1: Restraint firing time in NHTSA OMDB tests.....	11
Table 2: Occupant injury measures and mechanisms in the driver near-side oblique tests.....	13
Table 3: Injury measures and mechanisms in the driver far-side oblique tests.....	14
Table 4: Injury measures and mechanisms in the passenger near-side oblique tests.....	15
Table 5: Injury measures and mechanisms in the passenger far-side oblique tests.....	16
Table 6: Injury measure comparison between the baseline sled tests and the simulations.....	20
Table 7: Injury measure comparison between the US-NCAP/FMVSS No. 208 tests and simulations.....	22
Table 8: Design specifications of the seat belt and air bag technologies.....	27
Table 9: Injury measures and the associated injury risk curves.....	30
Table 10: D-ring location sensitivities on injury measures for driver far-side impact.....	31
Table 11: D-ring location sensitivities on injury measures for passenger far-side impact.....	31
Table 12: Injury measure reductions by using more rearward and inboard D-ring locations.....	32
Table 13: Injury measures with different 3-point belt designs in driver far-side crash.....	34
Table 14: Injury measures with different 4-point belt designs in driver far-side crash.....	35
Table 15: Parametric simulations with different suspender 4-point belt configurations.....	36
Table 16: Injury measures with different DAB designs in driver far-side crash.....	38
Table 17: Injury measures with different PAB designs in passenger far-side crash.....	40
Table 18: Injury measures with different KnAB designs in passenger far-side crash.....	41
Table 19: Injury measures with different CAB designs in driver near-side crash.....	42
Table 20: Injury measures with different CAB designs in passenger near-side crash.....	44
Table 21: Seat belt and air bag effects on injury measure in driver far-side impacts.....	48
Table 22: Head and neck injury measures in the parametric study with suspender 4-point belt and V13 PAB.....	51
Table 23: Modified prototype designs used in the final sled series.....	52
Table 24: Injury measures in baseline and final sled tests for driver near-side impact.....	53
Table 25: Injury measures in baseline and final sled tests for driver far-side impact.....	54
Table 26: Injury measures in baseline and final sled tests for passenger near-side impact.....	55
Table 27: Injury measures in baseline and final sled tests for passenger far-side impact.....	56
Table 28: Injury measures in 6YO OOP tests for modified passenger air bags.....	57
Table 29: Injury measures in 5th Female OOP tests for modified driver air bags.....	58
Table 30: Model-predicted driver injury measures in simulations for FMVSS No. 208 compliance.....	59
Table 31: Model-predicted front passenger injury measures in simulations for FMVSS No. 208 compliance.....	60
Table 32: Abdomen compressions between two THORs.....	63

## Executive Summary

The objective of this study was to develop and demonstrate possible improvements for occupant restraint systems for both the driver and front right passenger that can help provide reduced injury potential for the 50th percentile male THOR in both left and right oblique crashes.

A surrogate B-segment vehicle was selected as the baseline vehicle to build a sled buck representing the driver and front right passenger compartments. The B-segment vehicles are “small cars” defined by the European Commission, and are sometimes described as subcompacts in the United State with overall length roughly between 144 and 165 inches. A sled test procedure with an 18° sled angle was developed to replicate typical THOR kinematics and injury measures in NHTSA oblique moving deformable barrier (OMDB) tests with small/midsize passenger cars. Four baseline sled tests (i.e., driver near-side, driver far-side, passenger near-side and passenger far-side) were conducted, which produced similar THOR kinematics to those in the NHTSA OMDB full vehicle tests. In particular, the near-side impacts produced a scenario in which the head could roll off the air bag, resulting in lateral head rotation, high BrIC values (>1.0), and potential head-to-door contact; while the far-side impacts produced a scenario in which the torso rolled off the belt and the head rolled off the air bag, resulting in lateral head rotation, high BrIC values (>1.0), and potential head-to-instrument-panel contact. The values and locations of the maximal chest deflections in the sled tests were also consistent to the NHTSA OMDB full vehicle tests. These sled tests set up the baseline restraint performance to be tuned in this study.

A set of baseline MADYMO models were developed with detailed vehicle interior and restraint systems to represent the baseline B-segment vehicle. These models were validated against the four baseline sled tests as well as the FMVSS No. 208 unbelted frontal barrier tests and US-NCAP frontal barrier tests. The models generally provided accurate kinematics prediction and reasonable injury measure predictions. One of the observed limitations of this model is that the THOR model tended to under-estimate the maximal chest deflections in oblique crash conditions.

A wide variety of restraint designs were evaluated for improving occupant protection in oblique impacts. In total, five seat belt systems (reversed 3-point belt, rerouted 3-point belt, 3-point belt with relocated retractor, X-type 4-point belt, and suspender 4-point belt), four driver air bag (DAB) designs (cone DAB, square-shaped (SQS) DAB, DAB support bag, and inboard SAB), 5-passenger air bag (PAB) designs (V64 PAB, V13 PAB, Clapper PAB, parallel cell PAB, and kickstand PAB), and four curtain air bag (CAB) designs (three small chamber CAB, two medium chamber CAB, single large chamber CAB, and buckle CAB) for near-side impacts were proposed. The proposed air bag designs focused on helping to improve lateral support of the occupant’s head; while the proposed seat belt designs focused on improving engagement with the occupant’s torso longer and lowering the chest deflections.

To tune the proposed restraint systems, nearly 100 sled tests and hundreds of MADYMO simulations were conducted to systematically select and tune the proposed prototype seat belt and air bag designs to help reduce injury measures of THOR in the NHTSA OMDB crash conditions. Due to the complicated nature of far-side impacts, both sled tests and computational simulations focused on the far-side oblique impacts.

For both driver and passenger far-side impacts, two types of restraint systems provided the highest potential improvement among the prototypes that were tested. The first prototype system includes a 3-point belt with a relocated retractor that is closer to THOR’s shoulder and an

additional air bag (DAB support bag) or an air bag with additional features (kickstand PAB) to help reduce the lateral head rotation; and the other prototype system is equipped with a suspender 4-point belt with independently configured load limiting between two shoulder belts and minimal changes to current driver or passenger air bag content.

The relocated retractor for a 3-point belt can help the belt stay on the shoulder longer during a far-side impact and help reduce chest deflections by lowering the load limiting on the shoulder. An additional air bag or a new air bag feature that can support the head laterally help to reduce BrIC in a far-side oblique impact with a 3-point belt.

On the other hand, individually configured load limiting at two shoulders in a suspender 4-point belt can improve occupant kinematics without significant air bag changes. Typically, a higher load limiting should be assigned at the striking side of the shoulder, so that THOR's torso can rotate laterally towards the impact. Such kinematics can help to reduce the lateral head rotation, and consequently reduce the BrIC value. The suspender 4-point belt also reduced the chest deflections with belt loadings mainly transferred through the clavicles, not the ribs. In addition, only minimal changes in air bag designs were needed to lower the occupant's injury potential with the suspender 4-point belt.

Two modified restraint systems, one with a 3-point belt and relocated retractor, and one with a suspender 4-point belt, were used in the final sled tests. In all four testing conditions (driver near-side, driver far-side, passenger near-side, and passenger far-side), both modified, prototype restraint systems helped to reduce the head lateral rotation and the joint injury probabilities of THOR. The average BrIC and average maximal chest deflection in the four baseline sled tests were 1.32 and 51 mm; with the modified system using a 3-point belt, the average BrIC and average maximal chest deflection in the four final sled tests were reduced to 0.78, and 40 mm; and with the modified system using a suspender 4-point belt, the average BrIC and average maximal chest deflection in the four final sled tests were reduced to 0.70, and 29 mm. The average joint injury probability values for the baseline restraint, the modified restraint with 3-point belt, and the modified restraint with suspender 4-point belt were 0.92, 0.51, and 0.38.

In summary, although this study does not evaluate application or production feasibility, we systematically investigated prototype restraint system designs through multiple sled tests and computational simulations to evaluate the potential to achieve increased protection for front seat occupants in oblique crash conditions. The results demonstrated that certain modified, prototype restraint systems could be used and configured to help reduce the injury measures of THOR in oblique impacts.

# 1 Introduction

## 1.1 Significance of Oblique Crashes

For the past two decades, NHTSA has published numerous reports updating the seat belt and air bag effectiveness in different types of crashes, and they have consistently shown the benefit of occupant restraint technology (Kahane, 1996; NHTSA, 1999; Kahane, 2000; NHTSA, 2001). Based on the most recent analyses, the average combined fatality reduction for seat belts and air bags in all frontal crashes is over 60 percent relative to an unrestrained occupant without an air bag and the injury reduction is around 70 percent (NHTSA, 2001; Bean, Kahane, Mynatt, Rudd, Rush, & Wiacek et al., 2009). Even though these results showed the reduced injury potential of using restraint systems, no system can prevent all injuries in all situations. This means that properly restrained occupants can still be injured in certain crashes.

To answer the question “Why are people still dying in frontal crashes despite seat belt use, air bags, and the crashworthy structures of late-model vehicles?,” NHTSA conducted an in-depth review study on fatal frontal crash cases with belted occupants in newer vehicles (Bean, Kahane, Mynatt, Rudd, Rush, & Wiacek et al., 2009). Aside from a substantial proportion of these crashes that are exceedingly severe, one of the reasons occupants can still be fatally injured is because of the unique crash dynamics in oblique and small overlap crashes, which may result in less structural engagement between the vehicle and its collision partner. This conclusion is consistent with the findings from other recent field data analyses (Brumbelow & Zuby 2009; Rudd, Bean, Cuentas, Kahane, Mynatt, & Wiacek, 2009). Further analyses of injury causation in small overlap and oblique frontal crashes showed that the crash angle could influence injury causation more than crash type (Rudd, Scarboro, & Saunders, 2011). Specifically, oblique crashes may change head and chest injury sources, as occupants can move more toward the A-pillar or the center of the instrument panel (IP), potentially reducing the effectiveness of the seat belt and air bag systems (Bean, Kahane, Mynatt, Rudd, Rush, & Wiacek et al., 2009; Rudd, Scarboro, & Saunders, 2011).

## 1.2 NHTSA Oblique Moving Deformable Barrier Test

NHTSA developed a test procedure that involves an oblique moving deformable barrier (OMDB) with 90 km/h (56 mph) travelling speed impacting a stationary vehicle with a 35-percent overlap and a 15° angle in both left- and right-side impacts (left-side impact example shown in Figure 1) to further evaluate occupant protection technology in oblique crashes. To help simulate occupant responses in the field, the most recent version of Test device for Human Occupant Restraint (THOR) 50th percentile male anthropomorphic test device (ATD) was used. This version of the THOR is called THOR Mod Kit with SD-3 shoulder (referred as “THOR” in this report). THOR has a more flexible spine/torso and a more humanlike shoulder than the Hybrid-III 50th percentile male ATD, so that it can better represent occupant kinematics in oblique crashes. Before this study started in late 2015, NHTSA had conducted over 30 full vehicle, either left- or right-side, OMDB tests. The results of these tests demonstrated kinematics and injury responses to the driver and front right passenger that are consistent with field data. In particular, in NHTSA OMDB tests, the near-side occupant could engage the air bag at an angle, potentially resulting in higher head angular velocity and Brain Injury Criteria (BrIC) values than in pure frontal crashes (Takhounts, Craig, Moorhouse, McFadden, & Hasija, 2013). On the other hand, the far-side occupant could roll out of the seat belt system and contact the IP. Prototype

designs or modifications could tune restraint systems to help better protect occupants in those oblique crash situations.

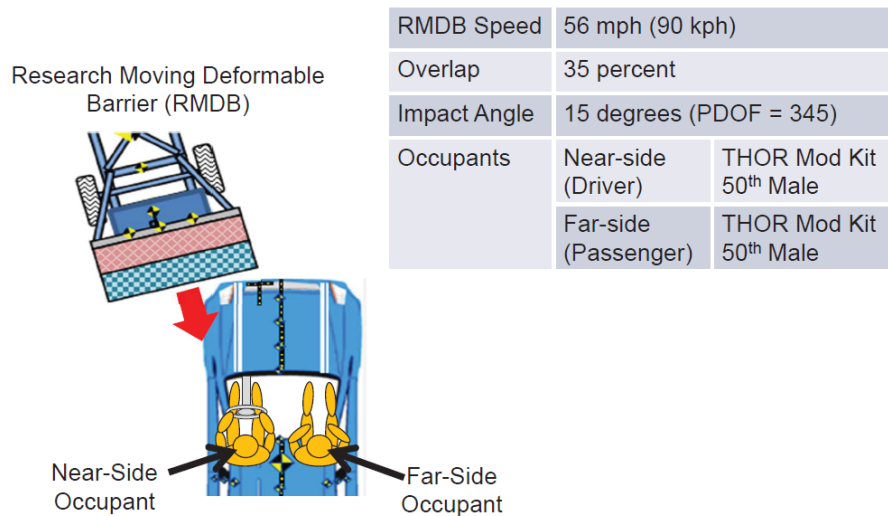


Figure 1: Illustration of NHTSA (left) OMDB test procedure (Saunders & Parent 2014)

Note: The NHTSA OMDB test procedure includes both the left and right impacts.

### 1.3 Potential Technologies for Improved Occupant Protection in Oblique Crashes

Although many restraint technologies are currently available for drivers and front seat passengers, there is opportunity to improve protection for the occupant kinematics that occurred in NHTSA OMDB crash conditions. Several seat belt and air bag designs have the potential to help reduce the occupant injury potential in oblique crashes.

For example, a 4-point seat belt system provides two webbing straps, one over each shoulder, thus helping to better prevent occupants from rolling out of the belt in oblique crashes. Previous sled tests with post-mortem human subjects (PMHSs) and ATDs have shown that the 4-point seat belt can help to reduce the chest deflection in frontal crashes, and provide extra constraint for far-side occupants in side impact crashes (Rouhana et al., 2003; Rouhana, Kankanala, Prasad, Rupp, Jeffreys, & Schneider, 2006). However, the customer and vehicle manufacturer acceptance of this design needs to be further evaluated.

A reversed 3-point seat belt, whose upper anchor is located toward the middle of a vehicle, has been previously tested for helping to better protect far-side occupants in side impacts and occupants in rollover crashes (Bostrom, Haland, & Soderstrom, 2005). The reversed 3-point seat belt may reduce the chance of far-side occupants rolling out of the belt in oblique crashes. However, it may reduce the effectiveness for near-side occupants in side-impact and oblique crashes. Because the curtain air bag is generally available for near-side occupants, it is possible that this disadvantage can be reduced by redesigning the curtain air bag.

Because the far-side occupants could roll out of the shoulder belt in oblique crashes, a change to the shape of the driver and passenger air bags or an additional air bag on the IP may help improve occupant protection by covering larger areas. The curtain air bag might also be tuned to adapt to the occupant kinematics in near-side oblique crashes. Although no air bag designs have been published in the literature specifically for oblique crashes yet, several auto makers and safety suppliers have proposed air bags in a wide variety of sizes and shapes to help improve

occupant protections in oblique crashes (U.S. Patent No. 9499118 B2, 2016; U.S. Patent No. 9550465B1 et al., 2017; U.S. Patent No. 20170072897A1, 2017).

#### 1.4 Restraint Design Optimizations

Even though the aforementioned technologies have the potential to help reduce the occupant injury risks in oblique crashes, different seat belt characteristics as well as the size and shape of the air bags will need to be tuned and evaluated. The methodologies used previously to evaluate the restraint systems in frontal crashes can be adapted to oblique crashes. For example, in a recent NHTSA-funded study, the University of Michigan Transportation Research Institute (UMTRI) and ZF conducted three series of sled tests, two series of computational model validations, and thousands of MADYMO simulations to tune the design parameters of new air bag and seat belt designs for rear-seat occupants in both pure frontal and oblique crash conditions (Hu, Rupp, Reed, Kurt, Lange, & Adler, 2015; Hu, Reed, Rupp, Fischer, Lange, & Adler, 2017). It was found that by adding seat belt pretensioner, load limiting, and SCaRAB (self-conforming rear seat air bag), almost all the injury measures for all four ATDs (HIII 6-year-old, HIII 5th percentile female, HIII 95th percentile male, and THOR) were reduced from the baseline system in the tested conditions. In another recent NHTSA-funded study, UMTRI and General Motors conducted hundreds of finite element (FE) simulations to tune restraint systems for both the driver and passenger side with and without FMVSS208 unbelted requirements (Hu, Reed, Rupp, Fischer, Lange, & Adler, 2017). In that study, multiple objective functions and multiple constraints were used for seat belt and air bag design optimizations to minimize the occupant injury risks for both HIII 50th and 5th percentile ATDs in US-NCAP crash conditions, and at the same time meet other regulatory and consumer information crash test requirements. Response surface method (RSM), design of experiment (DoE), and genetic algorithms were used for the design optimizations, which helped to reduce the injury potential from the baseline system (Hu, Reed, Rupp, Fischer, Lange, & Adler, 2017). Similar methods have been used in restraint system optimization in other studies on occupant protection (Deng et al., 2013; Hu, Wu, Klinich, Reed, Rupp, & Cao, 2013; Hu, Wu, Reed, Klinich, & Cao, 2013; Bai et al., 2014; Ito, Yokoi, & Mizuno, 2015; Zhang & Zhou 2015).

#### 1.5 Objective and Research Tasks

The objective of this study was to develop prototype occupant restraint systems for both the driver and front right passenger and evaluate the possible reduced injury potential for the 50th percentile male THOR in both left and right oblique crashes.

Figure 2 shows a method overview with five interrelated *research tasks* addressed in this study.

- Task 1.** Select a baseline vehicle, propose sled test procedures to mimic the occupant responses in NHTSA OMDB tests, and conduct baseline sled tests using the proposed procedures.
- Task 2.** Validate the baseline models against the baseline sled tests in Task 1 as well as the regulatory and consumer information crash tests available.
- Task 3.** Propose modified, prototype restraint systems that could improve occupant protection in OMDB tests.
- Task 4.** Design, validate, and tune the proposed restraint systems with the objective of minimizing the risk of occupant injuries in oblique sled crash conditions.

**Task 5.** Fabricate and test the proposed restraint systems and evaluate the potential occupant injury measure reduction in oblique sled crash conditions without compromising the safety performance in other crash conditions.

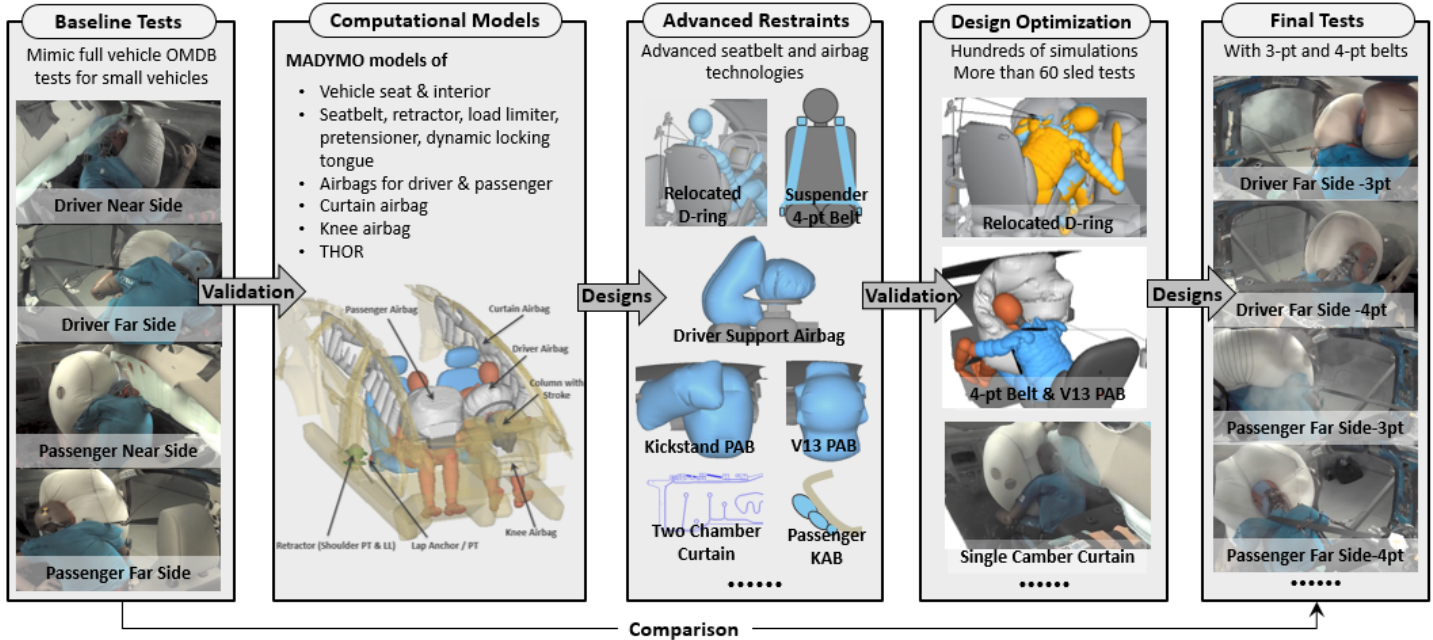


Figure 2: Method overview for developing modified, prototype restraint system in oblique crashes

## **2 Baseline Tests**

### **2.1 Goal**

The goals of Task 1 included choosing a baseline vehicle that met the following specific criteria.

- 1) Small or midsize passenger car
- 2) Good or acceptable structural rating on the Insurance Institute for Highway Safety (IIHS) small overlap
- 3) FMVSS compliant curtain air bag

The goals of Task 1 also included developing a sled test procedure to replicate the typical THOR kinematics and injury measures in the NHTSA OMDB tests with small/midsize passenger cars, and establishing the baseline crash performance with baseline restraint systems in oblique crash conditions.

### **2.2 Baseline Vehicle Selection**

A search of the NHTSA test database showed that 36 full vehicle tests following the NHTSA OMDB test procedure were available by the time when this project started, which covered 25 vehicle models. Among all these tests, 24 were conducted with two 50th percentile male THORs (1 test used modified HIII 50th male ATD) in the two front seat locations, 11 were conducted with THOR on the driver location and HIII 5th female ATD on the rear-seat, and one was conducted with only a 50th THOR on the driver location. The injury measures in all these tests are attached in the Appendix A. By reviewing the injury measures, the possible safety concerns for the drivers are high BrIC (mainly due to the potential head Z-rotation) and chest deflections, and the possible safety concerns for the front seat passengers are the high HIC and BrIC values (mainly due to potential head contact to the instrument panel and head Z-rotation) as well as the high chest deflections.

In this study, a surrogate B-segment vehicle was used as the baseline vehicle. The B-segment vehicles are “small cars” defined by the European Commission, and are sometimes described as subcompacts in the United State with overall length roughly between 144 and 165 inches. This decision was supported by the following rationale.

- 1) ZF is supplying almost all the occupant restraints (seat belts and air bags) for the surrogate B-segment vehicle. Therefore, it is faster and easier to access the baseline vehicle interior (IP, seat, steering wheel, etc.) and restraint systems (seat belt and air bag) used in the surrogate vehicle than any other vehicles.
- 2) ZF has a full set of restraint system models available that can simulate the surrogate vehicle’s crash performance.
- 3) The surrogate B-segment vehicle is a compact/sub-compact vehicle, which will pose challenges on restraint design optimizations in the OMDB testing condition due to the relative severe crash pulse.
- 4) In the surrogate B-segment vehicle oblique crash test, the BrIC values of the THOR at the driver location can exceed the thresholds due to the head rotation, and the chest deflection is high, both of which are consistent to the general trend found in other vehicles.
- 5) In a recent NHTSA-funded project on rear-seat occupant protection conducted by UMTRI and ZF, sled tests have already been conducted in oblique crash conditions. Comparison of

the ATD responses between those sled tests and surrogate B-segment vehicle OMDB crash test is useful to design sled test procedures.

In summary, the THOR kinematics and injury measures in the selected surrogate B-segment vehicle were representative of the general vehicle fleet in oblique crash tests, and the study’s research team possesses the physical and computational tools to replicate the occupant responses in full vehicle oblique crashes. However, it should be noted that the surrogate B-segment vehicle was rated as “4 Star” for the front seat passenger in US-NCAP full frontal crash test and is rated as “Marginal” in IIHS small overlap crash test. The surrogate B-segment vehicle was rated as “Good” in IIHS moderate overlap crash test, and met other NHTSA requirements based on FMVSS No. 208 unbelted and out-of-position (OOP) tests. The surrogate B-segment vehicle met the passenger OOP requirements through suppression, not air bag performance.

### 2.3 Baseline Sled Test Procedures

#### 2.3.1 THOR positioning

Because a surrogate B-segment vehicle was used to build the sled buck, it was necessary to ensure that the positions of THOR in both the driver and passenger side of surrogate B-segment vehicle were consistent to other small/midsize passenger cars. Figures 3 and 4 show THOR’s positions in the driver and passenger side of the surrogate B-segment vehicle and several other vehicles that have been tested in NHTSA oblique crash conditions.

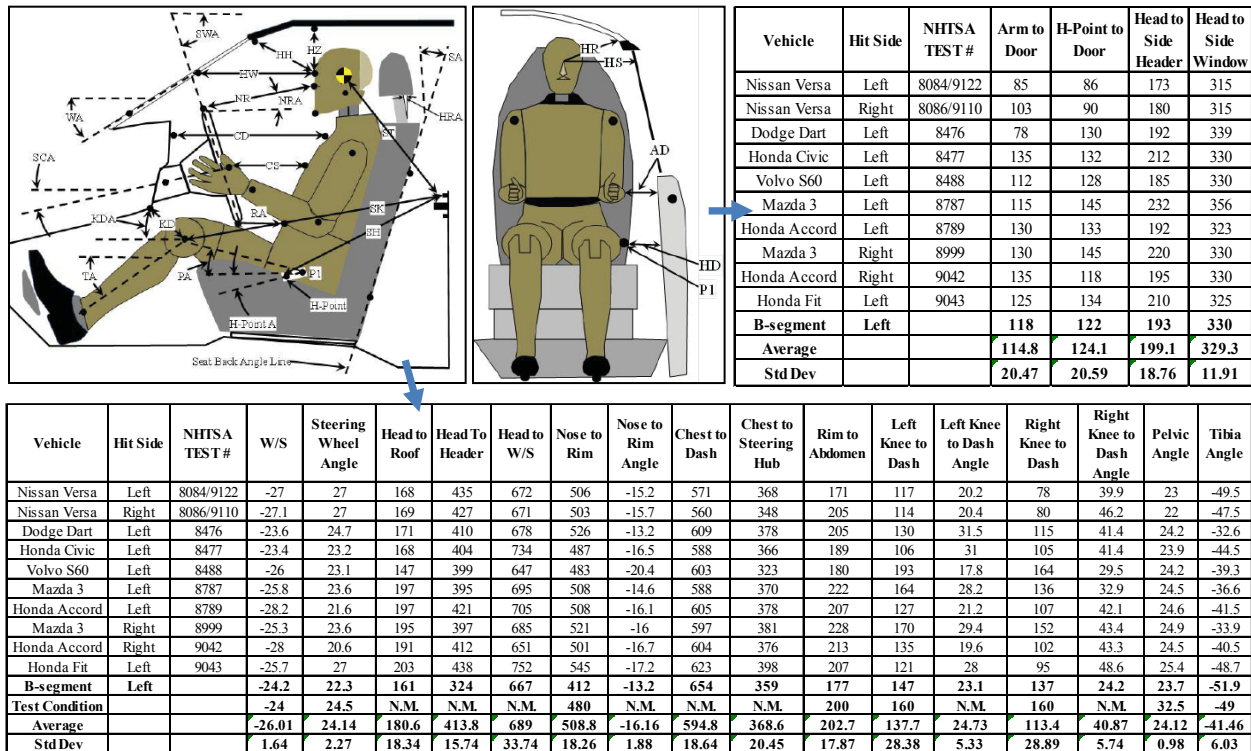
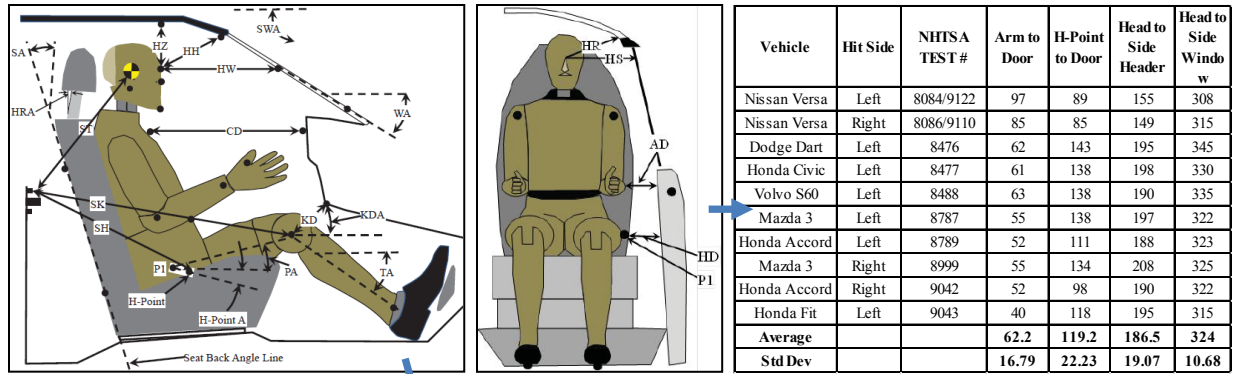


Figure 3: THOR position relative to the driver interior in small/midsize passenger cars



Vehicle	Hit Side	NHTSA TEST #	Head to Roof	Head To Header	Head to W/S	Nose to Rim	Nose to Rim Angle	Chest to Dash	Left Knee to Dash	Left Knee to Dash Angle	Right Knee to Dash	Right Knee to Dash Angle	Pelvic Angle	Tibia Angle
Nissan Versa	Left	8084/9122	158	434	644	675	-27.6	538	93	28.8	112	25.2	-21.4	-46.2
Nissan Versa	Right	8086/9110	146	433	636	680	-29.7	561	105	33.1	111	24.1	-21.8	-47.4
Dodge Dart	Left	8476	89	406	703	691	-25.1	565	127	39	142	42.8	-24.2	-37.7
Honda Civic	Left	8477	149	409	663	678	-32.2	549	108	32	105	32.6	-23.8	-42.4
Volvo S60	Left	8488	146	420	663	723	-33	602	203	31.5	207	30.8	-23.2	-37
Mazda 3	Left	8787	178	386	592	708	-30.2	552	142	32.5	151	31.9	-24.2	-34.4
Honda Accord	Left	8789	174	418	628	718	-35.1	561	127	28.6	137	29.8	-23.1	-40.8
Mazda 3	Right	8999	169	386	604	703	-29.9	563	135	30.2	155	28.5	-24.7	-35.5
Honda Accord	Right	9042	181	408	608	708	-33.8	568	115	29.2	129	30.7	-24.8	-43.1
Honda Fit	Left	9043	180	426	666	713	-32.9	568	73	30.4	92	26.1	-24.8	-51.6
<b>Test Condition</b>			N.M.	N.M.	N.M.	720	N.M.	580	145	N.M.	160	N.M.	32.5	-44
<b>Average</b>			<b>157</b>	<b>413</b>	<b>641</b>	<b>700</b>	<b>-31</b>	<b>563</b>	<b>123</b>	<b>32</b>	<b>134</b>	<b>30</b>	<b>-24</b>	<b>-42</b>
<b>Std Dev</b>			<b>27.7</b>	<b>17.1</b>	<b>34.2</b>	<b>17.5</b>	<b>3.0</b>	<b>16.7</b>	<b>34.9</b>	<b>3.1</b>	<b>33.0</b>	<b>5.3</b>	<b>1.2</b>	<b>5.6</b>

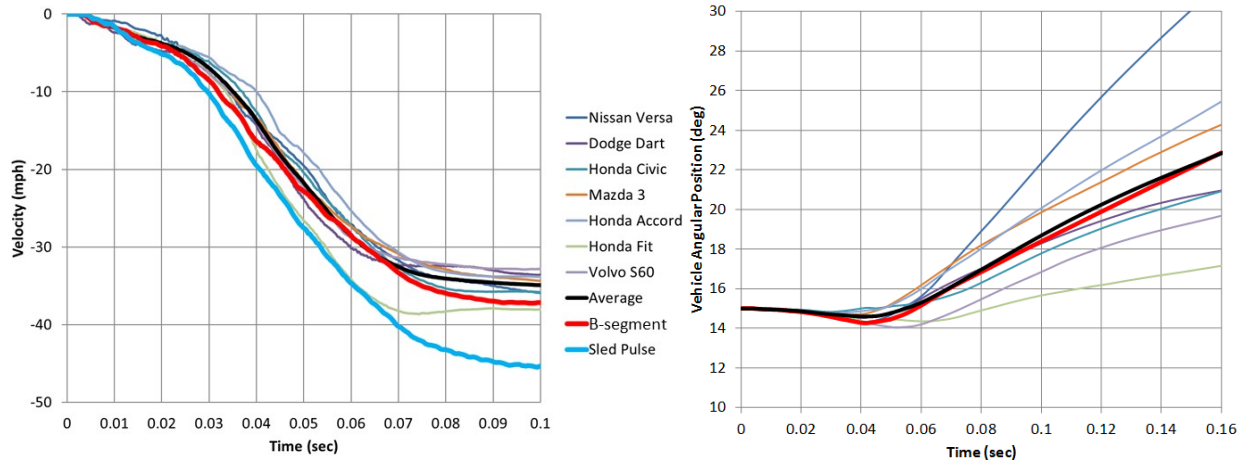
Figure 4: THOR position relative to the passenger interior in small/midsize passenger cars

For the driver side, the surrogate B-segment vehicle had shorter “Nose to Rim” and “Rim to Abdomen” distances compared to other vehicles, but other measurements in surrogate B-segment vehicle seemed representative for compact/small passenger cars. However, in the current study, it was found that THOR’s position in the driver side of the sled buck was close to the fleet average and it was representative of the fleet condition. The position of THOR on the passenger side of the sled buck was moved 40 mm rearward from the seat mid-track position to help match the general trend from the oblique crashes in other vehicles. The resulted THOR positioning measures in the testing condition were generally within the mean±1 standard deviation of THOR positions in the selected vehicles in Figures 3 and 4.

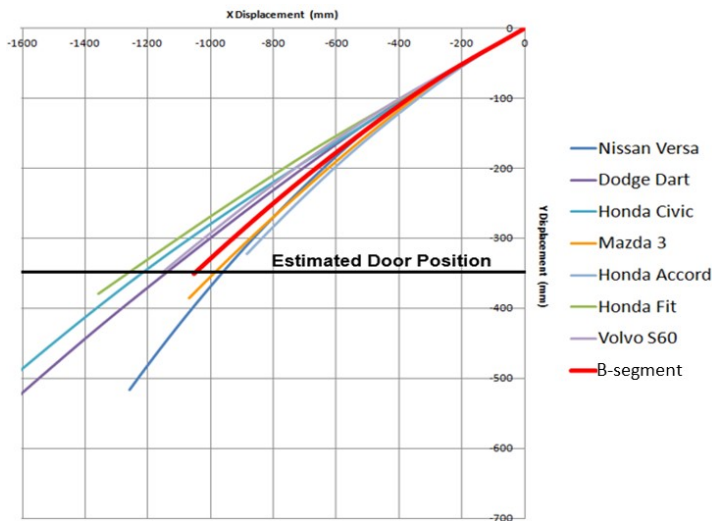
### 2.3.2 Crash pulse and impact angle

Figure 5 shows the vehicle velocity profiles and angular rotations of the surrogate B-segment vehicle and seven other small/midsize passenger cars in the NHTSA OMDB crash conditions. Note that the velocity profiles were generated by integrating the longitudinal acceleration component of the vehicle center of gravity. This was represented by the “Average” pulse curve. The vehicle kinematics of the surrogate B-segment vehicle were representative for all the tested small/midsize vehicles. Initially, the surrogate, “Average,” vehicle crash pulse was used as the baseline crash pulse for the sled tests. However, such a pulse could not generate the occupant kinematics that were representative of those in the NHTSA OMDB crash tests. Therefore, the surrogate “Average” vehicle pulse was re-calculated using the resultant acceleration of the vehicle center of gravity and represented by the “Sled Pulse” curve in Figure 5.

In a sled test, the sled (yaw) angle is generally fixed. Figure 6 shows the free flight head trajectory comparison among different vehicles tested in NHTSA OMDB crash conditions. The free flight head trajectory was calculated by applying the vehicle accelerations to an imaginary head. The calculated free flight head trajectory was then used to estimate the proper sled angle to be used in the current study. The average of the equivalent sled angle for all the tested vehicles is 17.92°. The surrogate B-segment vehicle (17.71°) was representative in terms of the trajectory as well as the equivalent sled angle. Therefore, in the current study, an 18° sled angle was used.



(a) Velocity profile  
 (b) Angular rotation  
 Figure 5: Vehicle kinematics for 8 vehicles in NHTSA oblique crash tests



(a) Free flight head trajectory

Vehicle	Free Flight Head Trajectory ( $R^2$ )
Mazda 3	19.16° (0.9932)
Honda Accord	19.24° (0.9927)
Volvo S60	16.19° (0.9957)
Nissan Versa	20.51° (0.9821)
Dodge Dart	17.77° (0.9955)
Honda Fit	15.45° (0.9988)
Honda Civic	17.12° (0.9959)
<b>B-Segment</b>	<b>17.71° (0.9945)</b>
<b>Average*</b>	<b>17.92°</b>

(b) Equivalent sled angle

Figure 6: Comparison of free flight head trajectories among different vehicles

### 2.3.4 Restraint firing time

Table 1 shows the estimated restraint firing times for the vehicles tested in the NHTSA OMDB crash conditions, which provided the references for the baseline sled tests.

Table 1: Restraint firing time in NHTSA OMDB tests (unit: ms)

	Vehicle	DAB/PAB TTF	KAB TTF	CAB TTF	SAB TTF	Seatbelt PT
Driver Near-side	Mazda 3	8/13	--	38	38	8
	Honda Accord	14/19	--	42	42	13
	Volvo S60	9/14	--	13	68	8
	Nissan Versa	15/19	--	41	41	15
	Dodge Dart	20/40	20	46	46	20
	Honda Fit	18/38	--	34	36	17
	Honda Civic	16/21	--	42	42	14
	<b>B-Segment</b>	16/26	4	--	--	4
	<b>Average*</b>	<b>14/23</b>	<b>--</b>	<b>37</b>	<b>45</b>	<b>14</b>
Passenger Near-side	Mazda 3	10/15	--	39	39	10
	Honda Accord	13/53	--	37	37	13
	Nissan Versa	10/14	--	33	33	9
	<b>Average</b>	<b>11/27</b>	<b>--</b>	<b>36</b>	<b>36</b>	<b>11</b>
Driver Far-side	Mazda 3	10/15	--	--	--	10
	Honda Accord	14/54	--	--	--	13
	Nissan Versa	9/14	--	--	--	10
	<b>Average</b>	<b>11/28</b>	<b>--</b>	<b>--</b>	<b>--</b>	<b>11</b>
Passenger Far-side	Mazda 3	8/13	--	--	--	8
	Honda Accord	13/28	--	--	--	13
	Volvo S60	9/19	--	--	--	16
	Nissan Versa	15/19	--	--	--	15
	Dodge Dart	20/40	20	--	--	20
	Honda Fit	17/57	--	--	--	17
	Honda Civic	16/56	--	--	--	14
	<b>Average</b>	<b>14/33</b>	<b>--</b>	<b>--</b>	<b>--</b>	<b>15</b>

\*Average does not include the surrogate B-segment vehicle fire times

### 2.3.5 Summary of baseline sled setup and targets

A sled buck representing the surrogate B-segment vehicle driver and front-seat passenger compartments was adapted to be positioned at two initial sled angles +18° (rotate the sled to the right) and -18° (rotate the sled to the left) to replicate the left and right oblique crashes, respectively. This resulted in four crash conditions: driver left (near-side), driver right (far-side), passenger left (far-side) and passenger right (near-side).

The 50th percentile male THOR was used in all the sled tests. THOR was positioned following the NHTSA OMDB THOR positioning procedure (NHTSA, 2015). The driver seat was in the

mid-track location, and the passenger seat was moved 40 mm rearward from the mid-track position to be more representative for small/midsize passenger cars. A 3-D coordinate measurement device was used to measure the initial ATD position/posture and restraint system configuration in each test to achieve test repeatability and document initial conditions that were used in the simulation studies. The measurements in each test followed NHTSA's specifications on THOR.

The restraint systems used in the baseline sled tests were consistent to those used in the surrogate B-segment vehicle, which included a two-stage driver air bag, a two-stage passenger air bag, a knee air bag for the driver, curtain air bags for both driver and front passenger, and 3-point belts with retractor pre-tensioner and load limiting (digressive load limiting [DLL] for the driver and switchable load limiting [SLL] for the passenger). The restraint firing times were based on the references provided in Table 1. Specific firing times were as the following.

- Driver air bag stage 1 and stage 2 – 13/23 ms
- Passenger air bag stage 1 and stage 2 – 13/23 ms
- Knee air bag – 7 ms
- Curtain air bag – 34 ms
- Seat belt retractor pre-tensioner – 11 ms

In the baseline sled tests, the major occupant kinematics to be reproduced were as follows.

- Near-side occupant: Occupant experiences movement off the air bag and the head hits the door
- Far-side occupant: Occupant rolls out of the shoulder belt and the head hits the IP

In any of the baseline sled tests, the BrIC should be greater than 0.87 and/or the maximal chest deflection should be at the “near nothing/near buckle” location and around 50 mm. The “near nothing” location is at the upper and inboard chest; while the “near buckle” location is at the lower and inboard chest. THOR's kinematics in all four crash conditions were compared to the small/oblique vehicle oblique tests to ensure that they were representative for the tested vehicle fleet.

## **2.4 Baseline Sled Test Results**

Overall, the baseline sled tests produced similar THOR kinematics to those in the NHTSA OMDB full vehicle tests; and the injury measures, especially the BrIC and maximal chest deflections, were also consistent to the OMDB tests. Figures 7 to 10 show THOR's kinematics in the baseline sled tests with the baseline restraint systems in four impact conditions. Tables 2 to 5 show some of the critical injury measures along with some basic occupant kinematic characteristics for both the OMDB full vehicle tests and the baseline sled tests. The far-side impacts tended to have higher BrIC values and a larger tendency to roll out of the belts and contact the IP; while the near-side impacts had BrIC values close to 1.0 and tended to contact the door without sufficient curtain air bag support.

### 2.4.1 Driver near-side baseline sled test

In the driver near-side oblique impact, as shown in Figure 7, the torso of THOR rotated substantially toward the impact direction, and the head rolled laterally off the driver bag. Although, these kinematics did not cause a head to door contact, it led to a high BrIC value ( $>1.0$  as shown in Table 2). The sled test generated higher HIC value than those in the vehicle OMDB tests, but the BrIC and chest deflections were consistent to the vehicle OMDB tests.

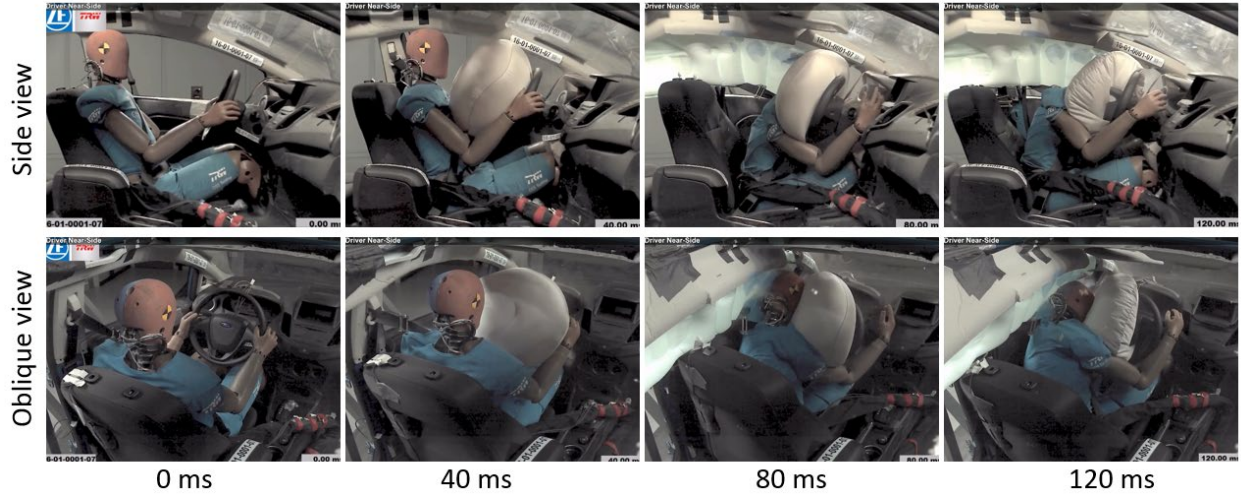


Figure 7: Occupant kinematics in the driver near-side baseline sled test

Table 2: Occupant injury measures and mechanisms in the driver near-side oblique tests

Vehicle	HIC	BrIC	ChestD (mm)	ChestD Location	Head Contact	Roll off bag
Mazda 3	267	1.19	41	Near Nothing /Near Buckle	Door	Yes
Honda Accord	185	0.61	49	Near Nothing	None	Yes
Volvo S60	151	1.1	37	Near Buckle	Door	Yes
Nissan Versa	137	0.89	36	Near Nothing	Door	Yes
Dodge Dart	313	0.73	49	Near Buckle	Header	No
Honda Fit	264	1.1	52	Near Nothing	Door	Yes
Honda Civic	201	0.85	43	Near Buckle	Door	Yes
B-Segment	145	1.52	46	Near Nothing	Door	Yes
<b>Average*</b>	<b>217</b>	<b>0.92</b>	<b>44</b>	<b>Near Nothing /Near Buckle</b>	<b>Door</b>	<b>Yes</b>
<b>Baseline Test Sled 0001-07</b>	<b>448</b>	<b>1.04</b>	<b>49</b>	<b>Near Nothing</b>	<b>None</b>	<b>Yes</b>

\*Average does not include the B-segment vehicle injury values

### 2.4.2 Driver far-side baseline sled test

In the driver far-side oblique impact, as shown in Figure 8, the torso of THOR rotated substantially toward the impact direction, the seat belt red off the shoulder, and the head rolled laterally off the driver bag. These kinematics caused a head to hand/IP contact, and it resulted in a high BrIC value ( $>1.0$  as shown in Table 3). The sled test generated HIC, BrIC and chest deflection within the range of those in vehicle OMDB tests.

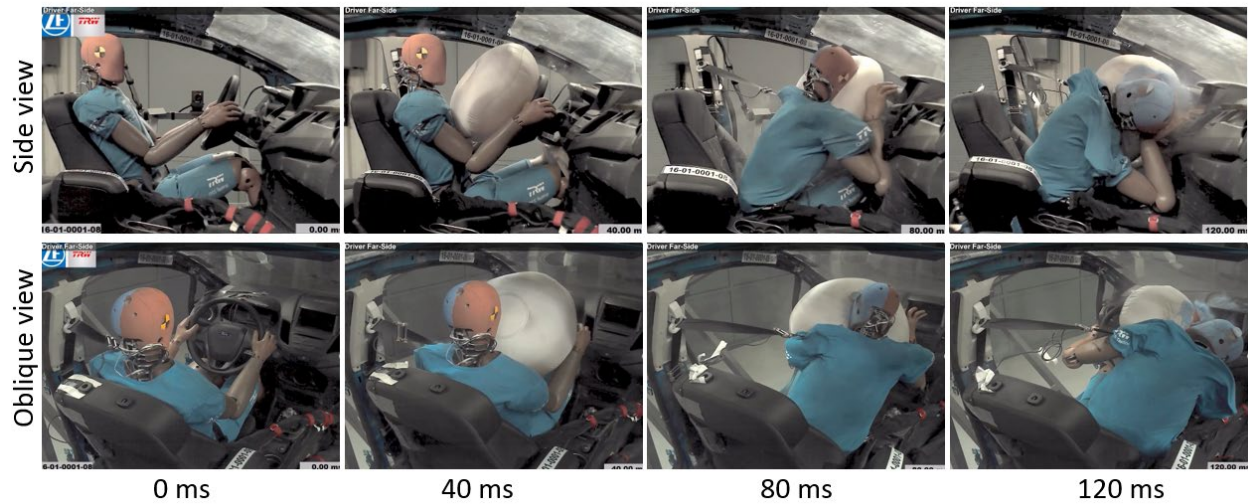


Figure 8: Occupant kinematics in the driver far-side baseline sled test

Table 3: Injury measures and mechanisms in the driver far-side oblique tests

Vehicle	HIC	BrIC	ChestD (mm)	ChestD Location	Head Contact	Belt Rollout
Mazda 3	747	1.48	41	Near Nothing	IP	Yes
Honda Accord	416	1.78	44	Near Nothing	IP	Yes
Nissan Versa	645	1.00	40	Near Nothing	IP	Yes
<b>Average</b>	<b>603</b>	<b>1.42</b>	<b>42</b>	<b>Near Nothing</b>	<b>IP</b>	<b>Yes</b>
<b>Baseline Test Sled 0001-03</b>	<b>496</b>	<b>1.73</b>	<b>44</b>	<b>Near Nothing</b>	<b>IP/Hand</b>	<b>Yes</b>

### 2.4.3 Passenger near-side baseline sled test

In the passenger near-side oblique impact, as shown in Figure 9, the torso of the THOR rotated substantially toward the impact direction, and the head rolled laterally off the passenger bag. These kinematics caused a head to door contact, which led to a high HIC and BrIC (Table 4). The sled test generated HIC, BrIC and chest deflection within the range of those in vehicle OMDB tests.

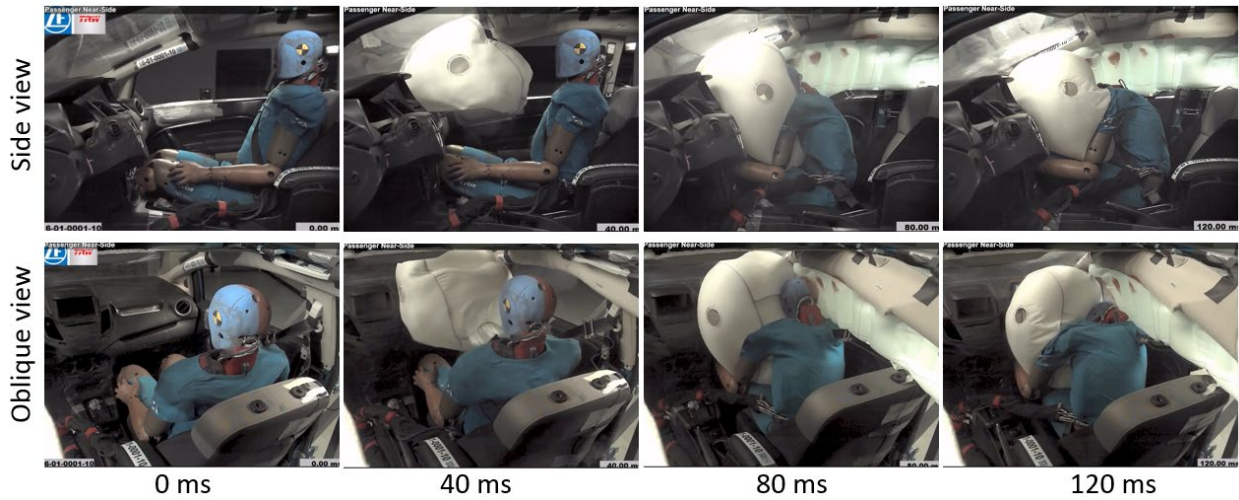


Figure 9: Occupant kinematics in the passenger near-side baseline sled test

Table 4: Injury measures and mechanisms in the passenger near-side oblique tests

Vehicle	HIC	BrIC	ChestD (mm)	ChestD Location	Head Contact	Roll off bag
Mazda 3	356	0.83	56	Near Buckle	None	Yes
Honda Accord	189	0.94	58	Near Buckle	None	Yes
Nissan Versa	824	1.01	42	Near Nothing	Door	Yes
<b>Average</b>	<b>456</b>	<b>0.93</b>	<b>52</b>	<b>Near Buckle</b>	<b>None / Door</b>	<b>Yes</b>
<b>Baseline Test Sled 0001-10</b>	<b>773</b>	<b>0.97</b>	<b>58</b>	<b>Near Nothing (UL)</b>	<b>Door</b>	<b>Yes</b>

#### 2.4.4 Passenger far-side baseline sled test

In the passenger far-side oblique impact, as shown in Figure 10, the torso of the THOR rotated substantially toward the impact direction, the seat belt rolled off the shoulder, and the head rolled laterally off the passenger bag. These kinematics caused a head to IP contact, and resulted in a high BrIC value ( $>1.0$  as shown in Table 5). The sled test generated HIC, BrIC and chest deflection within the range of those in vehicle OMDB tests.

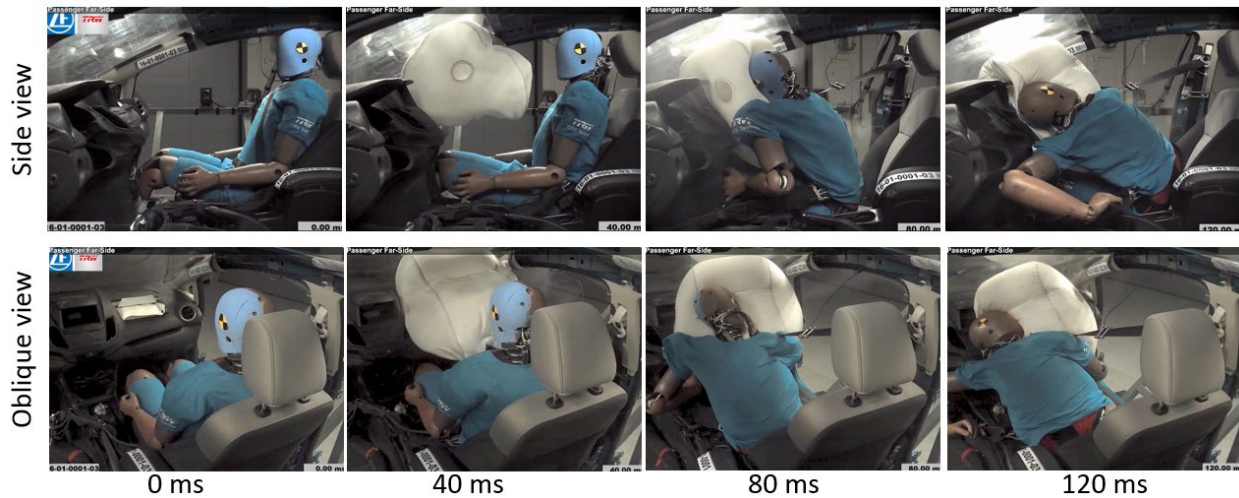


Figure 10: Occupant kinematics in the passenger far-side baseline sled test

Table 5: Injury measures and mechanisms in the passenger far-side oblique tests

Vehicle	HIC	BrIC	ChestD (mm)	ChestD Location	Head Contact	Belt Rollout
Mazda 3	806	1.12	38	Near Buckle	IP	Yes
Honda Accord	935	1.46	39	Near Buckle	IP	Yes
Volvo S60	223	1.46	31	Near Nothing	IP	Yes
Nissan Versa	543	1.91	41	Near Buckle	IP	Yes
Dodge Dart	113	2.21	35	Near Nothing	Header/ IP	Yes
Honda Fit	908	2.23	56	Near Buckle	IP	Yes
Honda Civic	272	2.81	42	Near Buckle	IP	Yes
<b>Average</b>	<b>543</b>	<b>1.89</b>	<b>40</b>	<b>Near Buckle / Near Nothing</b>	<b>IP</b>	<b>Yes</b>
<b>Baseline Test Sled 0001-03</b>	<b>332</b>	<b>1.54</b>	<b>48</b>	<b>Near Nothing (UL)</b>	<b>IP</b>	<b>Yes</b>

### 3 Baseline Model Validation

#### 3.1 Goal

The goals of Task 2 were to develop a set of computational models representing the occupant compartments, restraint systems, and occupants for both the driver and front seat passenger, and validate the model against the baseline tests as well as the regulatory and consumer information crash test results.

#### 3.2 Baseline Model Development and Validation

A set of baseline models in MADYMO (TASS International, Netherlands) were developed as shown in Figure 11. The models included detailed geometry of the vehicle interior (seat, instrument panel, crushable steering column, steering wheel, door interior, and windshield, etc.) and detailed restraint systems for both the driver and front seat passenger (3-point seat belt, seat belt retractor with pretensioner and load limiting, anchor pretensioner, driver air bag, passenger air bag, knee air bag for driver, knee bolster for the passenger, and curtain air bags).

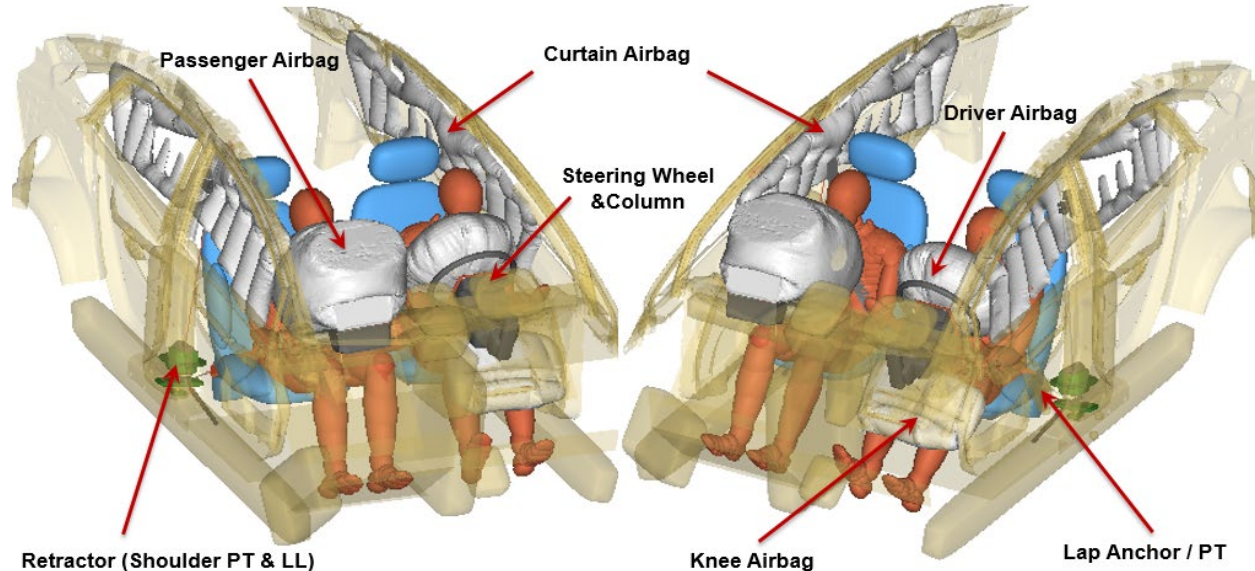


Figure 11: Baseline MADYMO model

The reason of selecting MADYMO models rather than FE models for this study was because an FE model is generally more computational expensive (more than 100 times) than a MADYMO model. Considering that design optimizations would be conducted, MADYMO models will provide faster solutions than the FE models. The seat belt and air bag models in MADYMO are FE-based, and have been validated at the component level previously by ZF. In this study, the vehicle and occupant models along with the restraint models were validated against results from the baseline sled tests, the US-NCAP full frontal barrier tests and FMVSS No. 208 unbelted barrier tests. The focus of the validation was to match the ATD kinematics and major injury measures of the head, neck, chest, and lower extremities to the test results. CORrelation and Analysis (CORA) scores were used to quantitatively evaluate the match between the tests and simulations for the associated time history curves.

### 3.3 Validation Against Baseline Oblique Sled Tests

The MADYMO THOR-NT v2.0 model with the SD-3 shoulder, along with the vehicle and restraint models, were used to validate against the baseline sled tests. Because a knee air bag was available in the driver side of the surrogate B-segment vehicle, the validity of the vehicle interior and restraint model were dominated by the accuracy of the seat belts and air bags, as well as the accuracy of the THOR model.

To validate the baseline models, simulations were set up to match the four baseline test configurations. The model validation process followed those from previous studies, in which sensitivity analyses and optimization techniques were used to validate ATD responses against multiple sled tests (Hu, Klinich, Reed, Kokkolaras, & Rupp, 2012; Wu, Hu, Reed, Klinich, & Cao, 2012; Hu, Rupp, Reed, Kurt, Lange, & Adler, 2015). In the current study, design of experiments (DoE, a data collection and analysis tool) was used to determine model parameters that matched THOR's responses in the four test conditions. ModeFRONTIER (ESTECO), a multi-objective optimization software program, was coupled with MADYMO to conduct the DoE.

THOR's responses that were used for model validation included the same measurements mentioned in Task 1. To evaluate the level of correlation between the test and simulation results, statistical assessments were performed in addition to visual comparisons between test and simulation results. CORA scores were calculated for each measurement of the tests to evaluate the model quality. A CORA score of 1.0 represents a perfect match between the test and simulation, while CORA score of 0.0 represents no correlation between the test and simulation results. More details about model evaluation can be found in previous work (Hu, Reed, Rupp, Fischer, Lange, & Adler, 2015).

Figures 12 to 15 show the occupant kinematics comparisons between the tests and simulations for the four baseline sled test conditions, namely the driver near-side, driver far-side, passenger near-side, and passenger far-side. Overall, the models provided high correlations to the baseline sled tests in terms of THOR's kinematics, especially the head, neck, and torso. These kinematics are important in design optimization because the high BrIC values and chest deflections are associated with the occupant kinematics (namely, occupants rolling off bag or rolling out of the belt).

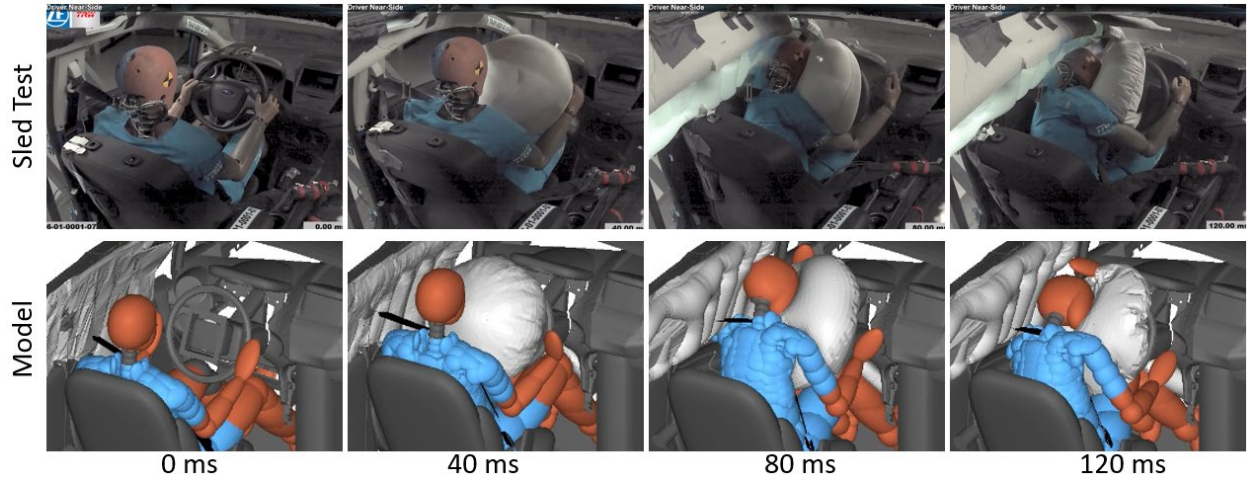


Figure 12: Model validation – Driver near-side baseline oblique

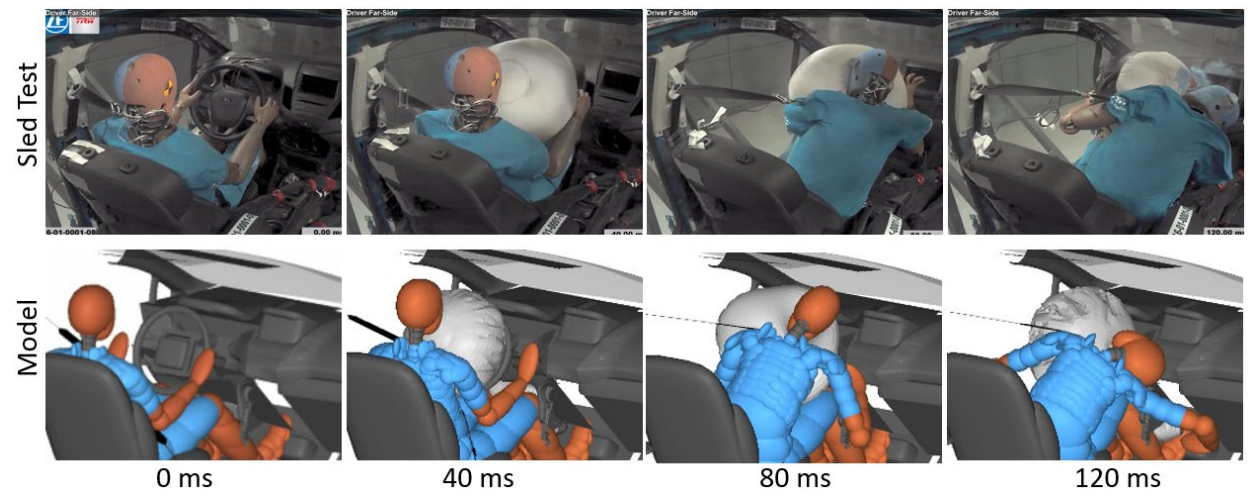


Figure 13: Model validation – Driver far-side baseline oblique

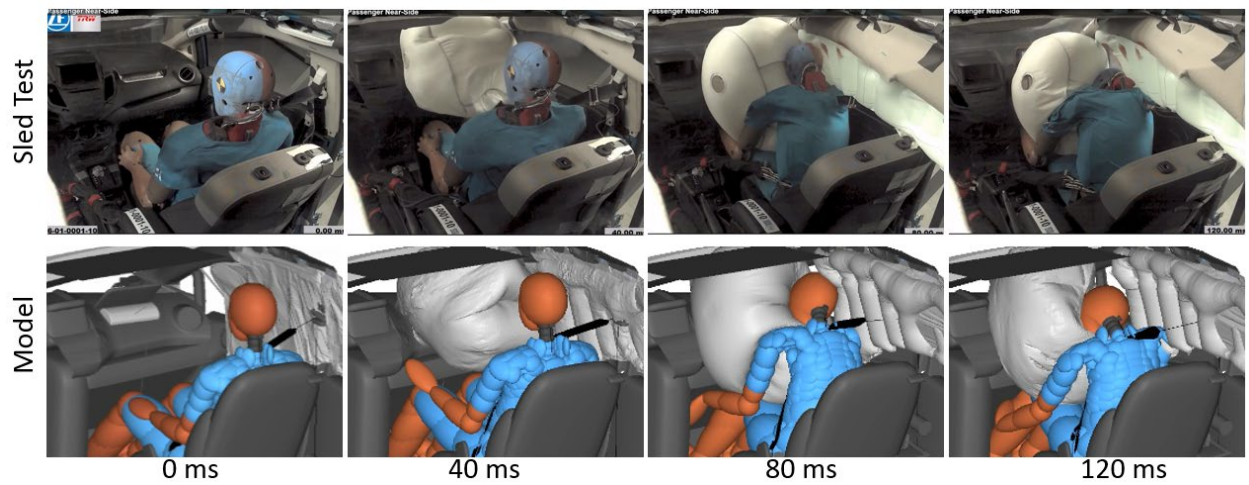


Figure 14: Model validation – Passenger near-side baseline oblique

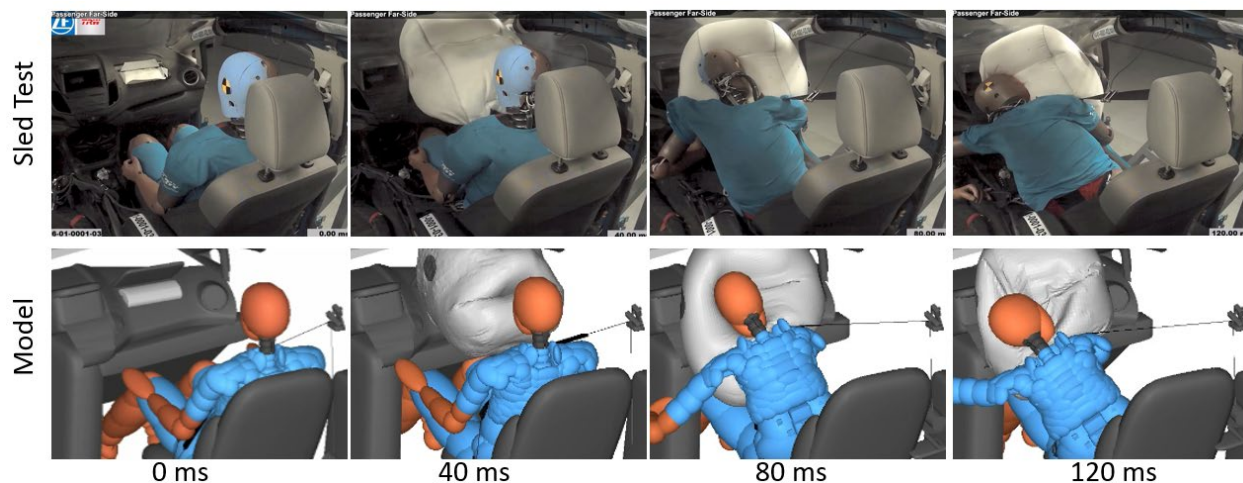


Figure 15: Model validation – Passenger far-side baseline oblique

Table 6 summarizes the injury measure comparisons between the baseline tests and simulations. All the model-predicted injury measures were consistent to the sled tests, except for the chest deflection, in which the model consistently under-estimated the maximal chest deflection.

Time history comparisons between the baseline sled tests and simulations as well as the CORA scores are shown in Appendix B.

Table 6: Injury measure comparison between the baseline sled tests and the simulations

Injury Measures	Unit	Driver Near-side		Driver Far-side		Passenger Near-side		Passenger Far-side	
		Test	Sim	Test	Sim	Test	Sim	Test	Sim
<b>HIC15</b>	-	448	814	496	596	773	587	332	560
<b>BrIC</b>	-	1.04	1.51	1.73	1.79	0.97	1.18	1.54	1.66
<b>Neck T</b>	kN	2.07	3.87	2.66	3.70	2.53	2.36	1.94	2.65
<b>Neck C</b>	kN	0.32	0.22	0.27	0.84	0.06	0.32	0.22	0.76
<b>Old Nij</b>	-	0.94	1.29	1.73	1.51	1.17	1.13	0.81	1.07
<b>Chest D</b>	mm	48.5	35.2	44.2	29.1	57.7	31.6	48.5	37.6
<b>Femur F</b>	kN	3.92	4.21	3.35	3.86	2.09	2.43	3.01	4.95

### 3.4 Validation Against US-NCAP or FMVSS No. 208 Crash Tests

To validate the models against US-NCAP and FMVSS No. 208 crash tests, the crash pulses and vehicle pitch angles measured in the tests were used as the pre-scribed motion of the vehicle model. A HIII 50th male ATD model and a HIII 5th female ATD model in MADYMO were used for the simulations. The ATDs were positioned based on the ATD positions and postures measured in the tests. Figures 16 to 19 show the occupant kinematics comparisons between the tests and simulations in US-NCAP and FMVSS No. 208 frontal crash conditions, including belted 50th HIII in driver side and belted 5th HIII in front seat passenger side under 56 km/h (35 mph) full frontal barrier crash, and unbelted 5th HIII in driver and front seat passenger sides

under 40 km/h (25 mph) full frontal barrier crash. The air bag deployment and occupant kinematics matched well against the test results.

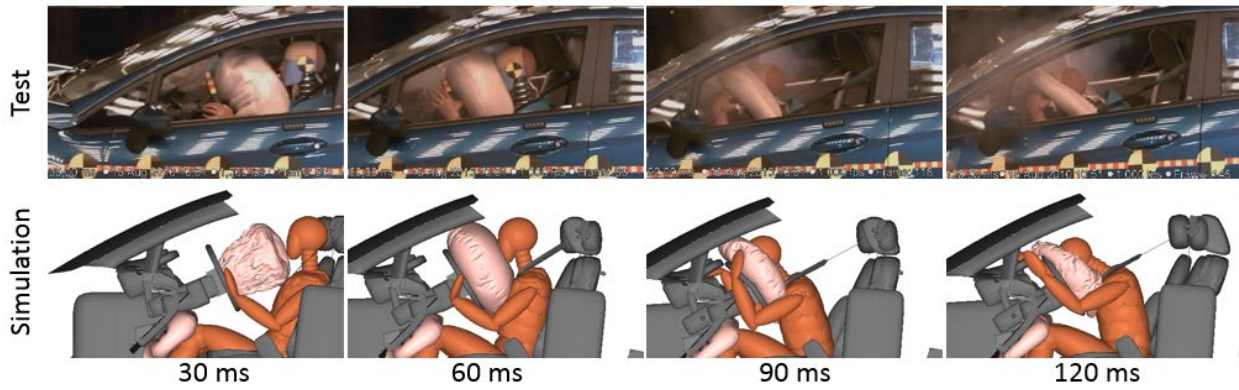


Figure 16: Model validation – US-NCAP driver 50th HIII

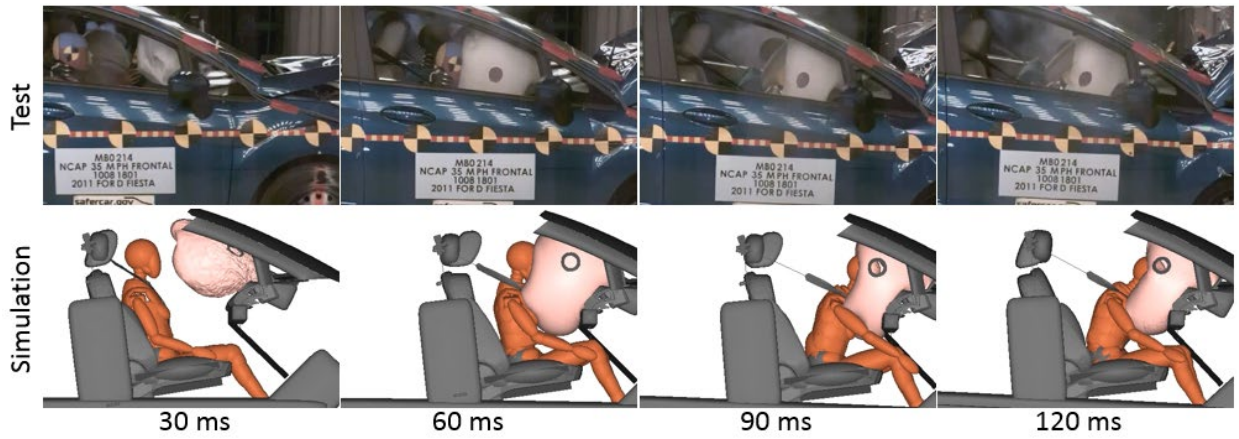


Figure 17: Model validation – US-NCAP passenger 5th HIII

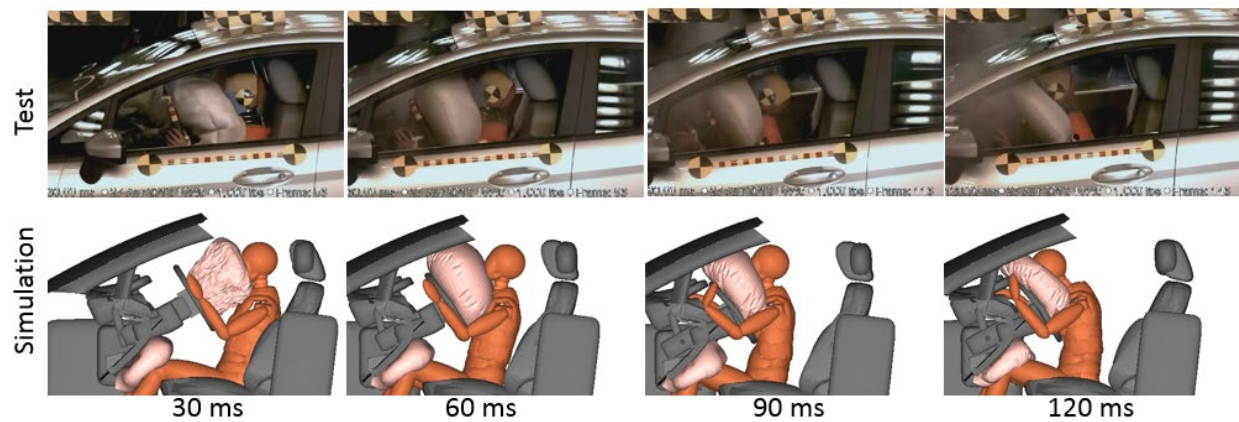


Figure 18: Model validation – FMVSS No. 208 unbelted driver 5th HIII

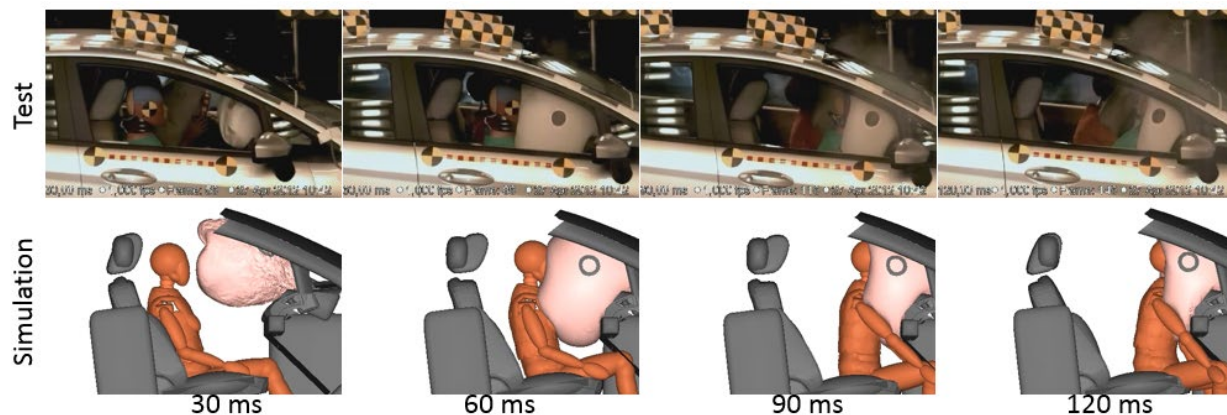


Figure 19: Model validation – FMVSS No. 208 unbelted passenger 5th HIII

The injury measures in the tests and simulations in both the US-NCAP and FMVSS No. 208 unbelted full frontal barrier crash conditions are shown in Table 7. For most of the injury measures, good correlations were achieved between the tests and simulations. However, the 5th female HIII ATD model over-estimated the chest deflections in all the three crash conditions, although none of those predictions were over 80 percent of the chest Injury Assessment Reference Value (IARV).

The time history comparisons between the US-NCAP/FMVSS No. 208 tests and corresponding simulations as well as the associated CORA scores are shown in the Appendix B.

Table 7: Injury measure comparison between the US-NCAP/FMVSS No. 208 tests and simulations

Injury Measures	Unit	US-NCAP		US-NCAP		FMVSS 208 Unbelted		FMVSS 208 Unbelted	
		Driver 50th HIII		Passenger 5th HIII		Driver 5th HIII		Passenger 5th HIII	
		Test	Sim	Test	Sim	Test	Sim	Test	Sim
<b>HIC15</b>	-	148	346	291	241	46	30	62	64
<b>Head Acc</b>	g	43	61	61	51	33	25	29	29
<b>Neck T</b>	kN	1.1	1.46	0.69	0.57	1.05	0.68	0.27	0.03
<b>Neck C</b>	kN	0.2	0.21	0.53	0.95	0.16	0.18	0.37	0.9
<b>NIJ</b>	-	0.25	0.25	0.52	0.43	0.60	0.34	0.40	0.54
<b>Chest Acc</b>	g	39	43	43	54	30	32	28	30
<b>Chest D</b>	mm	21	22	11	25	18	44	2	14
<b>Left Femur F</b>	kN	1.84	1.18	2.42	2.54	2.14	1.72	3.91	3.47
<b>Right Femur F</b>	kN	1.55	1.42	1.82	1.37	1.74	2.12	3.79	3.37

## **4 Modified restraint Selection**

### **4.1 Goal**

The goal of Task 3 was to identify different combinations of modified prototype restraint system technologies that had the potential to help improve occupant protection in oblique crash tests.

### **4.2 Rationale**

By using the above baseline sled tests and simulation models, safety concerns for both driver and passenger in both the near-side and far-side crashes were identified. These scenarios drove the technologies that were selected for the modified restraint system.

Potential safety concerns that were focused on include the following.

- For near-side occupants, potential:
  - Head contact with the door or A-pillar
  - Large lateral head rotation due to air bag interaction
  - High chest deflection values
- For Far-side occupants, potential:
  - Occupant rollout from the shoulder belt
  - Head contact with the IP
  - Large lateral head rotation due to air bag interaction
  - High chest deflection values

It was expected that protecting the far-side occupant would have been a challenging aspect of the study because a re-design of curtain air bag could help the restraint performance for near-side occupants. In a far-side oblique crash, both the driver and front-seat passenger tended to move toward the center of the IP, which was not covered by any air bag. Depending on the size and performance of the driver air bag and passenger air bag, a single air bag in the center of the IP might not have been a viable solution. It was also possible that the driver protection in far-side oblique crash would also pose a challenge, as a redesign of the original driver air bag could be considered to improve occupant protection.

The study focused on the traditional 3-point seat belts with additional air bags and/or air bag re-designs. However, other seat belt systems (4-point belts, reversed 3-point belt, etc.) were also investigated, as they may provide different solutions for helping to improve occupant protection in oblique crashes without additional air bags.

### **4.3 Countermeasures for Oblique Crashes**

The countermeasures considered in this study are shown in Figure 20, which included 3-point belt, X-type 4-point belt, rerouted 3-point belt, relocated D-ring, dynamic locking tongue (DLT), anchor pre-tensioner, digressive load limiting, and switchable load limiting at the retractor, anchor, and buckle locations, knee air bag (KnAB), SQS driver air bag (DAB), cone DAB, inboard support side air bag (SAB), driver support air bag, V13 passenger air bag (PAB), V64 PAB, clapper PAB, parallel cell PAB, kickstand PAB, three small chamber curtain air bag (CAB), two medium chamber CAB, single large chamber CAB, and buckle CAB. The study did not evaluate consumer acceptance or the receptivity of original equipment manufacturers to installing these technologies.

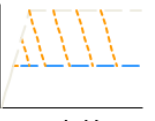
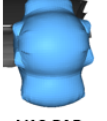
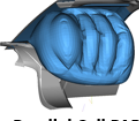
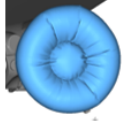
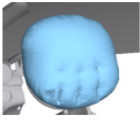
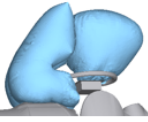
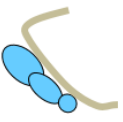
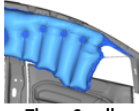
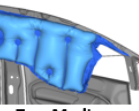
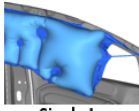
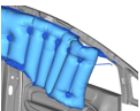
<b>Seat Belts</b>	 Reversed 3-Pt Belt	 'X-type' 4-Pt Belt	 Suspender 4-Pt Belt	 Rerouted 3-Pt Belt	 Relocated Retractor	
<b>Seat Belts Pre-tensioner (PT) Load Limiter (LL)</b>	 DLT	 Buckle PT	 Anchor PT	 Digressive LL	 Switchable LL	 Suspender Switchable LL
<b>Passenger Air Bags</b>	 V64 PAB	 V13 PAB	 Clapper PAB	 Parallel Cell PAB	 Kickstand PAB	
<b>Driver/Knee/Side Air Bags</b>	 Cone DAB	 SQS DAB	 Support Bag	 Inboard SAB	 Passenger KnAB	
<b>Curtain Air Bags</b>	 Three Small Chamber CAB	 Two Medium Chamber CAB	 Single Large Chamber CAB	 Buckle CAB		

Figure 20: An overview of countermeasures for oblique crashes

#### 4.3.1 3-point belt with pretensioner, load limiting, and dynamic locking tongue

The restraint components investigated for this study were intended to engage the occupant earlier in the event. This allowed the restraint systems to help absorb the energy with a lower load preventing occupant contact to the interior of the vehicle. Pre-tensioners were used to engage the occupant earlier by moving the onset of belt force earlier in the crash. A retractor pre-tensioner, the most common form of pre-tensioner, helped to reduce the slack in the shoulder portion of the belt system. An anchor pre-tensioner reduced slack in the lap portion, and a buckle pre-tensioner added pretension to both the lap and shoulder segments of the belt system. These pre-tensioner configurations were evaluated in this study.

In general, once a pre-tensioner fires, the load limiting in the retractor manages belt force to reduce loads on the occupant, allowing the occupant to travel further while absorbing energy. A constant load limiting (CLL) provides a constant belt force as the webbing is pulled out of the retractor at the controlled load regardless of the occupant size or crash pulse. In general, a larger occupant or more severe crash pulse will produce larger excursions. In contrast, a DLL has an initial peak in the belt force, but reduces to a constant lower level as the webbing is extracted. As a result, the increased belt force may limit the higher excursions at the beginning of the crash. Similarly, an SLL has two levels of constant belt forces, which can be switched during the crash depending on the occupant size and loading condition.

The DLT is a design consisting of a seat belt tongue (the plate which fastens into the buckle) with a rotating cam and a concealed spring. The DLT allows webbing to pass freely through the

tongue when buckling. However, in the event of hard braking or a crash resulting in greater than about 45 N of force on the belt, the DLT clamps the webbing to prevent the webbing transferring from the shoulder belt portion to the lap belt portion. It works with other seat belt technologies, helping to reduce loads on the occupant's chest.

#### *4.3.2 X-type 4-point belt*

A further option with a belt system was the 4-point belt. Two retractor pre-tensioners with CLLs positioned the belt over both shoulders, crossed over the chest, and two DLTs anchored the lap portion. Since this system engaged both shoulders, the load was more evenly distributed over the occupant with a more symmetrical loading to the left and right sides of the body than with a three-point belt.

#### *4.3.3 Suspender 4-point belt*

An alternative to the X-type 4-point belt is the suspender 4-point belt. This concept is similar to an airline flight attendant's jump seat, where the seat belt positions over the occupant's shoulders from behind the head and anchors on each side of the hip without crossing on the chest as the X-type system. This puts more of the restraining forces on the shoulders/clavicles and less on the ribs.

#### *4.3.4 Reversed 3-point belt*

The reverse 3-point belt system is the same as a conventional belt system except the routing of the belt is mirrored. Instead of the shoulder belt positioning over the outboard shoulder, it positions over the inboard shoulder. On far side impacts, the shoulder belt has the tendency to roll off the outboard shoulder. Having the belt on the inboard shoulder, the occupant will be moving inward and thus helping to keep the belt on the shoulder.

#### *4.3.5 Rerouted 3-point belt*

The re-routed belt is similar with the reversed 3-point belt in that it has the belt is going over the inboard shoulder. However, with this configuration the belt anchorages are not mirrored. The buckle, anchor, and D-ring are all in the same location as the standard belt configuration.

#### *4.3.6 Cone driver air bag*

The cone driver air bag can provide larger coverage than a typical driver air bag, which has the potential to help reduce the THOR lateral rotation in an oblique impact.

#### *4.3.7 SQS driver air bag*

The SQS (Square Shaped) driver air bag is a bag concept that has a conical back panel and a round front panel. This can provide added depth to the air bag without adding to the overall diameter. Since THOR tends to position further away from the steering wheel, the SQS driver air bag can help close that larger gap and provide earlier restraint.

#### *4.3.8 Driver support bag*

The driver support bag works with the driver air bag to restrain the occupant during oblique loading. Typically, in oblique tests, the occupant will roll off the driver air bag potentially causing the head to twist and contact the instrument panel. The driver support bag can provide improved lateral support to catch the head as it rolls off the driver air bag, thus minimizing the twist and head contact to the instrument panel.

#### *4.3.9 V13 PAB*

The V13 PAB (passenger air bag) is like the SQS driver bag, in that it provides a deeper bag so that the head restraint can start earlier. The portion of the bag that contacts the head consists of a series of pleats to increase bag volume. When the bag is inflated, the pleats unfold and balloon out towards the occupant.

#### *4.3.10 Clapper PAB*

The clapper PAB is a standard shaped bag except that has small pillows (or clappers) on each side of the head. These pillows are designed to help support the head as it rolls off the bag.

#### *4.3.11 Parallel Cell PAB*

The parallel cell bag is a PAB concept that uses a series of vertical cells on the front face of the air bag to give a non-uniform restraint to the head. The size of the cells varies across the bag. The bigger the cells result in larger restraining forces applied to the occupant and vice versa for the smaller cells. The larger cells are positioned on the left and right side of the bag while the smaller cells are in the middle. In an oblique impact, as the occupant moves to the left or right sides of the bag, the head will contact the larger cells. These larger cells can provide a higher force to counteract the occupant movement to the left or right.

#### *4.3.12 Kickstand PAB*

The kickstand PAB adds an external chamber, the kickstand, to the inboard side of a traditional 3-piece PAB. The kickstand uses the IP to provide support so the PAB does not roll inboard during a far-side impact. The kickstand will also provide lateral support to the inboard side of the occupant's head on a far-side impact, reducing the rotation of the head. Because the kickstand is attached to the side panel of the 3-piece PAB, it does not affect the normally seated occupants or near-side oblique impacts.

#### *4.3.13 Three-small-chamber CAB*

The three-small-chamber curtain air bag (CAB) is a baseline CAB that has three small chambers in the car forward section of the bag. It is also FMVSS 226 compliant.

#### *4.3.14 Buckle curtain*

The buckle CAB extends the car forward portion of the curtain. This extra material is then buckled by an exterior tether on the outboard side of the curtain. The buckled portion of the CAB extends inboard into the vehicle and interacts with the occupant's head. The buckle will reduce the outboard excursion of the head and will minimize the head rotation.

#### *4.3.15 Two-medium-chamber CAB*

The two-medium-chamber CAB is a modified version of the three-small-chamber CAB. The three small chambers in the car forward section are reconfigured into two medium chambers. By increasing the size of the chambers, the chambers became thicker and provided earlier support to the side of the occupant's head, therefore reducing the lateral head rotation.

#### *4.3.16 Single large chamber*

The single-large-chamber CAB is modified version of the three-small-chamber CAB. The three small chambers in the car forward section are reconfigured into one single large chamber. This

large chamber was much thicker than the three small chambers. The thicker chamber is capable of earlier and increased lateral head support to help reduce lateral head rotation.

Table 8 shows the baseline design specifications of the seat belt and air bag technologies.

Table 8: Design specifications of the seat belt and air bag technologies

Seat Belt	Specifications		
CLL/DLL/SLL	The 8, 9.5, 10, 10.5, and 12 mm torsion bars are approximately equivalent to 1.8, 3, 3.6, 4.2, and 4.5 kN load limiting.		
Pre-tensioner(s)	The stroke of the buckle pre-tensioner ranges from 15 to 45 mm, while the strokes of the anchor and retractor pre-tensioner range from 40 to 80 mm.		
PAB	Volume (L)	Inflator Output (kPa)	Vent Size (mm)
Baseline	110	440	2x65
Clapper	140	530	2x50
V13	140	440	2x65
V64	112	440	2x65
Parallel Cell	160	530	2x50
Kickstand	154	530	1x65
DAB	Volume (L)	Inflator Output (kPa)	Vent Size (mm)
Baseline	43	170	2x30
Cone DAB	58	205	2x30
SQS DAB	53	205	2x45
DAB Support	75	205	1x30

## 5 Develop, Validate, and Tune Proposed Restraint Systems

### 5.1 Goals

The goals of Task 4 were to develop and validate the physical prototype and computational models for the proposed restraint technologies, and to combine and tune these technologies to help minimize the injury risks in oblique crashes.

### 5.2 Design Optimization Method Overview

Figure 21 illustrates the process used for developing, validating and optimizing the proposed modified prototype restraint systems. First, models of modified restraint components were developed and validated against physical component test data. Such models were integrated into the baseline vehicle/occupant model in a parametric simulation study for design optimization. The model-predicted modified restraint designs were fabricated and tested in sled tests. If some of the design concepts did not show reduced injury potential in the tests, they were removed from the list of the final modified restraint designs. If the design performance was not as good as the model predictions but had the potential for further tuning, the models would be re-validated against the sled tests with prototype modified restraints and another parametric study and design optimization were conducted.

Examples of the model validations against sled tests with modified restraints are shown in the Appendix C.

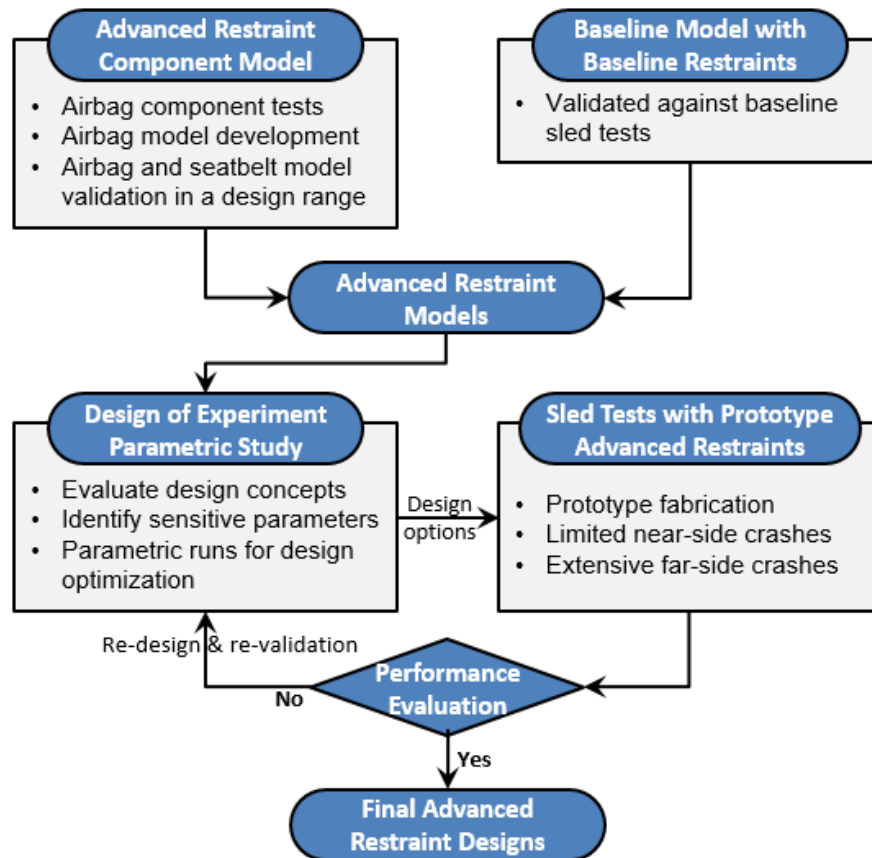


Figure 21: Design optimization process

The objective function and constraints that were used to perform design optimizations for each of the four oblique crash conditions are shown in equation 1. The joint probability of injuries for THOR ( $P_{joint\_THOR}$  in equation 2) in the oblique crash condition were considered as the objective function, while the final design had to ensure similar or reduced injury potential in US-NCAP frontal crash than the baseline vehicle, and compliance of the FMVSS No. 208 unbelted and OOP requirements. The driver and passenger air bags affected injury risks in both near-side and far-side oblique crashes; thus the same driver and passenger air bags were used in both near-side and far-side oblique crashes. However, the study was focused on the far-side occupant safety. Therefore, parametric studies were conducted for far-side occupants first, and then the same driver or passenger air bag was used for the near-side occupants for further evaluations. No parametric study was conducted for the near-side oblique crashes.

$$\left\{ \begin{array}{l} \min_{\mathbf{X}} [P_{joint\_THOR}(\mathbf{X}) \text{ in oblique crash}] \\ \text{s. t.} \\ \text{All THOR injury measures} < 80\% \times IARV \\ \text{NCAP frontal crash performance} \geq \text{Baseline performance} \\ \text{FMVSS 208 Unbelted performance} < 80\% \times IARVs \\ \text{FMVSS 208 5F OOP performance} < 80\% \times IARVs \\ \text{FMVSS 208 6YO OOP performance} < 80\% \times IARVs \\ \mathbf{X}_l \leq \mathbf{X} \text{ (Design parameters)} \leq \mathbf{X}_u \end{array} \right. \quad (1)$$

$$P_{joint\_THOR} = 1 - (1 - P_{head}) \times (1 - P_{neck}) \times (1 - P_{chest}) \times (1 - P_{abdomen}) \times (1 - P_{acetabulum}) \times (1 - P_{femur}) \quad (2)$$

The probability of each body region was calculated based on the NHTSA injury risk curves (NHTSA, 2015). The injury measures and the associated injury risk curves used in this study are shown in Table 9. The  $P_{head}$  equaled the highest injury probability predicted by HIC15 and BrIC. It should be noted that the  $N_{ij}$  calculation defined in Table 9 used different critical values from those defined by NHTSA in the current US-NCAP tests (Eppinger et al., 1999). Therefore, in this study, “Old  $N_{ij}$ ” refers to the  $N_{ij}$  defined in the current US-NCAP tests, while “New  $N_{ij}$ ” refers to the  $N_{ij}$  defined in Table 9. The  $P_{joint\_THOR}$  values were all calculated based on the “New  $N_{ij}$ ”.

To enable the large-scale parametric analyses, an automated computer program was developed using a combination of MADYMO and ModeFRONTIER. Similar work has been done in previous studies (Hu, Reed, Rupp, Fischer, Lange, & Adler 2017; Hu, Wu, Reed, Klinich, & Cao, 2013).

The purpose of this series of sled tests was to explore the effectiveness of modified prototype restraint design concepts with preliminary modified design parameters for better protecting occupants in four oblique crash conditions described in Task 1. Furthermore, this series of tests provided additional test data to further validate the computational models. Because the modified restraint models were only validated at the component level, sled test results were necessary to further validate the accuracy of those models with the occupant and vehicle models. In general, without this validation, the safety performance of modified restraint systems may not be accurately predicted by the computational models alone. Therefore, at least 1-2 iterations (Figure 21) were necessary to ensure that the model-predicted tuned designs were indeed the tuned designs based on the test results. In the following sections, the performance for each of the proposed modified prototype restraint designs are presented through computational modeling and sled testing.

Table 9: Injury measures and the associated injury risk curves

Criterion [ref]	Calculation	Variable	Variable Definition	Risk Function
$HIC_{15}$ [NCAP Final Decision Notice, 2008]	$HIC_{15} = \left[ (t_2 - t_1) \left[ \frac{1}{(t_2 - t_1)} \int_{t_1}^{t_2} a(t) dt \right]^{2.5} \right]_{max}$	$t_1$ $t_2$ $a(t)$	Beginning of time window in $s$ End of time window in $s$ Head CG resultant acceleration in $g$ , $x$ , $y$ , $z$ components filtered at CFC1000	$p(AIS \geq 3) = \Phi \left[ \frac{\ln(HIC_{15}) - 7.45231}{0.73998} \right]$
$BrIC$ [Takhounts, 2013]	$BrIC = \sqrt{\left( \frac{\max( \omega_x )}{\omega_{xc}} \right)^2 + \left( \frac{\max( \omega_y )}{\omega_{yc}} \right)^2 + \left( \frac{\max( \omega_z )}{\omega_{zc}} \right)^2}$	$\omega_{[x,y,z]}$ $\omega_{[x,y,z]c}$ $\omega_{xc}$ $\omega_{yc}$ $\omega_{zc}$	Angular velocity of the head about the local [ $x$ , $y$ , or $z$ ] axis, in $rad/s$ , filtered at CFC60 Critical angular velocities in $rad/s$ 66.25 $rad/s$ 56.45 $rad/s$ 42.87 $rad/s$	$p(AIS \geq 4) = 1 - e^{-\left( \frac{BrIC - 0.523}{0.647} \right)^{1.8}}$
$N_{ij}$ [Injury Criteria for the THOR 50 <sup>th</sup> Male ATD]	$N_{ij} = \frac{F_z}{F_{zc}} + \frac{M_y}{M_{yc}}$	$F_z$ $F_{zc}$ $M_y$ $M_{yc}$	Z-axis force measured at upper neck load cell in $N$ , filtered at CFC600 Critical force (tension or compression) in $N$ [4200/-6400] Y-axis moment measured at upper neck load cell $Nm$ , filtered at CFC600 Critical moment (flexion or extension) in $Nm$ [88.1/-117]	$p(AIS \geq 2) = \frac{1}{1 + e^{(4.3085 - 5.4079N_{ij})}}$ $p(AIS \geq 3) = \frac{1}{1 + e^{(4.9372 - 4.5294N_{ij})}}$
Multi-point Thoracic Injury Criterion – Peak Resultant Deflection	$R_{max} = \max(UL_{max}, UR_{max}, LL_{max}, LR_{max})$ where $\left[ \frac{U/L/R/L}{R/L} \right]_{max} = \max \left( \sqrt{[L/R]X_{[u/l]s}^2 + [L/R]Y_{[u/l]s}^2 + [L/R]Z_{[u/l]s}^2} \right)$	$R_{max}$ $\left[ \frac{U/L}{R/L} \right]_{max}$	Overall peak resultant deflection in $mm$ Peak resultant deflection of the [upper/lower   left/right] quadrant in $mm$	$p(AIS \geq 3) = 1 - e^{-\left( \frac{R_{max}}{59.865} \right)^{2.7187}}$
[Injury Criteria for the THOR 50 <sup>th</sup> Male ATD]		$\left[ \frac{L/R}{Y/Z} \right]_{[u/l]s}$	Time-history of the [left/right] chest deflection along the [ $X/Y/Z$ ] axis relative to the [upper/lower] spine segment in $mm$ , filtered at CFC180	
Abdomen Compression [Injury Criteria for the THOR 50 <sup>th</sup> Male ATD]		$\delta_{max}$	Peak X-axis deflection of the left or right abdomen in $mm$ , filtered at CFC600	$p(AIS \geq 3) = \frac{1}{1 + e^{(7.849 - 0.0886\delta_{max})}}$
Peak Resultant Acetabulum Force [Injury Criteria for the THOR 50 <sup>th</sup> Male ATD]	$F_{AR} = \sqrt{F_x^2 + F_y^2 + F_z^2}$	$F_{AR}$	Peak resultant acetabulum force in $kN$ , $x$ , $y$ , $z$ , components filtered at CFC600	$p(Hip\ fracture) = \Phi \left[ \frac{\ln(1.429F_{AR} - 1.6058)}{0.2339} \right]$
Femur Axial Load [Injury Criteria for the THOR 50 <sup>th</sup> Male ATD]		$F_{LC}$	peak compressive Z-axis force, in $kN$ , measured in the left and right femur, filtered at CFC600	$p(AIS \geq 2) = \frac{1}{1 + e^{5.7949 - 0.6748F_{LC}}}$

### 5.3 Relocated D-ring/Retractor, Reversed, or Rerouted 3-point Belts

One concern for protecting occupants in far-side oblique crash was that the 3-point belt tended to roll off the shoulder quickly, which adversely affected the occupant kinematics. This had the potential to cause higher head and torso rotations, as a result increasing the occupant head and chest injury risks. Therefore, a variety of modified 3-point belt designs were investigated with the baseline air bag design using the computational models and sled tests. These designs included 3-point belts with a wide range of relocated D-rings/retractors, reversed 3-point belt, and rerouted 3-point belt.

### 5.3.1 Parametric simulations

Different D-ring locations for both the driver and passenger in far-side oblique crashes were simulated with the baseline driver and passenger air bags. Because in the baseline tests the D-ring was on the B-pillar and away from the shoulder, the intuition was that moving the D-ring close to the shoulder may have helped the seat belt stay on the shoulder longer in a far-side impact than the original setup. Therefore, the D-ring location varied in the fore-aft (0, 100, 200 mm more rearward), lateral (0, 30, and 60 mm more inboard), and vertical (0, 80, and 160 more downward) directions, which resulted in 27 (3x3x3) simulations for both the driver and passenger in far-side oblique crash condition.

The sensitivity of the D-ring locations for different injury measures for both the driver and passenger in far-side oblique crash are shown in Tables 10 and 11. Overall, moving the D-ring locations more rearward and inboard, closer to the occupant, had resulted in less occupant rotation, as well as lower injury potential in the head, neck, and chest compared to the baseline D-ring locations. This was true for both driver and passenger far-side impacts.

Table 10: D-ring location sensitivities on injury measures for driver far-side impact

D-ring	HIC	BrIC	Old Nij	NeckT	ChestD	FemurF
More rearward	↓	↓	↓	↓	○	○
More inboard	↓	↓	↓	↓	↓	○
Lower	↓	↑	↓	↓	○	○
Baseline Ranking *	27	8	26	27	10	10
Lowest LIP Design **	(200, 60, -160)	(200, 60, -80)	(200, 30, -160)	(200, 60, -160)	(200, 60, -80)	(200, 0, -160)

\* Ranking was based on a total of 27 designs with 1 having the lowest injury potential (LIP)

\*\* Reported as location changes in (X, Y, Z) in mm, from (0, 0, 0) to (200, 60, -160)

Table 11: D-ring location sensitivities on injury measures for passenger far-side impact

D-ring	HIC	BrIC	Old Nij	NeckT	ChestD	FemurF
More rearward	↓	↓	↓	↓	↓	○
More inboard	↓	↓	↓	↓	↓	○
Lower	↑	○	↓	↓	↑	↑
Baseline Ranking *	24	27	27	26	10	2
Lowest LIP Design **	(200, -30, 0)	(200, -60, 0)	(0, -60, -160)	(200, -30, -0)	(200, -30, -0)	(0, 0, -160)

\* Ranking is based on a total of 27 designs with 1 having the LIP

\*\* Reported as location changes in (X, Y, Z) in mm, from (0, 0, 0) to (200, -60, -160)

Figure 22 shows the occupant kinematic comparison between the baseline and relocated D-ring locations with the lowest injury potential based on the MADYMO simulations. With more rearward and inboard D-ring locations, the seat belt stayed on the shoulder longer than the baseline D-ring location. This trend was found for both driver and passenger far-side impacts. Although large head and torso rotations still existed with the simulated relocated D-ring locations, most injury measures reduced slightly from the baseline tests, as shown in Table 12. The higher BrIC values were not addressed by the relocated D-ring, which may be improved by modified air bag designs.

The safety performances in the near-side oblique crashes with the adjusted D-ring locations were also simulated. Most injury measures reduced with the relocated D-ring locations compared to the baseline tests (Table 12), even though large lateral head rotations still existed, which could be improved by modified air bag designs.

It should be noted that the MADYMO THOR model under-estimated the chest deflections in all baseline oblique sled tests, which may have affected the trends presented in Table 12.

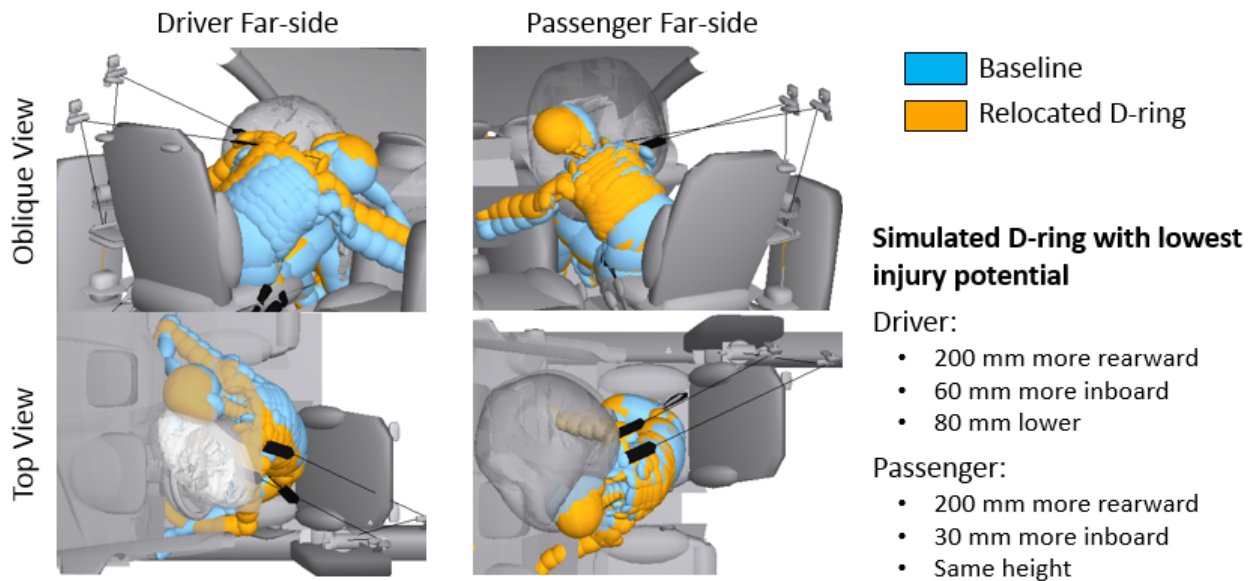


Figure 22: Simulated occupant kinematics between baseline and relocated D-ring locations

Table 12: Injury measure reductions by using more rearward and inboard D-ring locations

Injury Measures	Driver Near-side		Driver Far-side		Passenger Near-side		Passenger Far-side	
	Baseline	Relocated	Baseline	Relocated	Baseline	Relocated	Baseline	Relocated
<b>HIC15</b>	100%	73%	100%	53%	100%	90%	100%	79%
<b>BrIC</b>	100%	79%	100%	91%	100%	111%	100%	90%
<b>NIJ</b>	100%	69%	100%	75%	100%	75%	100%	77%
<b>Neck T (N)</b>	100%	67%	100%	72%	100%	75%	100%	69%
<b>Chest D (mm)</b>	100%	87%	100%	95%	100%	94%	100%	86%
<b>Femur F (N)</b>	100%	103%	100%	100%	100%	101%	100%	103%

### 5.3.2 Sled Tests

Sled tests using one of the relocated D-ring/shoulder retractor locations from the above simulation study, a reversed belt, and a rerouted belt were conducted with a baseline driver air bag in the driver far-side oblique condition. The retractor load limiting was the same for all the tests, except that no actual D-ring was presented in the relocated retractor design and the reversed belt, which reduced the actual shoulder belt force slightly from the baseline test. The occupant kinematics and injury measures with these 3 modified 3-point belt, as well as the baseline test, are shown in Figure 23, and Table 13.

Overall, the “relocated retractor” and the “reserved belt” provided similar joint injury probabilities to the baseline tests. However, the chest deflection decreased from 45 mm in the baseline test to 35 mm with the relocated retractor. Such a decrease may have been attributed to the longer stay of belt on the shoulder and the slightly reduced shoulder belt force without the D-ring friction. On the other hand, the rerouted belt reduced the BrIC and chest deflection, and consequently reduced the joint injury probability from the baseline test. The reduced BrIC may have been a result of a belt loading direction that prevented the occupant’s torso from moving more laterally, which lead to lower rotation in the torso and head/neck. In addition, the belt routed to the opposite side of the shoulder allowed loads on the shoulder rather than the chest, which reduced the maximal chest deflection.

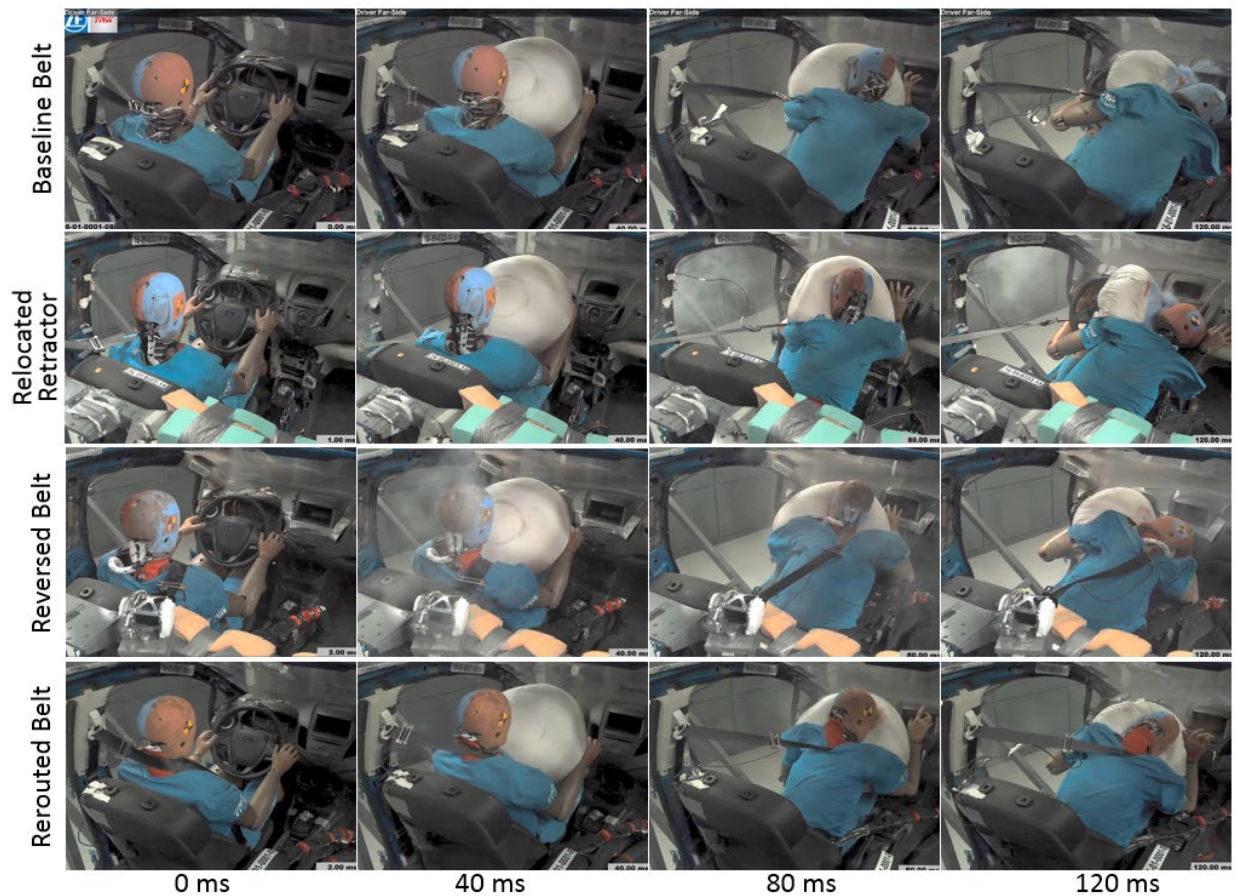


Figure 23: Occupant kinematics with different 3-point belt designs in driver far-side crash

Table 13: Injury measures with different 3-point belt designs in driver far-side crash

Series No.	Test No.	Restraint	Head		Neck		Chest		Abdomen		Acetabular		Femur		Pjoint
			HIC	BrIC	Old Nij	New Nij	R <sub>MAX</sub>	PCA Score	D <sub>max</sub> (L)	D <sub>max</sub> (R)	F <sub>max</sub> (L)	F <sub>max</sub> (R)	Comp (L)	Comp (R)	
16-01-0001	08	Baseline	496	1.73	1.00	0.58	45	5.22	71	75	2031	2476	3354	3185	0.980
16-09-0323	14	Relocated Retractor	518	1.80	0.83	0.48	35	4.33	Lost	64	2073	2400	3560	3010	0.979
16-05-0156	10	Reversed	515	1.67	1.07	0.63	43	6.23	79	76	2072	1709	3740	2820	0.975
16-01-001	09	Rerouted	504	0.86	1.14	0.69	29	3.74	85	83	3227	1624	3332	3954	0.785

## 5.4 Suspender 4-Point Belt and X-Type 4-Point Belt

### 5.4.1 Sled Tests

Sled tests with two X-type 4-point belts and a suspender 4-point belt were conducted with the baseline air bag in the driver far-side oblique crash condition. In each 4-point belt design two buckle pre-tensioners and two DLTs were used. Parametric simulations (explained later in this report) and previous experiences indicated that a higher potential for submarining may occur without buckle pre-tensioners for 4-point belt designs (Rouhana et al., 2003). The DLTs were used to help further reduce the pelvis and lower torso excursions to help reduce femur forces and chest deflections. In the X-type 4-point belt design #1, two CLLs, each with an 8-mm torsion bar, were used as the two shoulder belts; while in the X-type 4-point belt design #2 and the suspender 4-point belt, a CLL with 8-mm torsion bar was used for the left (outboard) shoulder belt and a CLL with 12-mm torsion bar was used for the right (inboard) shoulder belt.

The occupant kinematics of the sled tests for the three 4-point belts, as well as the baseline test, are shown in Figure 24. The occupant rotation in all three tests with 4-point belts were lower than the baseline test. The belt on the right (inboard) shoulder limited the occupant's lateral excursions, and in turn reduced lateral head rotations. The belts with uneven load limiting on the shoulder belts allowed the occupant's torso to rotate towards the impact direction, and reduced the lateral head rotations.

The injury measures of those tests are shown in Table 14. All three 4-point belts provided lower joint injury probability, BrIC, and Nij. There were slight reductions of HIC values with all three 4-point belts, but abdomen deflections, acetabular loads, and femur forces were almost unchanged from the baseline test. It was interesting to note that 4-point belt had the potential to reduce chest deflections as well, as those with X-type 4-point belt #1 and the suspender belt shown in Table 14. Based on the belt geometry, the suspender belt used the clavicles as the main loading path without touching the ribcage. The test results confirmed that the suspender belt could help reduce the chest deflections.

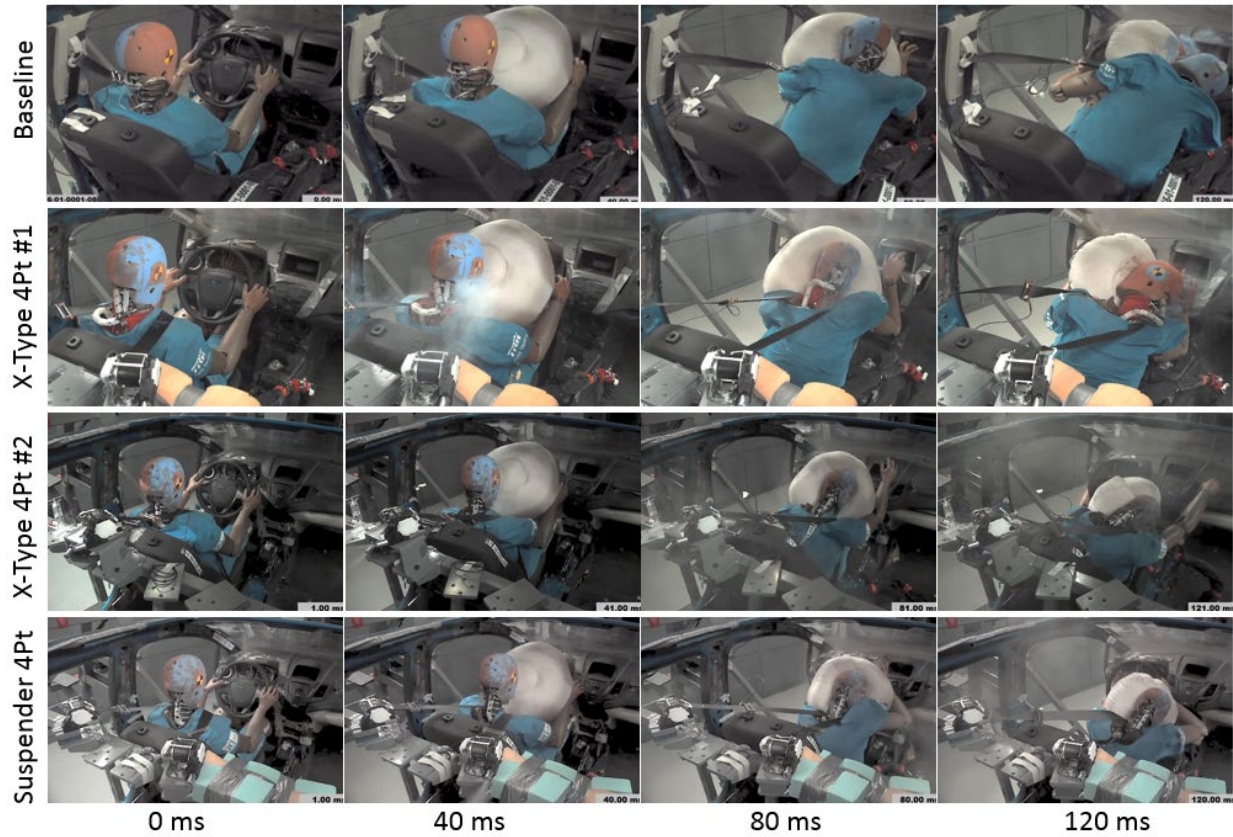


Figure 24: Occupant kinematics with different 4-point belt designs in driver far-side crash

Table 14: Injury measures with different 4-point belt designs in driver far-side crash

Series No.	Test No.	Restraint	Head		Neck		Chest		Abdomen		Acetabular		Femur		Pjoint
			HIC	BrIC	Old Nij	New Nij	R <sub>MAX</sub>	PCA Score	Dmax (L)	Dmax (R)	Fmax (L)	Fmax (R)	Comp (L)	Comp (R)	
16-01-0001	08	Baseline	496	1.73	1.00	0.58	45	5.22	71	75	2031	2476	3354	3185	0.980
16-05-0156	09	X-type 4-Point #1	425	1.31	0.58	0.34	38	5.25	74	79	1675	1331	3430	3620	0.877
16-09-0323	10	X-type 4-Point #2	343	0.71	0.65	0.39	49	5.36	71	Lost	1595	1644	3690	3100	0.600
16-09-0323	09	Suspender 4-Point	451	0.81	0.65	0.40	35	4.69	72	72	2399	1641	4570	3290	0.555

#### 5.4.2 Parametric Simulations

Given the potential of the suspender 4-point belt, several sets of parametric simulations were conducted to investigate the effects from shoulder retractor locations, retractor load limiting, buckle pre-tensioner, and DLT on the ATD kinematics and injury measures in the driver far-side impacts.

The first parametric study (first eight simulations in Table 15) focused on the buckle pre-tensioner and DLT effects. A pair comparison between with and without buckle pre-tensioner and DLT showed that adding buckle pre-tensioners and DLTs had the potential to reduce almost all injury measures, except for neck compression. It was also shown that having uneven load limiting between the left and right shoulders had the potential to reduce the BrIC value. Specifically, a higher load limiting on the right side (the side of impact) allowed the torso to rotate laterally to the right, which avoided the large lateral head rotation.

The second parametric study (six simulations in the middle of Table 15) focused on the D-ring/retractor locations for the suspender belts. Pair comparisons with locations A, B, and C, shown in Figure 25, showed that D-ring/retractor locations closer to the neck (Location C) provided slightly lower BrIC values. Once again, the simulations demonstrated that uneven load limiting could result in lower values for almost all injury measures.

The third parametric study (four simulations at the bottom of Table 15) focused on the load limiting effects. In these simulations, the load limiting for the left shoulder was fixed at a lower level, while the load limiting for the right shoulder varied. New D-ring/retractor location (Location D) was used, which was similar to Location C but the D-ring/retractor were laterally closer. The larger load limiting differences between the left and right shoulders tended to provide lower BrIC and chest deflections.

In summary, the parametric studies suggested that buckle pre-tensioner and DLT were necessary for the suspender 4-point belt in driver far-side oblique impact condition; D-ring/retractor closer to each other and close to the neck/shoulder could have been beneficial; and higher load limiting on the striking side of the shoulder than the non-striking side is needed to control the ATD torso rotation.

Table 15: Parametric simulations with different suspender 4-point belt configurations

Study	Dring Location	Retractor Torsion Bar Diameter & Type		Buckle PT & DLT	Head		Neck			Chest	Femur		
					HIC15	BrIC	T (N)	C (N)	Old NIJ	Dmax (mm)	Left F (N)	Right F (N)	
Buckle PT and DLT Effects	A	R8mm	L8mm	DLL	No	1383	1.33	4140	507	1.87	35.8	5384	3569
	A	R10mm	L10mm	DLL	No	561	0.96	2841	691	1.38	34.5	5812	4058
	A	R10mm	L8mm	DLL	No	949	1.03	3851	510	1.82	38.7	5647	3900
	A	R12mm	L8mm	DLL	No	760	0.99	3374	507	1.6	37.6	5988	4009
	A	R8mm	L8mm	DLL	Yes	661	0.97	2329	1043	1.06	30.5	2982	2162
	A	R10mm	L10mm	DLL	Yes	391	0.82	2064	1033	0.92	26.2	3075	2254
	A	R10mm	L8mm	DLL	Yes	535	0.75	2172	1015	1.01	27.0	2961	2135
	A	R12mm	L8mm	DLL	Yes	534	0.7	2211	1026	1.13	28.0	2966	2171
D-ring Location Effects	A	R8mm	L8mm	DLL	Yes	661	0.97	2329	1043	1.06	30.5	2982	2162
	A	R12mm	L8mm	DLL	Yes	534	0.7	2211	1026	1.13	28.0	2966	2171
	B	R8mm	L8mm	DLL	Yes	556	1.07	2241	1212	1.00	37.3	3033	2044
	B	R12mm	L8mm	DLL	Yes	381	0.77	2228	1220	1.08	31.0	2986	1965
	C	R8mm	L8mm	DLL	Yes	447	0.95	1991	1062	0.91	33.1	3004	2061
Load limit Effects	C	R12mm	L8mm	DLL	Yes	411	0.73	1857	1036	1.00	23.8	3053	1992
	D	R8mm	L8mm	CLL	Yes	317	1.47	2283	777	0.94	40.0	3279	2156
	D	R9mm	L8mm	CLL	Yes	306	1.22	1620	777	0.81	39.3	3319	2136
	D	R10.5mm	L8mm	CLL	Yes	281	0.83	1425	779	0.78	30.4	3260	2095
	D	R12mm	L8mm	CLL	Yes	345	0.73	1608	770	0.86	28.5	3353	2067

Note: The D-ring locations are shown in Figure 25. Higher torsion bar diameter is associated with higher load limiting, but the relationship between them is not linear.

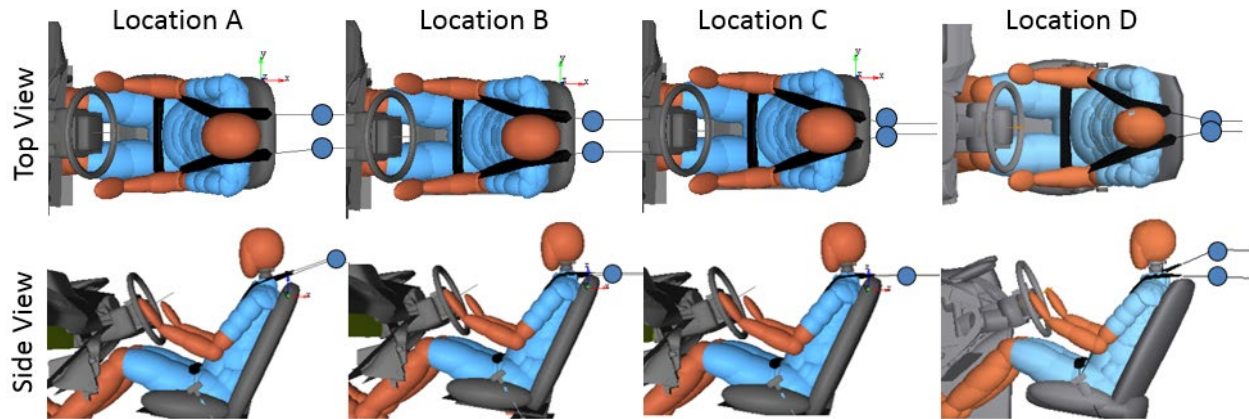


Figure 25: D-ring locations in the parametric simulation study

### 5.5 Various Driver Air Bags

Various driver air bag designs, including the cone bag, cone bag+trampoline/support, inboard SAB, and multiple versions of DAB+support bag, were tested in the driver far-side oblique impact condition. The ATD kinematics are shown in Figure 26, and the injury measures are shown in Table 16.

Overall, the cone bag, cone bag+trampoline/support, and inboard SAB did not show reduced ATD head rotation and injury measures compared to the baseline sled test. It was anticipated that the cone bag or cone bag+trampoline/support may have provided large coverage for the potential head contact, and in turn prevent the head from rotating off the edge of the air bag. However, because it was the steering wheel that generated the impact stiffness change between the air bag and the ATD's head, a wider air bag, even with supports behind the bag, did not provide enough stiffness to prevent the lateral head rotation. Therefore, the opportunity to reduce the lateral head rotation was not to widen the driver air bag, but to reduce the lateral head excursion or support the head from the side. The inboard SAB was designed to reduce the lateral ATD excursion. However, because lateral ATD excursion occurred toward the end of the impact, the inboard SAB design did not reduce the lateral ATD motion enough to reduce the head lateral rotation. On the other hand, the DAB support bag was designed to support the head from the side, which helped prevent a large lateral head rotation. As shown in Figure 26 and Table 16, the DAB support bag changed the head motion during the impact, and consequently reduced the BrIC and Nij from the baseline test.

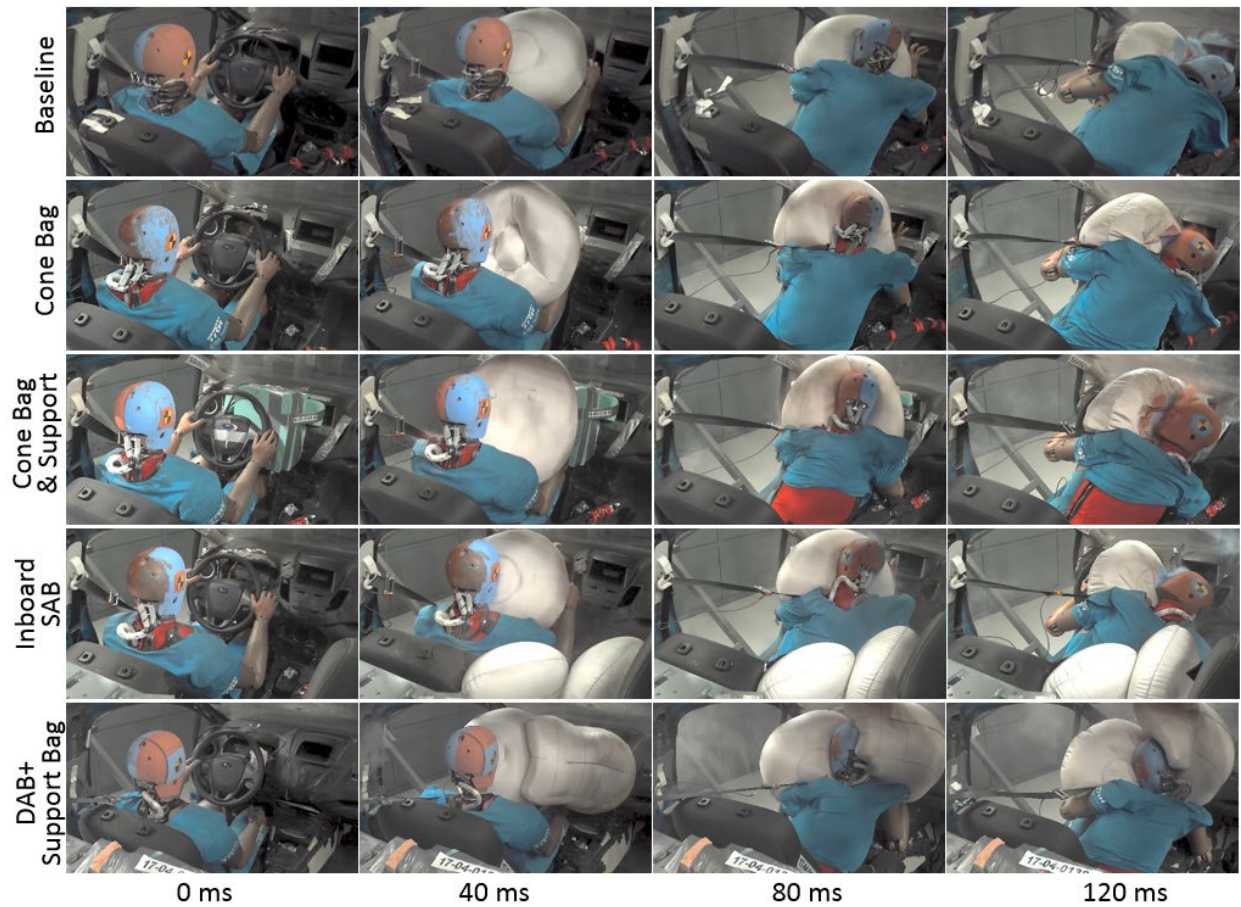


Figure 26: Occupant kinematics with different DAB designs in driver far-side crash

Table 16: Injury measures with different DAB designs in driver far-side crash

Series No.	Test No.	Restraint	Head		Neck		Chest		Abdomen		Acetabular		Femur		Pjoint
			HIC	BrIC	Old Nij	New Nij	R <sub>MAX</sub>	PCA Score	Dmax (L)	Dmax (R)	Fmax (L)	Fmax (R)	Comp (L)	Comp (R)	
16-01-0001	08	Baseline	496	1.73	1.00	0.58	45	5.22	71	75	2031	2476	3354	3185	0.980
16-05-0156	07	Cone	528	1.64	1.30	0.77	39	5.01	69	81	2527	1777	3470	3960	0.975
16-05-0156	08	Cone+ Trampoline/ Support	738	1.72	0.64	0.38	33	4.71	68	78	2577	1946	2500	3220	0.975
16-05-0156	11	Inboard SAB	548	1.82	0.97	0.57	43	5.18	Lost	77	2030	2154	3130	3180	0.987
17-04-0138	07	DAB+ Support Bag	582	0.97	0.53	0.31	36	5.95	46	Lost	2083	1429	2966	1802	0.573

Note: Several versions of DAB+support bag were tested. Only the design with the lowest injury potential is shown in this table.

## 5.6 Various Passenger Air Bags

Various passenger air bag designs, including parallel cell bags, V13 PAB, kickstand bags, and V64 PABs were tested in the passenger far-side impact condition. The ATD kinematics are shown in Figure 27, and the injury measures are shown in Table 17. The kickstand bag was tested with baseline D-ring location as well as a relocated D-ring/retractor.

Overall, all the modified passenger air bag designs showed the potential to reduce the occupant's injury measures, especially the BrIC value. The lateral head rotation was reduced by the special-design feature in each of the modified PAB designs, while the relocated D-ring/retractor provided additional help to keep the belt on the ATD's shoulder. The kickstand bag with the relocated D-ring/retractor provided the lowest injury potential to the ATD. Specifically, the additional chamber in the kickstand bag provided a lateral support to the head, which reduced the lateral head rotation and led to a lower BrIC value. At the the same time, the relocated D-ring/retractor helped reduce the chest deflection, which was similar to what had been discussed for the driver far-side impact in section 5.3.

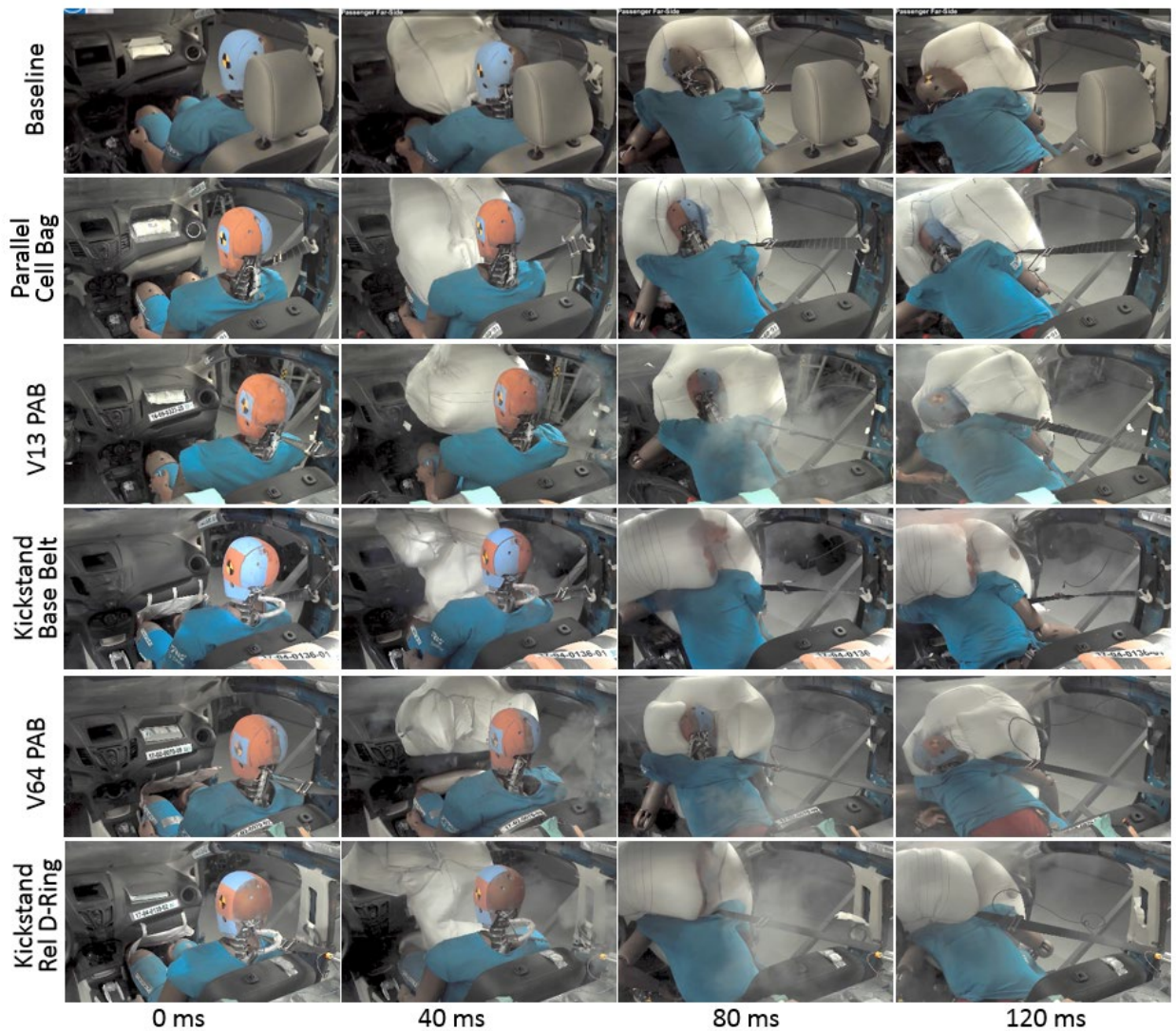


Figure 27: Occupant kinematics with different PAB designs in passenger far-side crash

Table 17: Injury measures with different PAB designs in passenger far-side crash

Series No.	Test No.	Air Bag	Belts	Head		Neck		Chest		Abdomen		Acetabular		Femur		Pjoint
				HIC	BrIC	Old Nij	New Nij	R <sub>MAX</sub>	PCA Score	Dmax (L)	Dmax (R)	Fmax (L)	Fmax (R)	Comp (L)	Comp (R)	
16-01-0001	03	Baseline	Base	332	1.55	0.81	0.47	50	6.36	82	75	1657	4430	3010	990	1.00
16-09-0323	06	Parallel Cell Bag	Base	667	0.80	0.74	0.45	54	6.86	67	66	1222	4268	3730	1400	0.972
16-09-0323	20	v13 PAB	Base	248	1.08	0.58	0.34	43	5.77	66	Lost	1853	4571	3330	1030	0.970
17-04-0136	01	Kickstand	Base	549	0.93	0.86	0.52	47	6.22	47	Lost	3231	3255	3629	3855	0.878
17-02-0070	09	v64	Rel	335	0.96	0.63	0.38	36	Lost	Lost	65	3170	3120	3984	2704	0.801
17-04-0138	02	Kickstand	Rel	378	0.62	0.71	0.43	33	5.08	29	27	2179	2388	3520	3737	0.447

Note: Base= B-Pillar mounted D-Ring/SLL, Rel= Relocated D-ring/DLL. A few versions of each modified PAB designs were tested. Only the design with the lowest injury potential is shown in this table.

## 5.7 Knee Air Bag

In the baseline sled tests, a knee air bag was equipped for the driver side but not the passenger side. As a result, there were higher acetabular loads for the passenger. The right acetabulum sustained a high load, which resulted in more than 60 percent of the injury potential. To address this, a variety of knee air bags, including a generic KnAB, a large-top KnAB, and a narrow/deep KnAB, were introduced and tested. The ATD lower-extremity kinematics are shown in Figure 28, and the acetabular and femur loads are shown in Table 18.

Overall, all knee air bag designs reduced the acetabular loads, and increased the femur loads. However, the reduction in the injury probabilities of the acetabulum measured higher than the increase in the injury probabilities of the femurs. The narrow/deep KnAB provided the highest reduction of the acetabulum injury values due to the early engagement to the knee.

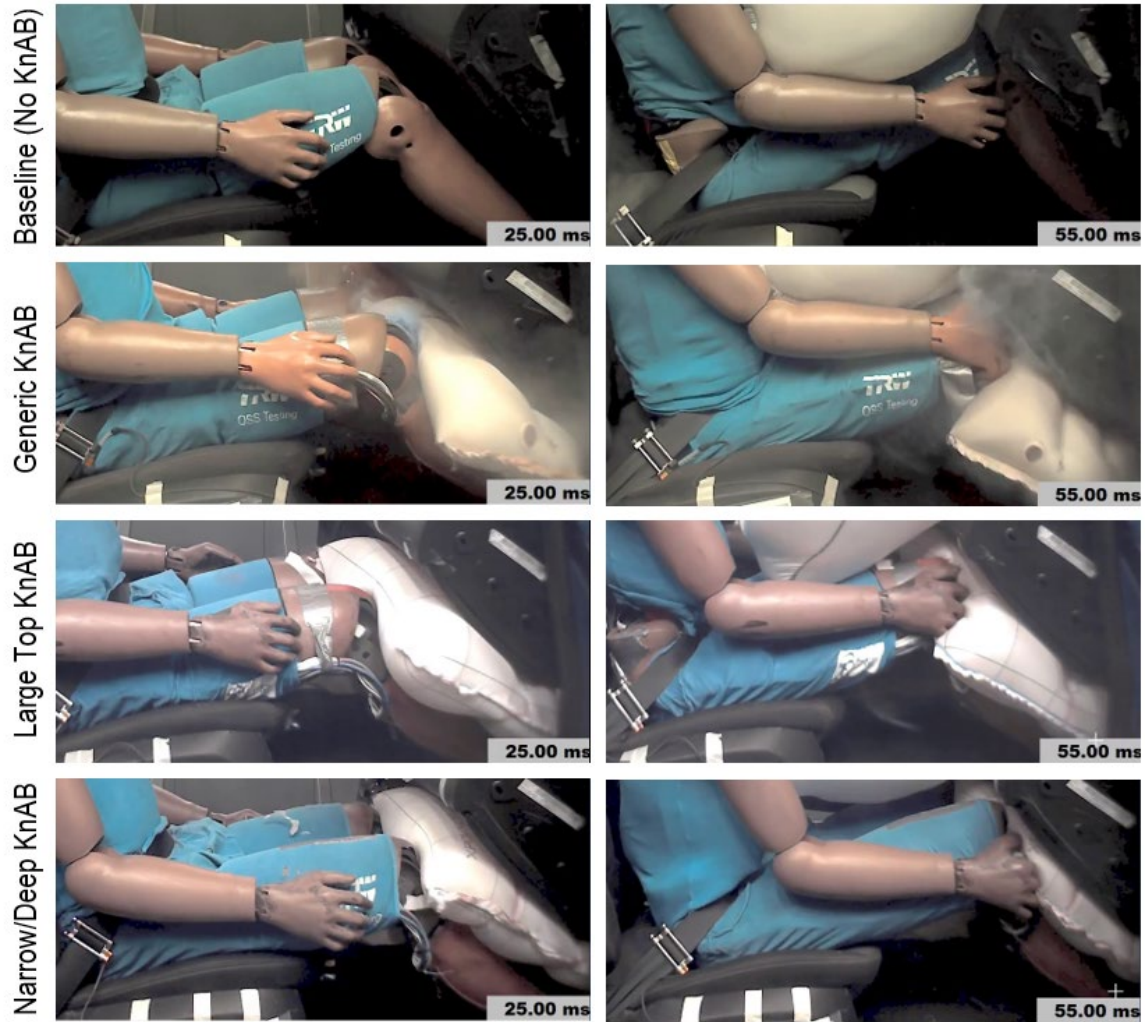


Figure 28: Occupant kinematics with different KnAB designs in passenger far-side crash

Table 18: Injury measures with different KnAB designs in passenger far-side crash

Series No.	Test No.	Air Bag	Acetabular		Femur		Injury Probability	
			Fmax (L)	Fmax (R)	Comp (L)	Comp (R)	Acetabulum	Femur
16-01-0001	03	Baseline (No KnAB)	1657	4430	3010	990	0.689	0.002
17-02-0070	01	Generic KnAB	3040	3550	1928	4366	0.268	0.029
17-04-0136	04	Large Top KnAB	2197	2802	3024	4043	0.035	0.024
17-04-00138	04	Narrow/Deep KnAB	1898	2395	3699	4202	0.005	0.026

## 5.8 Curtain Air Bags

Various curtain air bag designs, including buckle CAB, two medium chamber CAB, single large chamber, and telephone CAB, were tested in the driver near-side impact condition. All the sled

tests were equipped with a baseline 3-point belt, driver air bag, and knee air bag. The ATD kinematics are shown in Figure 29, and the injury measures are shown in Table 19.

The two-medium chamber CAB provided the lowest BrIC values among all the curtain air bag designs, and the reduction in BrIC was attributed to the reduction of lateral head rotation with lateral curtain air bag support.

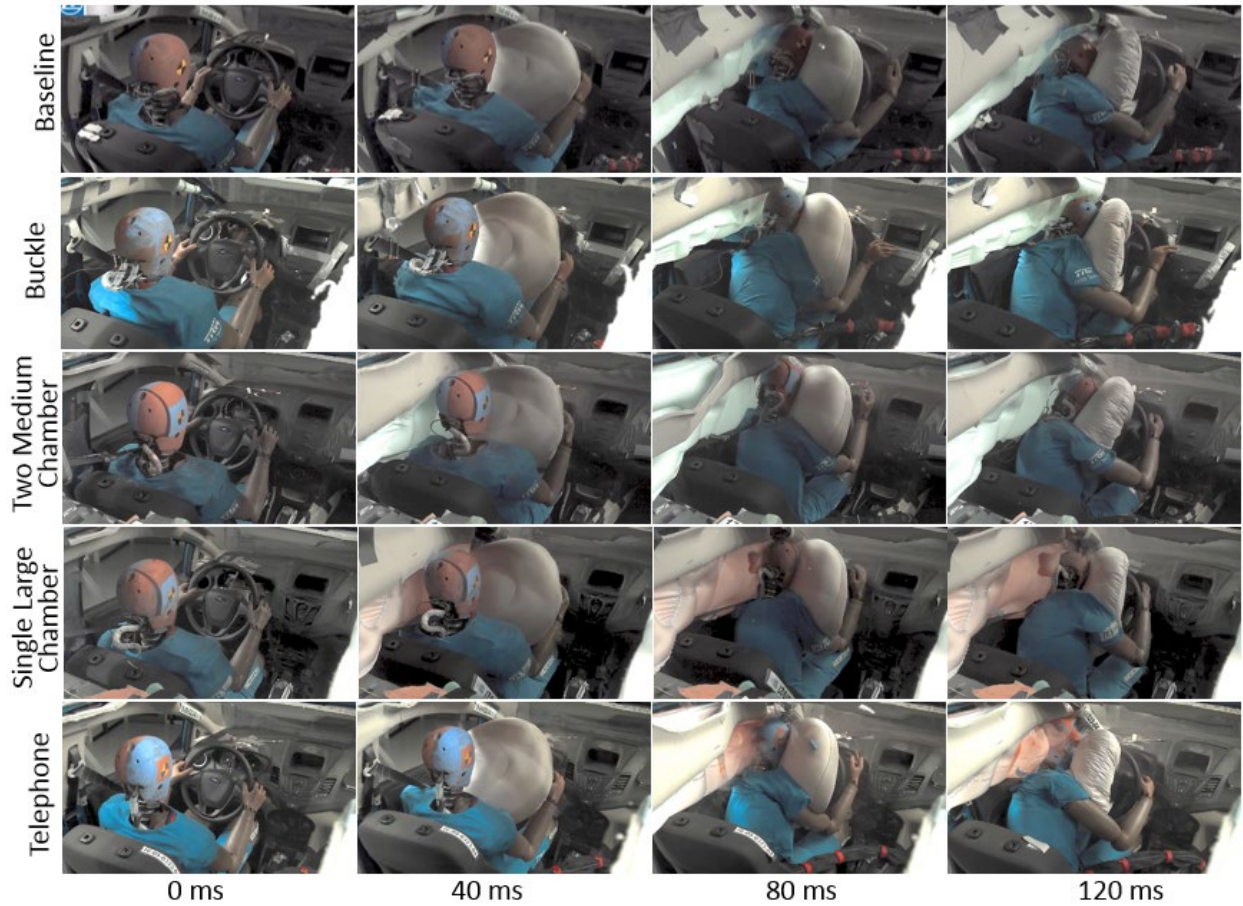


Figure 29: Occupant kinematics with different CAB designs in driver near-side crash

Table 19: Injury measures with different CAB designs in driver near-side crash

Series No.	Test No.	Restraint	Head		Neck		Chest		Abdomen		Acetabular		Femur		Pjoint
			HIC	BrIC	Old Nij	New Nij	R <sub>MAX</sub>	PCA Score	D <sub>max</sub> (L)	D <sub>max</sub> (R)	F <sub>max</sub> (L)	F <sub>max</sub> (R)	Comp (L)	Comp (R)	
16-01-0001	07	Baseline	448	1.04	0.94	0.56	51	6.62	73	76	1935	2065	1858	3916	0.809
16-05-0156	06	Buckle CAB	549	0.98	0.49	0.29	49	6.94	67	76	1978	2021	3010	4320	0.767
17-04-0136	05	Two Medium Chamber CAB	473	0.79	0.62	0.36	47	6.53	37	Lost	2660	2059	3938	3766	0.610
17-02-0070	27	Single Large Chamber	442	1.06	0.60	0.35	37	5.61	30	39	1950	1694	2826	2334	0.653
16-09-0323	04	Telephone CAB	407	1.06	0.85	0.50	46	5.72	58	75	2138	1095	3750	1960	0.789

Note: If multiple versions of a CAB design were tested, only the design with the lowest injury potential is shown in this table.

Various curtain air bag designs, including buckle CAB, two-medium-chamber CAB, single-large-chamber, telephone CAB, two-medium-chamber CAB with kickstand PAB, and single-large-chamber with kickstand PAB, were tested in the passenger near-side impact condition. All the sled tests were equipped with a 3-point belt with relocated D-ring/retractor, except for the two-medium chamber CAB design, in which the baseline 3-point belt was used. The ATD kinematics are shown in Figure 30, and the injury measures are shown in Table 20.

Like the driver near-side impacts, the two-medium chamber CAB provided the lowest BrIC values among all the curtain air bag designs, regardless of the passenger air bag (kickstand or baseline).

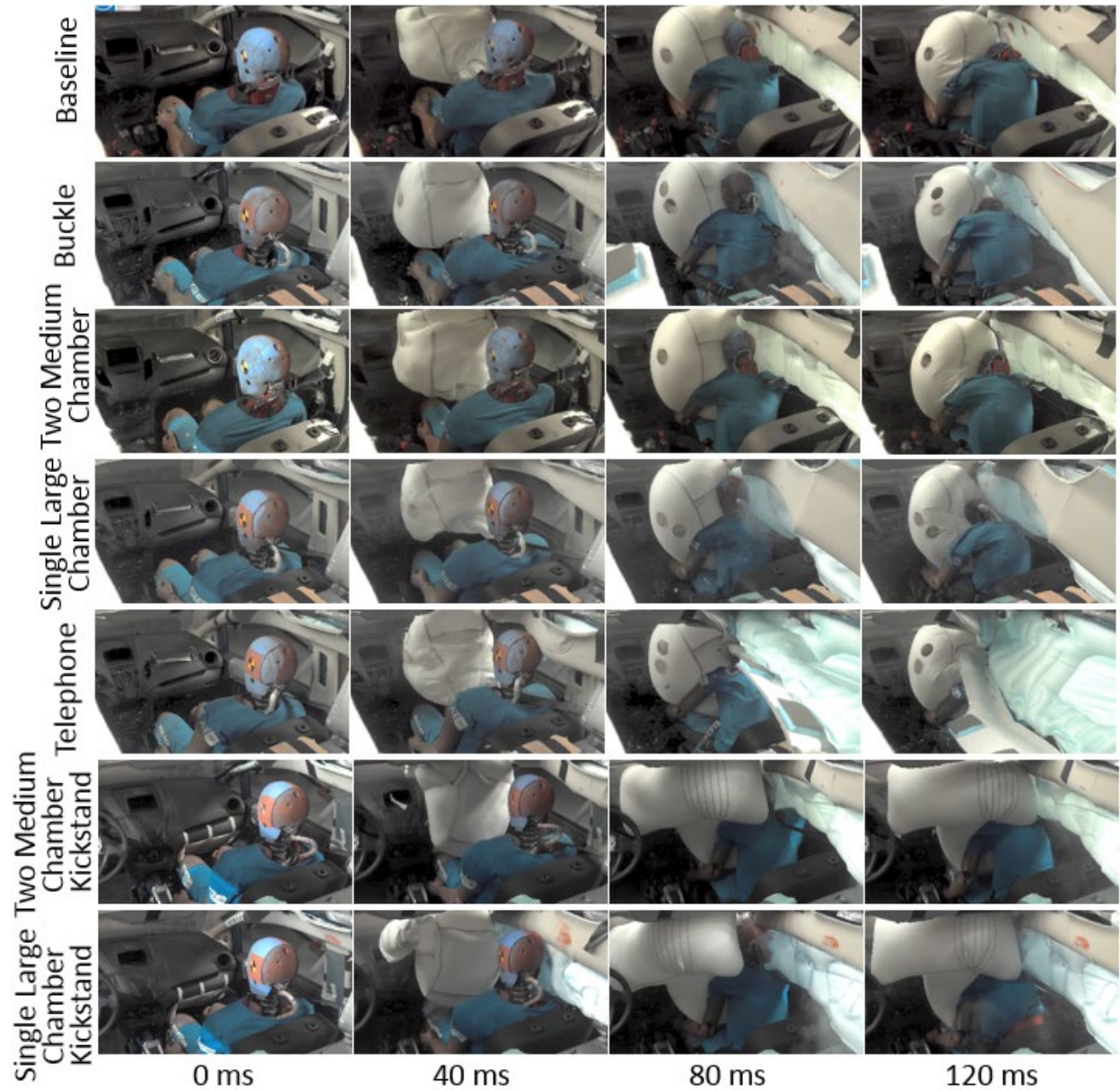


Figure 30: Occupant kinematics with different CAB designs in passenger near-side crash

Table 20: Injury measures with different CAB designs in passenger near-side crash

Series No.	Test No.	Air Bags	Head		Neck		Chest		Abdomen		Acetabular		Femur		Pjoint
			HIC	BrIC	Old Nij	New Nij	R <sub>MAX</sub>	PCA Score	D <sub>max</sub> (L)	D <sub>max</sub> (R)	F <sub>max</sub> (L)	F <sub>max</sub> (R)	Comp (L)	Comp (R)	
16-01-0001	10	Baseline	773	0.97	1.17	0.71	59	7.28	78	74	2840	2437	-2095	-1395	0.883
17-02-0070	19	Buckle CAB	666	1.03	1.03	0.62	44	7.25	43	39	3318	4072	1778	2002	0.925
16-01-0001	11	Two Medium Chamber CAB	548	0.75	0.84	0.51	63	7.71	86	76	3430	2912	-1220	-860	0.919
17-02-0070	20	Single Large Chamber	689	0.75	0.82	0.50	39	5.90	28	52	2631	2768	4154	1565	0.547
17-02-0070	21	Telephone CAB	170	1.25	2.27	1.33	42	7.36	50	50	3479	6558	2209	1788	1.000
17-04-0136	17	Two Medium Chamber CAB/Kickstand	444	0.68	1.03	0.62	47	6.33	45	Lost	1976	2147	2746	3766	0.538
17-04-0136	13	Single Large Chamber/Kickstand	420	0.90	1.03	0.62	45		42	Lost	2005	2234	3463	4444	0.652

Note: If multiple versions of a CAB design were tested, only the design with the lowest injury potential is shown in this table.

## 5.9 Air Bag and Seat belt Optimization in Driver Far-Side Impact

Several sets of parametric simulations were conducted to investigate the combination effects from driver air bag and seat belt designs on occupant protection in the driver far-side impact condition.

### 5.9.1 SQS air bag parameter optimization

The first parametric study was conducted with a 3-point belt with relocated D-ring and a variety of SQS air bag designs. Air bag design parameters that varied in this parametric study included the tether length (245, 275, 375, and 500 mm), vent diameter (30, 40, and 50 mm), and air bag depth (100%, 105%, and 110% from the baseline), which resulted in a total of 32 (4x3x3) simulations. Figure 31 shows the SQS design parameter effects on ATD injury measures, in which the injury measures were reported as the percentage of injury measures with the baseline restraint model shown in Table 6. The SQS air bag helped to reduce the BrIC, HIC, and even Nij. Longer tether and larger vent within the design range were beneficial for reducing the BrIC, HIC, and chest deflection. The air bag depth was insensitive for all the injury measures.

The second parametric study was conducted with a suspender 4-point belt (8 mm torsion bar on the left shoulder and 12 mm torsion bar on the right shoulder) and a variety of SQS air bag designs. Since the air bag depth was not likely to be sensitive, in this parametric study a fixed air bag depth of 110 percent from the baseline was used. The tether length (175, 275, 375, and 475 mm) and vent diameter (30, 40, 50, and 60 mm) were varied, which resulted in a total of 16 (4x4) simulations. Figure 32 shows the design parameter effects on the ATD injury measures. Similar to the results with the 3-point belt, longer tether and vent size, around 40-50 mm,

provided the lowest injury potential to the occupant with the suspender 4-point belt. It was also worth noting that the vent diameter posed conflicting effects on the BrIC and Nij.

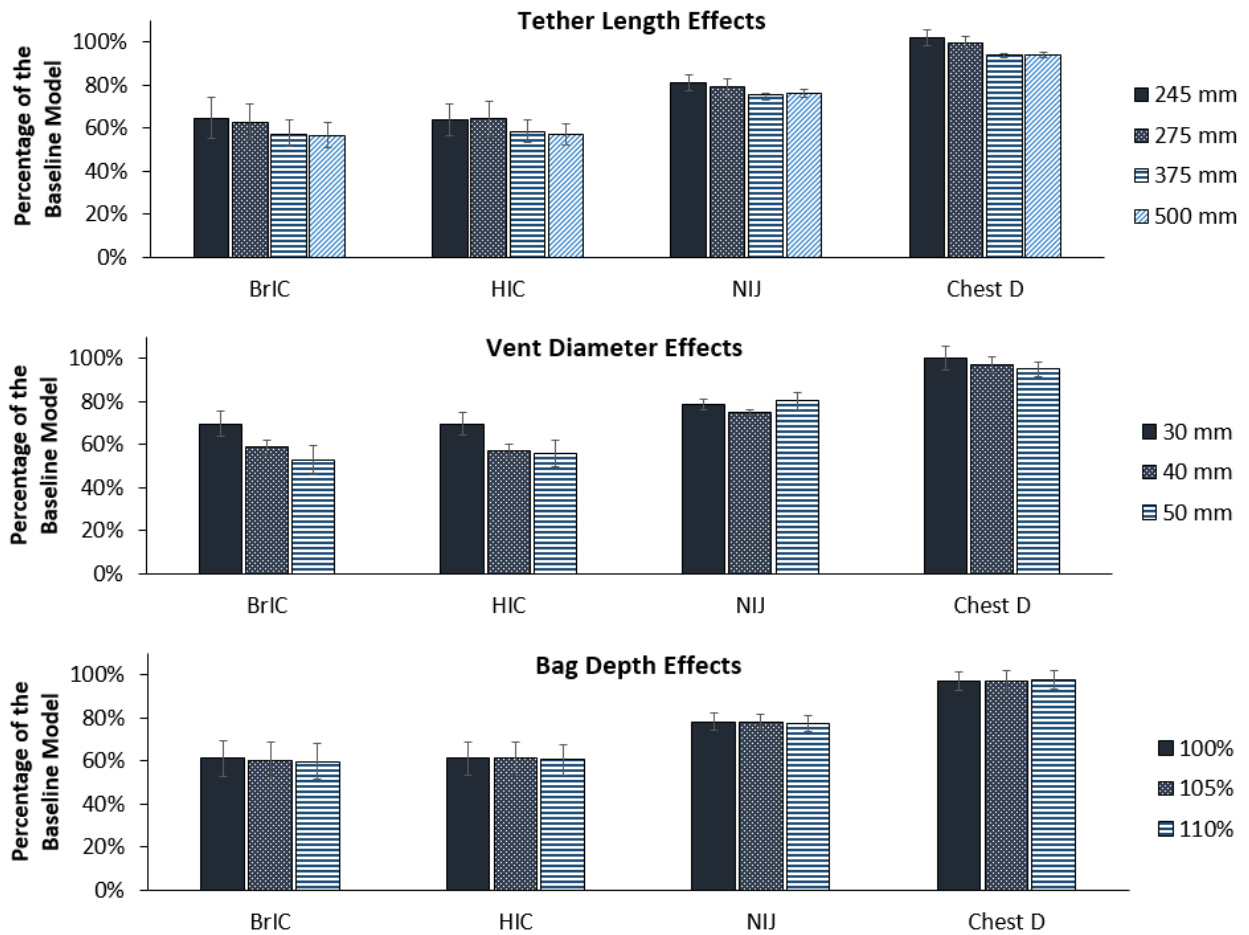


Figure 31: SQS DAB parameter effects on ATD injury measures with a 3-point belt

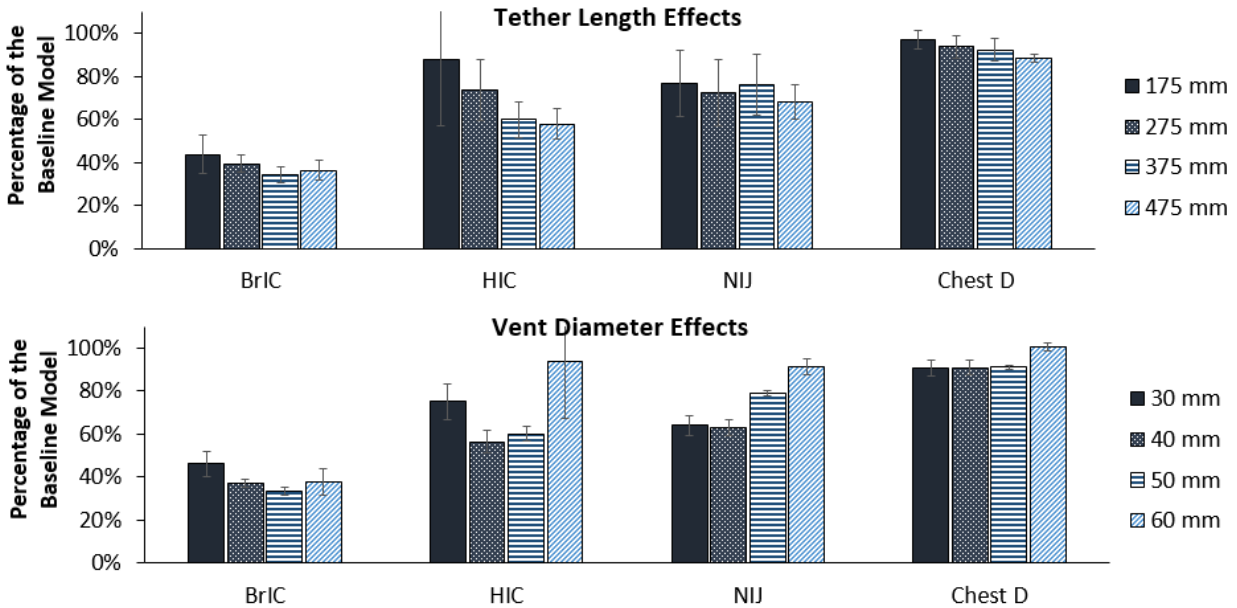


Figure 32: SQS DAB parameter effects on ATD injury measures with a suspender 4-point belt

The first two parametric studies were with different seat belt systems, but showed consistent trends regarding the SQS air bag design parameter effects on ATD injury measures. A longer tether, close to 400-500 mm, and vent size, around 40-50 mm, were the ranges of SQS air bag that resulted in the lowest injury potential. Although the bag depth was not sensitive, conceptually, a deeper air bag could catch the occupant earlier, which could be helpful for reducing the head and neck injury measures. It is possible that in the parametric study, the tether length controlled the actual depth of the air bag more than scaling the bag depth did. Nevertheless, a deeper SQS bag should be considered as the alternate DAB design.

### 5.9.2 Combined seat belt and air bag design effects

With the above findings, another parametric study was conducted to compare seat belt and air bag designs in a systematic manner. In this parametric study, two driver air bag designs (baseline bag and alternate SQS bag), support bag presence (Yes and No), and four seat belt designs (3-point baseline, 3-point with relocated D-ring, suspender R12mm/L8mm, and suspender R10.5mm/L7.5mm), were varied. This resulted in a total of 16 (2x4x2) simulations.

Figure 33 shows the seat belt and air bag effects on the ATD injury measures. Overall, the suspender 4-point belts provided lower injury potential to the 3-point belt; the suspender belt with higher load limiting provided reduced occupant rotation than that with lower load limiting; and the relocated D-ring reduced the injury potential when compared to the baseline 3-point belt. In terms of the air bag, the SQS bag provided lower injury potential compared to the baseline air bag; while adding support bag reduced head and neck injury measures. It should be noted that the baseline model under-estimated the ATD chest deflection, which reduced the sensitivity for the seat belt and air bag designs on the chest deflection. However, the chest deflection trends in simulations were consistent between the tests and simulations.

Table 21 shows the injury measures of all 16 simulations. It is interesting that the suspender belt helped reduce the BrIC, regardless of the air bag designs, while the 3-point belt relies on the support air bag to reduce the BrIC. In other words, if suspender 4-point belt were used, the research indicates less efforts are needed to tune the driver air bag. If 3-point belt were used, additional support bag may be necessary to achieve similar occupant protection improvements.

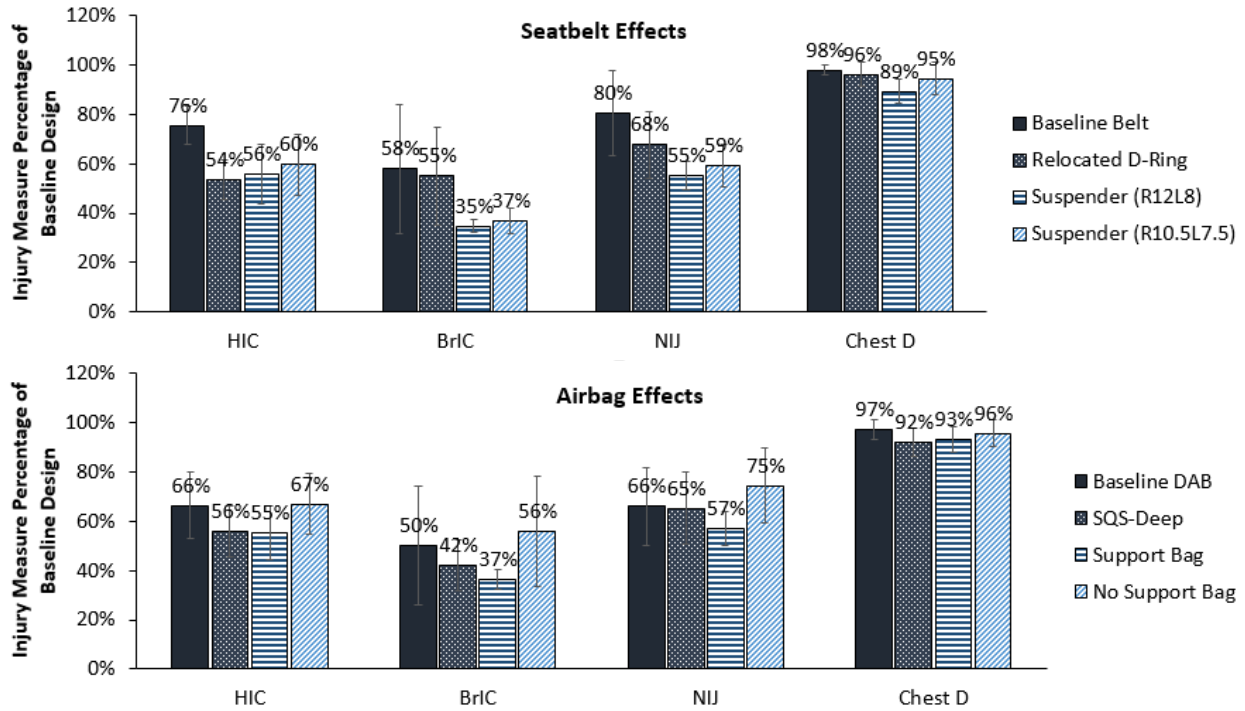


Figure 33: Air bag and seat belt effects on ATD injury measures in driver far-side impacts

Table 21: Seat belt and air bag effects on injury measure in driver far-side impacts

DAB	Support Bag	Belt System	HIC	BrIC	Old Nij	Chest D
Baseline	No	Baseline 3-point	518	1.67	1.47	28
Baseline	No	3-point Relocated D-Ring	388	1.49	1.25	30
Baseline	No	Suspender (R12L8)	438	0.68	0.86	27
Baseline	No	Suspender (R10.5L7.5)	459	0.77	0.89	30
Baseline	Yes	Baseline 3-point	434	0.69	0.96	28
Baseline	Yes	3-point Relocated D-Ring	277	0.75	0.91	28
Baseline	Yes	Suspender (R12L8)	321	0.57	0.75	27
Baseline	Yes	Suspender (R10.5L7.5)	331	0.54	0.9	28
SQS-Deep	No	Baseline 3-point	422	1.12	1.4	29
SQS-Deep	No	3-point Relocated D-Ring	319	0.98	1.13	27
SQS-Deep	No	Suspender (R12L8)	304	0.62	0.94	26
SQS-Deep	No	Suspender (R10.5L7.5)	347	0.65	1.06	26
SQS-Deep	Yes	Baseline 3-point	426	0.67	1.03	29
SQS-Deep	Yes	3-point Relocated D-Ring	293	0.72	0.8	27
SQS-Deep	Yes	Suspender (R12L8)	269	0.62	0.79	24
SQS-Deep	Yes	Suspender (R10.5L7.5)	285	0.67	0.74	26

### 5.10 Air Bag and Seat Belt Optimization in Passenger Far-Side Impact

Two sets of parametric simulations were conducted to investigate the combined effects from passenger air bag and suspender 4-point belt designs on occupant protection in the passenger far-side impact condition.

#### 5.10.1 Baseline air bag and suspender belt parameter optimization

A parametric study was conducted with a variety of suspender 4-point belt and baseline PAB designs. The design parameters that varied in this parametric study included the inflator (baseline and large), air bag depth (100% and 110% from the baseline), vent diameter (65, 75, and 85 mm), right shoulder retractor torsion bar (7.0, 7.5, and 8.0 mm), and left shoulder retractor torsion bar (9.5, 10.5, and 11.5 mm), which resulted in a total of 108 (2x2x3x3x3) simulations. Figure 34 shows the design parameter effects on ATD head and neck injury measures, which were reported as the percentage of injury measures in the baseline restraint model shown in Table 6.

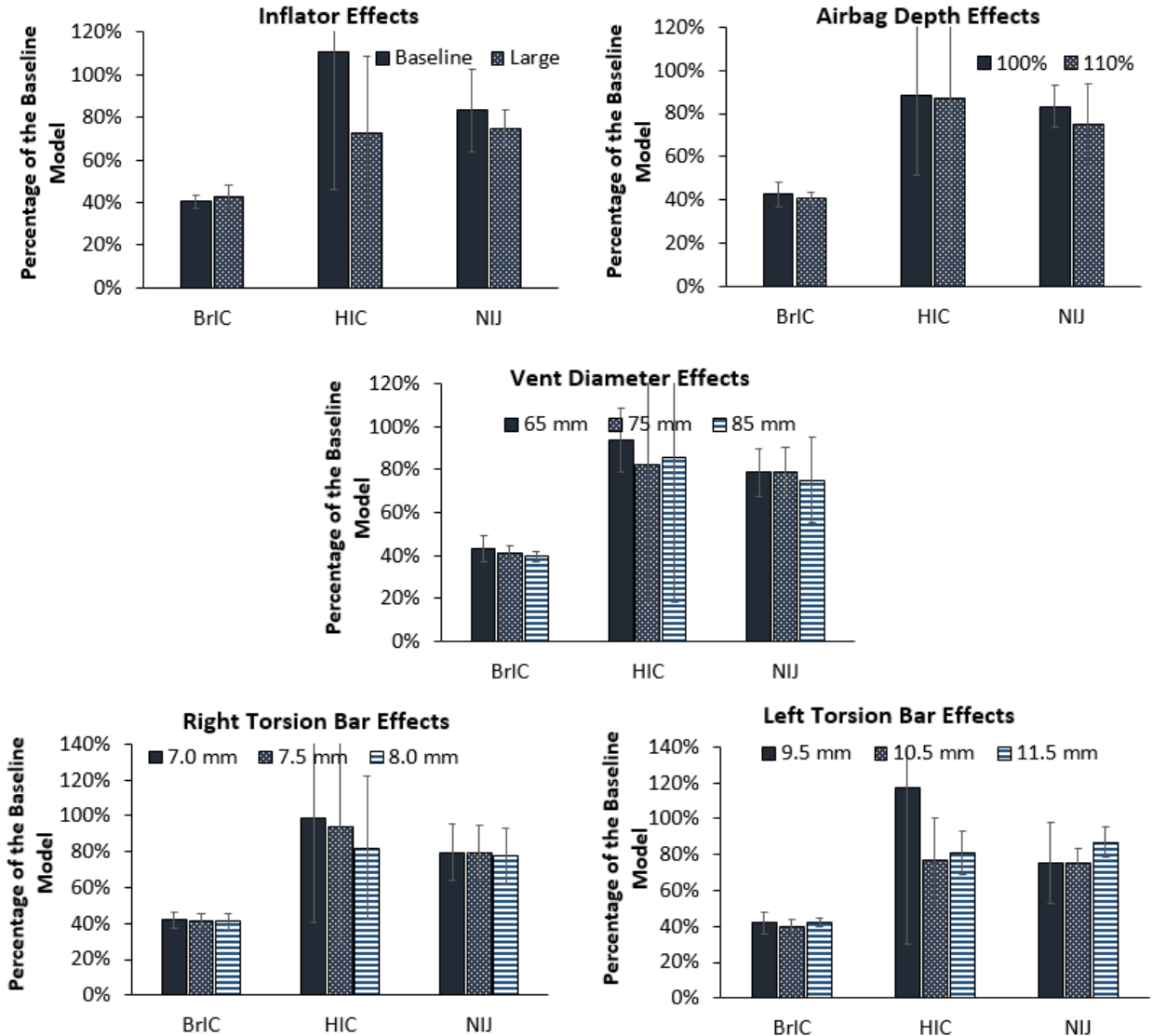


Figure 34: Air bag and seat belt effects on ATD injury measures in passenger far-side impacts

Overall, the suspender 4-point belt resulted in lower injury values than the baseline 3-point belt design, as majority of the injury measures were below the baseline model (<100%). There were large variations in HIC values, due in part to some soft restraint designs, which caused the ATD to strike through the air bag. Some general trends were worth noting, including the injury measure reductions to having a larger inflator with a deeper air bag, and using an 8-mm torsion bar on the right shoulder. The effects of the air bag vent diameter and the left shoulder torsion bar had on the head and neck injury measures are nonlinear.

Figure 35 shows a comparison on ATD kinematics and head/neck injury measures between the simulated baseline restraint and one of the alternate prototype restraints based on the parametric simulations. The suspender 4-point belt and the alternate air bag reduced the lateral head rotation and in turn reduced the BrIC by holding the left (inboard) shoulder tighter than the right (outboard) shoulder. The deeper air bag and larger inflator led to an earlier engagement between the air bag and the ATD's head, which reduced the HIC and Nij.

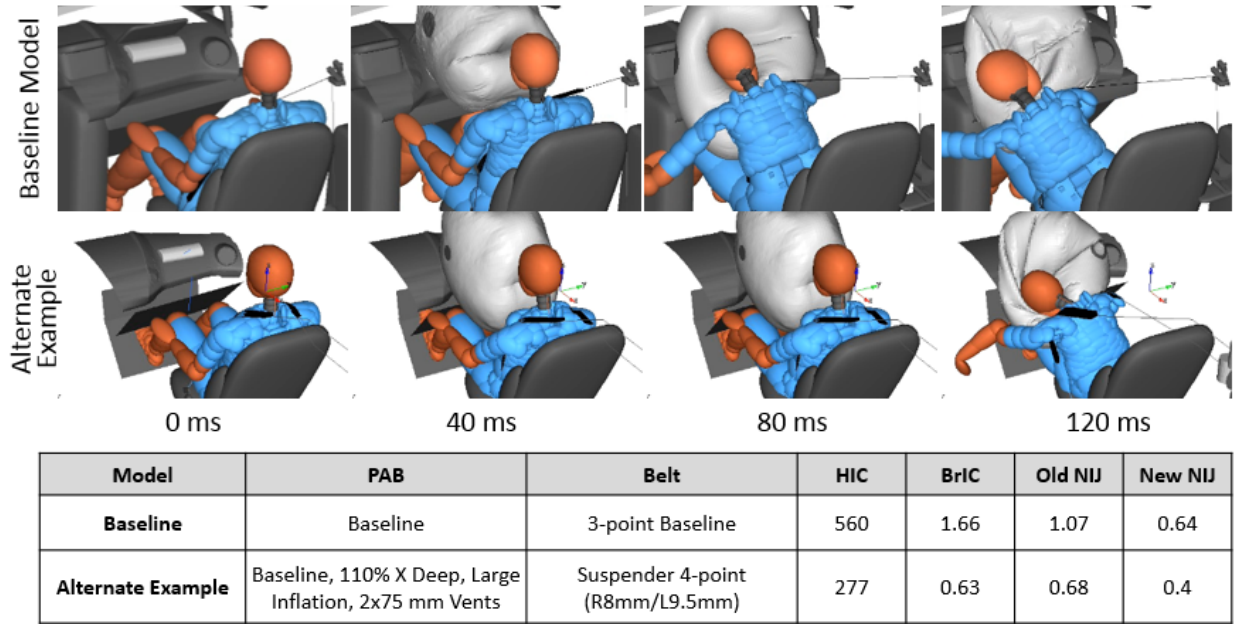


Figure 35: ATD kinematics and head/neck injury measures with the baseline restraint and an alternate PAB and suspender belt in passenger far-side impact condition

### 5.10.2 V13 PAB and suspender belt parameter optimization

Another parametric study was conducted with a variety of suspender 4-point belts and V13 PAB designs. The previous parametric study with the baseline PAB designs had revealed that the occupant could experience load reductions from a deeper air bag with a larger inflator and an 8-mm torsion bar on the right shoulder. Therefore, the design parameters that varied in this parametric study only included the vent diameter (40, 50, 60 and 70 mm), and left shoulder retractor torsion bar (9.5, 10.5, and 11.5 mm), which resulted in a total of 12 (4x3) simulations. Table 22 shows the head and neck injury measures for all the 12 simulations. Simulation No. 4 provided the lowest HIC and BrIC values. There were conflicting effects between BrIC and Nij, but many designs provided lower head and neck injury measures than the baseline design.

Table 22: Head and neck injury measures in the parametric study with suspender 4-point belt and V13 PAB

ID	Vent Size (mm)	Belt	HIC	BrIC	Old Nij	New Nij
1	40	Suspender (R8L9.5)	997	1.20	0.59	0.35
2	50	Suspender (R8L9.5)	799	0.76	0.68	0.40
3	60	Suspender (R8L9.5)	639	0.57	0.79	0.47
4	70	Suspender (R8L9.5)	520	0.54	0.87	0.52
5	40	Suspender (R8L10.5)	959	0.81	0.68	0.41
6	50	Suspender (R8L10.5)	798	0.58	0.71	0.43
7	60	Suspender (R8L10.5)	642	0.56	0.90	0.54
8	70	Suspender (R8L10.5)	536	0.55	1.02	0.61
9	40	Suspender (R8L11.5)	932	0.73	0.85	0.51
10	50	Suspender (R8L11.5)	764	0.70	0.97	0.58
11	60	Suspender (R8L11.5)	644	0.66	1.11	0.66
12	70	Suspender (R8L11.5)	542	0.67	1.18	0.71

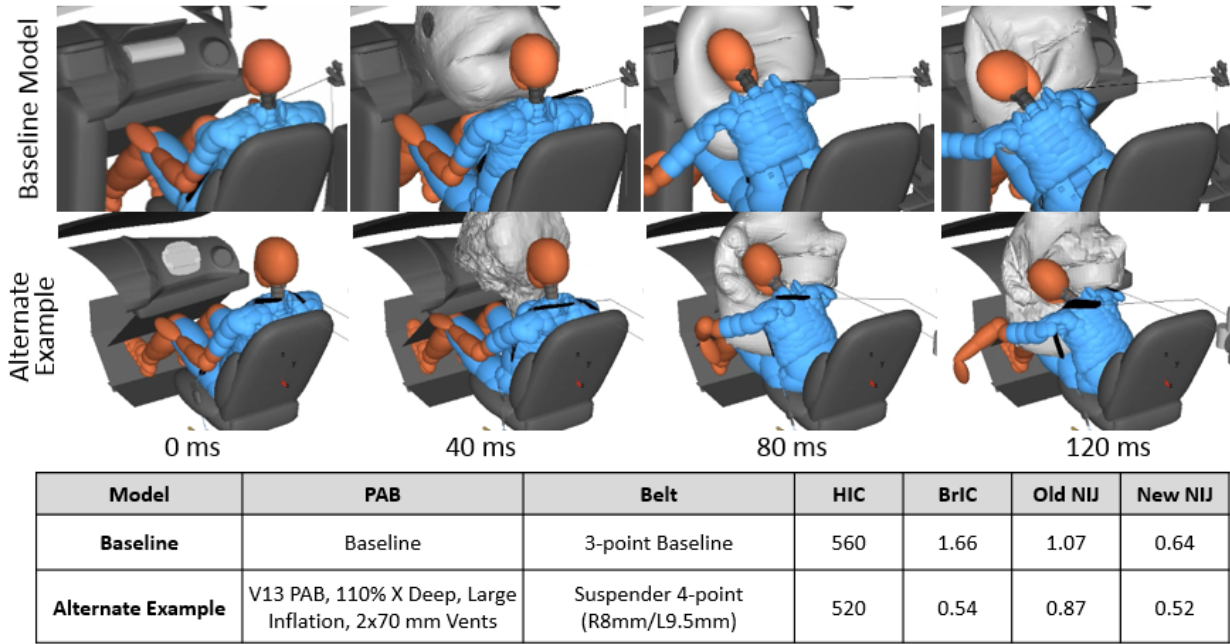


Figure 36: ATD kinematics and head/neck injury measures with the baseline restraint and a V13 PAB and suspender belt in passenger far-side impact condition

## 6 Final Series of Sled Tests With Modified Restraints

### 6.1 Goal

The goal of Task 5 was to fabricate the prototype modified restraint systems above for oblique crashes and to conduct sled tests to evaluate the reduced injury potential from these systems.

### 6.2 Modified Restraints and Testing Matrix

Two types of modified restraint designs, one with 3-point belt and one with suspender 4-point belt, as shown in Table 23, were identified through the design optimization analysis using sled tests and computational simulations. Consequently, two final sled tests were conducted in each of the four oblique impact conditions (i.e., driver near-side, driver far-side, passenger near-side, and passenger far-side), which resulted in a total of eight final sled tests.

Table 23: Modified prototype designs used in the final sled series

	Baseline	Advanced with 3-Point Belt	Advanced with 4-Point Belt
Driver			
Passenger			

Position	Belt	Modified restraint Details
Driver	3-Point	3-point belt with relocated D-ring, retractor with SLL and pre-tensioner, DLT, baseline DAB, two-medium chamber CAB, and baseline KnAB
	4-Point	4-point suspender belt with two CLLs (8 mm inboard torsion bar / 10 mm outboard torsion bar) and two pre-tensioners, SQS DAB, two-medium chamber CAB, and baseline KnAB
Passenger	3-Point	3-point belt with relocated D-ring, retractor with DLL and pre-tensioner, DLT, kickstand PAB, two-medium chamber CAB, and a new KnAB
	4-Point	4-point suspender belt with two CLLs (8 mm inboard torsion bar / 9 mm outboard torsion bar) and two pre-tensioners, V13 PAB, three small chamber CAB, and no KnAB

## 6.3 Results

### 6.3.1 Final sled tests

The ATD kinematics in the baseline test, the test with the modified 3-point belt and air bag, and the test with the suspender 4-point belt and air bag for the driver near-side impact condition are shown in Figure 37. The associated injury measures are shown in Table 24. Both the modified designs reduced injury measures for the head, neck, and chest, as well as the Pjoint. The restraint system with the suspender 4-point belt provided a lower Pjoint than that with the 3-point belt, which was largely due to the lower chest deflection measurements.



Figure 37: Occupant kinematics in baseline and final sled tests for driver near-side impact

Table 24: Injury measures in baseline and final sled tests for driver near-side impact

Occupant Side	Added Technology	Head		Neck		Chest		Abdomen		Acetabular		Femur		Pjoint
		HIC	BrIC	Old $N_{Ij}$	New $N_{Ij}$	$R_{MAX}$	PCA Score	Dmax (L)	Dmax (R)	Fmax (L)	Fmax (R)	Comp (L)	Comp (R)	
Driver Near-side (Left)	Baseline	448	1.04	0.94	0.56	51	6.62	73	76	1935	2065	1858	3916	0.809
	3-Pt System	402	0.72	0.63	0.36	40	5.99	45	51	1862	2121	2551	2774	0.426
	4-Pt System	448	0.75	0.88	0.53	20	2.51	-	35	1934	1294	3192	3050	0.267

The ATD kinematics in the baseline test, the test with the modified 3-point belt and air bag, and the test with the suspender 4-point belt and air bag for the driver far-side impact condition are shown in Figure 38. The associated injury measures are shown in Table 25. Like the driver near-side impact, both the modified prototype designs reduced injury measures for the head, neck, and chest, as well as the Pjoint. The restraint system with the suspender 4-point belt provided a lower Pjoint than that with the 3-point belt, which was due to the lower BrIC and chest deflection measurements. The  $N_{ij}$  with the suspender belt increased slightly from the baseline test due to a

larger head whipping motion, but such motion helped reduce the lateral head rotation and BrIC. The tradeoff between BrIC and  $N_{ij}$  with the suspender belt was discussed in the design optimization section, and is shown here.

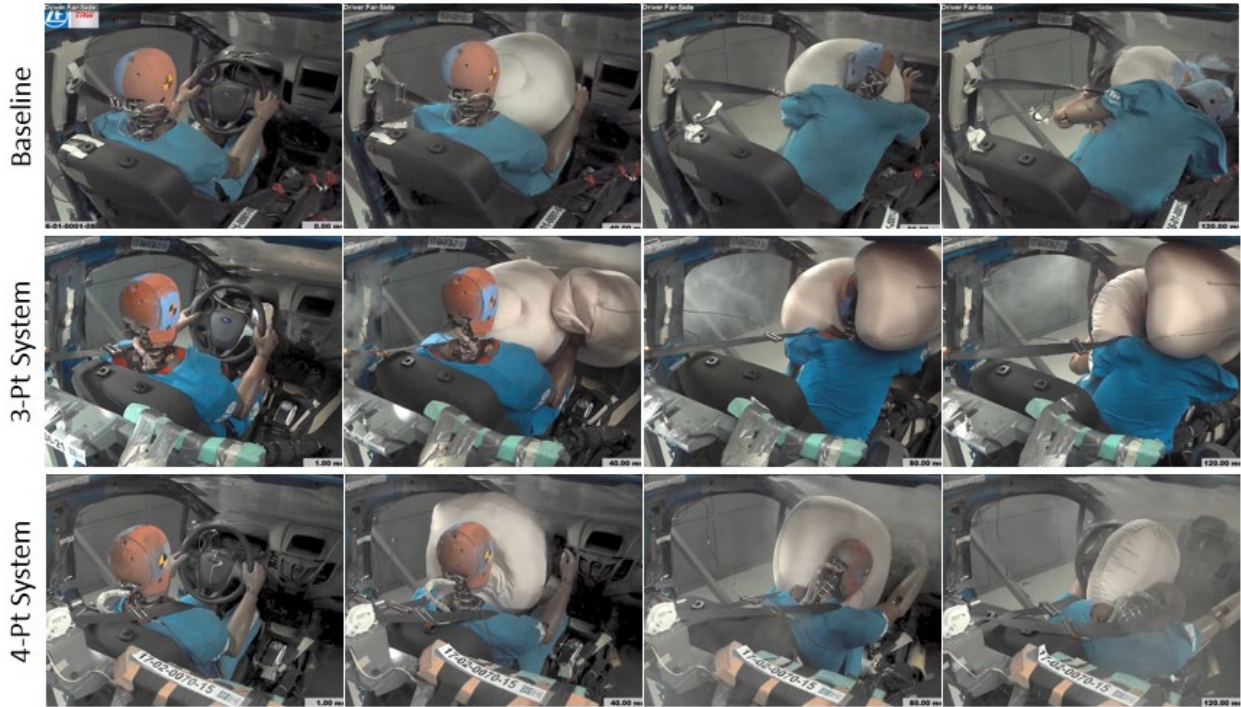


Figure 38: Occupant kinematics in baseline and final sled tests for driver far-side impact

Table 25: Injury measures in baseline and final sled tests for driver far-side impact

Occupant Side	Added Technology	Head		Neck		Chest		Abdomen		Acetabular		Femur		Pjoint
		HIC	BrIC	Old $N_{ij}$	New $N_{ij}$	$R_{MAX}$	PCA Score	Dmax (L)	Dmax (R)	Fmax (L)	Fmax (R)	Comp (L)	Comp (R)	
Driver Far-side (Right)	Baseline	496	1.73	1.00	0.58	45	5.22	71	75	2031	2476	-3354	-3185	0.98
	3-Pt System	500	0.94	0.72	0.43	37	5.31	40	-	2565	1648	3750	3332	0.603
	4-Pt System	405	0.70	1.07	0.65	33	3.26	62	61	1731	1434	3152	2883	0.411

The ATD kinematics in the baseline test, the test with the modified 3-point belt and air bag, and the test with the suspender 4-point belt and air bag for the passenger near-side impact condition are shown in Figure 39. The associated injury measures are shown in Table 26. Both the modified designs reduced injury measures for the head, neck, and chest, as well as the Pjoint. The restraint system with the suspender 4-point belt provided a lower Pjoint than that with the 3-point belt, which was largely due to the lower chest deflection measurements. However, the modified design with the 3-point belt provided lower BrIC and Nij than that with the suspender belt.

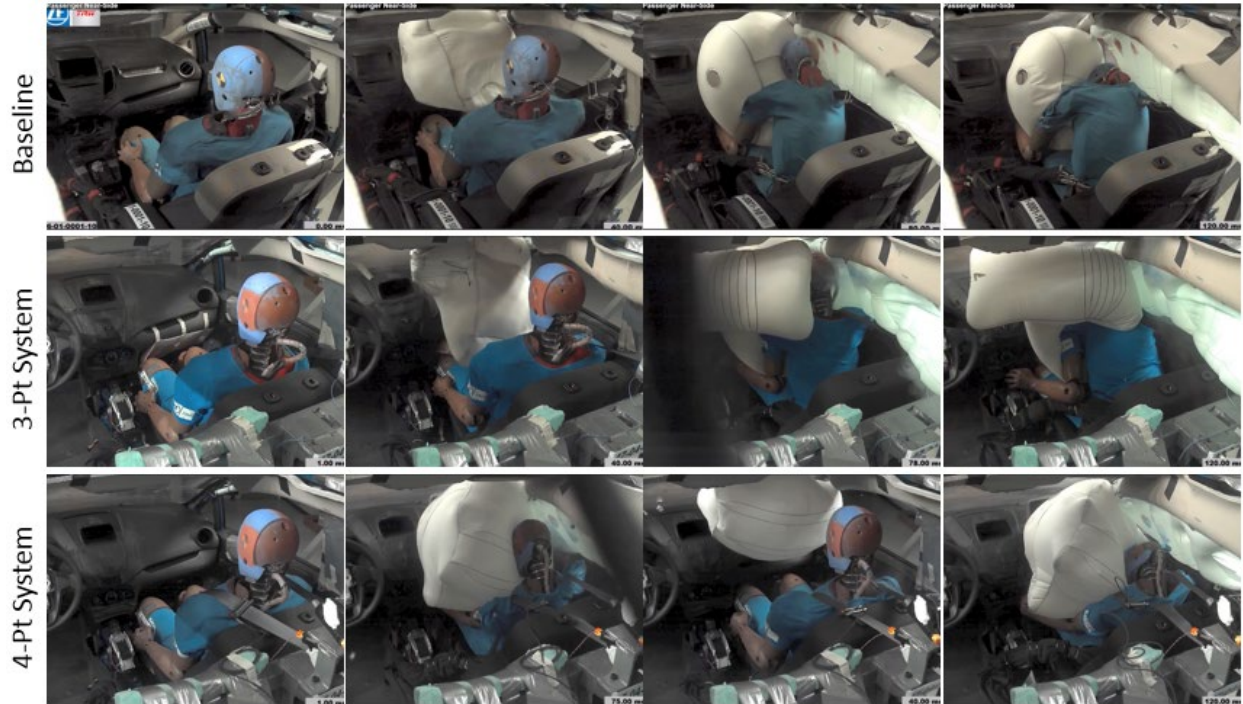


Figure 39: Occupant kinematics in baseline and final sled tests for passenger near-side impact

Table 26: Injury measures in baseline and final sled tests for passenger near-side impact

Occupant Side	Added Technology	Head		Neck		Chest		Abdomen		Acetabular		Femur		Pjoint
		HIC	BrIC	Old N <sub>IJ</sub>	New N <sub>IJ</sub>	R <sub>MAX</sub>	PCA Score	Dmax (L)	Dmax (R)	Fmax (L)	Fmax (R)	Comp (L)	Comp (R)	
Passenger Near-side (Right)	Baseline	773	0.97	1.17	0.71	59	7.28	78	74	2840	2437	-2095	-1395	0.883
	3-Pt System	489	0.69	0.75	0.45	45	5.93	45	-	1843	2861	2561	4504	0.589
	4-Pt System	476	0.83	0.83	0.49	26	3.39	44	-	2411	1906	4074	2671	0.423

The ATD kinematics in the baseline test, the test with the modified 3-point belt and air bag, and the test with the suspender 4-point belt and air bag for the passenger far-side impact condition are shown in Figure 40. The associated injury measures are shown in Table 27. Both the modified designs reduced the BrIC, chest deflection, as well as the Pjoint. The two modified restraint systems provided similar Pjoint values. The HIC and Nij with the modified suspender belt increased slightly from the baseline test due to a larger head whipping motion, but such motion helped reduce the lateral head rotation and BrIC. The tradeoff between BrIC and Nij with the suspender belt was discussed in the design optimization section, and is shown here.

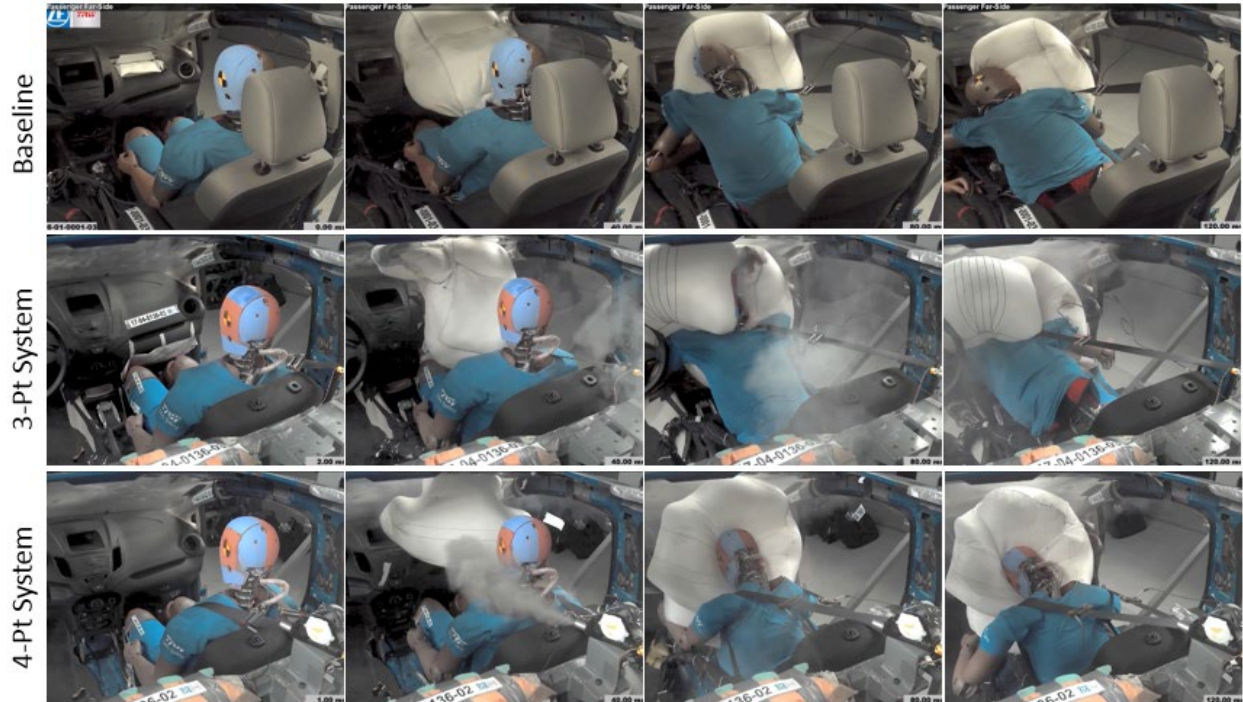


Figure 40: Occupant kinematics in baseline and final sled tests for passenger far-side impact

Table 27: Injury measures in baseline and final sled tests for passenger far-side impact

Occupant Side	Added Technology	Head		Neck		Chest		Abdomen		Acetabular		Femur		Pjoint
		HIC	BrIC	Old N <sub>IJ</sub>	New N <sub>IJ</sub>	R <sub>MAX</sub>	PCA Score	Dmax (L)	Dmax (R)	Fmax (L)	Fmax (R)	Comp (L)	Comp (R)	
Passenger Far-side (Left)	Baseline	332	1.55	0.81	0.47	50	6.36	82	75	1657	4430	-3010	-990	0.995
	3-Pt System	372	0.75	0.72	0.44	38	5.79	42	-	1944	2231	3492	3850	0.438
	4-Pt System	543	0.53	0.96	0.58	38	5.07	39	-	2310	2450	3550	2250	0.427

### 6.3.2 Out-of-position tests

FMVSS No. 208 OOP tests were conducted using the 6-year-old HIII ATD (6 YO) with both the kickstand PAB and V13 PAB, which were used in the final sled tests. For each air bag, two ATD positions (as shown in Figure 41) were evaluated. Table 28 and Figure 41 show the 6YO injury measures and kinematics in the OOP tests. All injury measures were well below the IARVs defined in the FMVSS No. 208 standards.

Table 28: Injury measures in 6YO OOP tests for modified passenger air bags

Injury Measure	IARV	Kickstand PAB		V13 PAB	
		6YO Position 1	6YO Position 2	6YO Position 1	6YO Position 2
HIC	700	141	254	28	109
NeckT (N)	1,490	1,121	215	385	431
NeckC (N)	1,820	4	1,062	221	1,386
Old Nij	1.00	0.79	0.46	0.24	0.56
ChestG (g)	60	15	9	9	11
ChestD (mm)	40	11	1	4	1

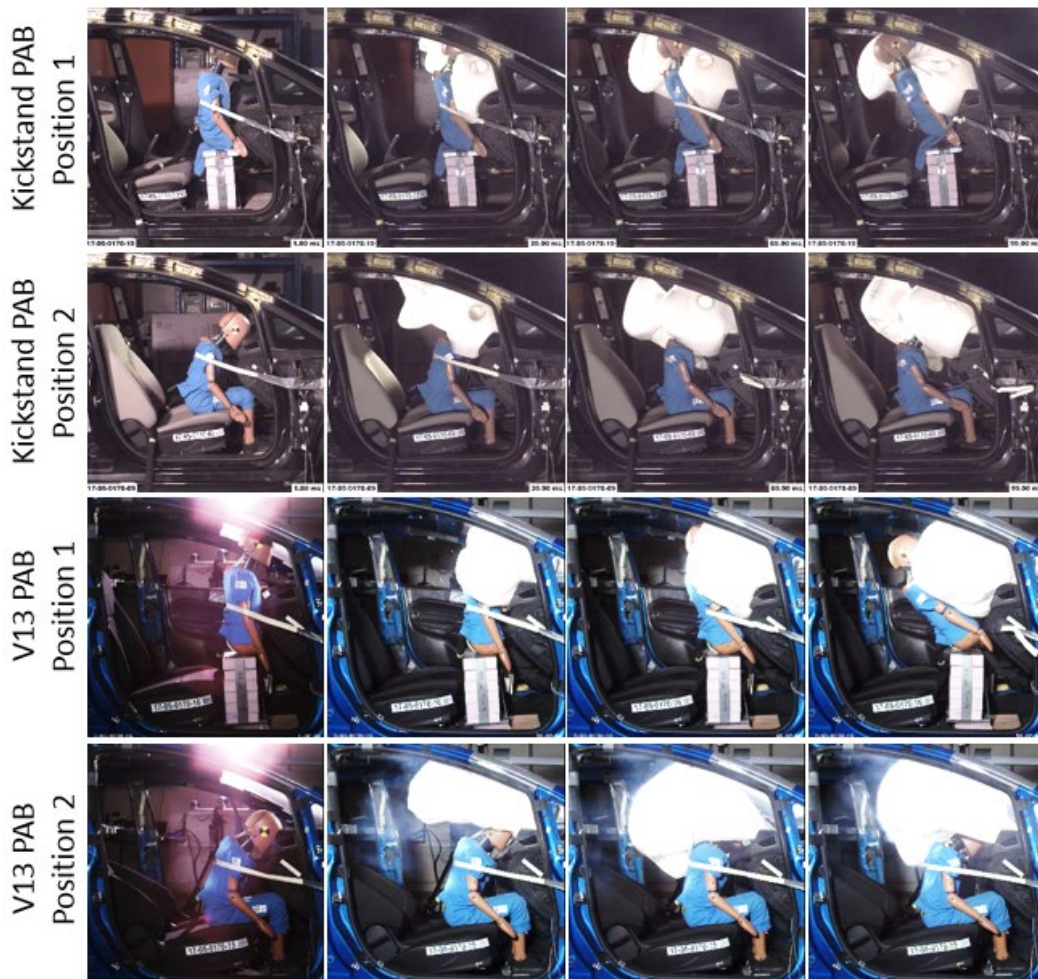


Figure 41: Occupant kinematics in 6YO OOP tests for modified prototype passenger air bags

FMVSS No. 208 OOP tests were also conducted using the HIII 5th female ATD (H5) on the driver seat with the SQS DAB, which were used in the final sled tests. Two ATD positions (as shown in Figure 42) were evaluated. Table 29 and Figure 42 show the H5 injury measures and kinematics in the OOP tests. All injury measures were below the IARVs defined in the FMVSS No. 208 standards.

Table 29: Injury measures in 5th female OOP tests for modified driver air bags

Injury Measure	IARV	SQS DAB	
		5th Female Position 1	5th Female Position 2
HIC	700	11	9
NeckT (N)	2,070	233	910
NeckC (N)	2,520	976	81
Old Nij	1.00	0.22	0.42
ChestG (g)	60	11.5	25.9
ChestD (mm)	52	5.6	31.4



Figure 42: Occupant kinematics in H5 OOP tests for modified driver air bags

### 6.3.3 FMVSS No. 208 simulations

The modified prototype systems were evaluated for FMVSS No. 208 compliance. Simulations under 56 km/h (35 mph) full barrier frontal crash condition with belted occupants and 40 km/h (25 mph) full barrier frontal crash condition for unbelted occupants were conducted with HIII 50th male and 5th female ATDs for both the driver side and front passenger side. The crash pulses were based on the full vehicle crash tests shown in Figures 16 to 19. Tables 30 and 31 show all the injury measures and the associated IARVs. All the injury measures are below the IARVs, although a few injury measures are over 80 percent of the IARVs but below 90 percent of the IARVs.

Table 30: Model-predicted driver injury measures in simulations for FMVSS No. 208 compliance

<b>HIII 50 Driver</b>		<b>Unbelted</b>	<b>Unbelted</b>	<b>3-Pt Baseline</b>	<b>3-Pt Belt Modified</b>	<b>4-Pt Belt</b>
<b>Injury Measures</b>	<b>IARV</b>	<b>Baseline DAB</b>	<b>SQS DAB</b>	<b>Baseline DAB</b>	<b>Baseline DAB</b>	<b>SQS DAB</b>
HIC15	700	100	440	346	349	234
Neck T (N)	4,170	1,391	1,609	1,456	1,020	1,751
Neck C (N)	4,000	361	363	214	171	56
Old Nij	1.00	0.31	0.63	0.25	0.22	0.83
Chest D (mm)	63	40.8*	38.9	21.7	22.1	11.3
Femur F L (N)	10,000	5,223	5,558	1,177	1,519	1,692
Femur F R (N)	10,000	8,569	8,233	1,424	1,503	1,633
<b>HIII 5th Driver</b>		<b>Unbelted</b>	<b>Unbelted</b>	<b>3-Pt Baseline</b>	<b>3-Pt Belt Modified</b>	<b>4-Pt Belt</b>
<b>Injury Measures</b>	<b>IARV</b>	<b>Baseline PAB</b>	<b>SQS</b>	<b>Baseline DAB</b>	<b>Baseline DAB</b>	<b>SQS DAB</b>
HIC15	700	30	26	172	169	114
Neck T (N)	2,620	681	722	1,138	1,118	1,128
Neck C (N)	2,520	184	133	24	117	29
Old Nij	1.00	0.34	0.38	0.67	0.71	0.59
Chest D (mm)	52	44.4*	43.1	38.2	35.5	8.8
Femur F L (N)	6,800	1,718	1,747	1,620	1,543	1,640
Femur F R (N)	6,800	2,121	2,146	1,559	1,543	1,072

\*Over prediction of the injury measure compared to the vehicle tests

Table 31: Model-predicted front passenger injury measures in simulations for FMVSS No. 208 compliance

HIII 50th Passenger		Unbelted	Unbelted	Unbelted	3-Pt Belt Baseline	3-Pt Belt Modified	4-Pt Belt
Injury Measures	IARV	Baseline PAB	Kickstand PAB & KnAB	V13 PAB	Baseline	Kickstand PAB & KnAB	V13 PAB
HIC15	700	462	185	161	519	292	394
Neck T (N)	4,170	3,757	591	631	1,202	1,246	1,378
Neck C (N)	4,000	864	697	613	151	726	654
Old Nij	1.00	0.58	0.29	0.26	0.35	0.33	0.39
Chest D (mm)	63	12.6	13.3	18.9	27.4	14.8	11.1
Femur F L (N)	10,000	4,831	4,231	4,625	3,069	4,178	3,739
Femur F R (N)	10,000	4,303	3,711	4,380	2,206	3,574	3,364
HIII 5th Passenger		Unbelted	Unbelted	Unbelted	3-Pt Belt Baseline	3-Pt Belt Modified	4-Pt Belt
Injury Measures	IARV	Baseline PAB	Kickstand PAB & KnAB	V13 PAB	Baseline	Kickstand PAB & KnAB	V13 PAB
HIC15	700	58	170	148	241	569	401
Neck T (N)	2,620	56	263	87	571	1,477	635
Neck C (N)	2,520	929	352	1,370	948	393	1,444
Old Nij	1.00	0.53	0.26	0.6	0.43	0.69	0.41
Chest D (mm)	52	13.8	8.1	17	24.8	30.7	11.6
Femur F L (N)	6,800	3,465	2,781	3,442	2,542	3,670	1,984
Femur F R (N)	6,800	3,370	2,490	3,319	1,370	3,249	893

## 7 Discussion

### 7.1 Challenges for Occupant Protection in Oblique Crashes

The NHTSA OMDB crash condition is a new and different crash condition to NHTSA's existing frontal crash tests requirements, and poses unique challenges for occupant protection. First, in an oblique impact, the ATD could contact the edge/side of the driver or passenger air bag, inducing possible lateral head rotation and a potential contact between the ATD's head and vehicle interior (e.g., door and IP). Such kinematics can result in higher HIC and/or BrIC values. Regarding the head injury measures, typically far-side oblique impacts are more challenging than near-side impacts, because in near-side impacts the vehicle front door may limit the ATD torso's lateral movement and curtain air bags may provide lateral support to the ATD's head. Second, THOR, used in the NHTSA OMDB tests, provides more sophisticated measurements than prior ATDs. Such change increase the biofidelity of the ATD creating both challenges and opportunities to tune the seat belt geometry. In a far-side oblique impact, the shoulder belt of a typical 3-point belt could shift off the shoulder, which may reduce the seat belt effectiveness and potentially limit the possibility of reducing the chest deflection by lowering the shoulder belt load limiting.

In this study, two types of modified, prototype restraint systems were used to address the above challenges and were focused on the far-side oblique impacts.

The first type of the prototype restraint system was a combination of a 3-point belt and a special designed air bag with an additional lateral support component. For the driver side, a support bag behind the driver air bag was designed, which could reduce the lateral rotation of the ATD's head. For the passenger side, the kickstand bag had an additional chamber on the inboard side of the passenger air bag, which could also reduce the lateral head rotation. Mitigating the lateral head rotation helped lessen the potential for a hard head contact and high BrIC value. With the 3-point belt, the retractor was moved closer to the shoulder of the ATD and the D-ring was removed, which lowered the shoulder belt force and the chest deflection measurements of the ATD.

The second type of the prototype restraint system included a suspender 4-point belt with slightly modified air bag. The observed advantages of the suspender 4-point belt were: 1) two shoulder belts apply loading on the clavicles, which helped reduce the chest deflection measurements; 2) different load limiting could be assigned to the two shoulder belts, which helped control the torso rotation during the oblique impact and consequently prevented a large lateral head rotation measurement; 3) with a proper sensing system, the shoulder belt load limiting could adapt to the impact direction (higher load limiting on the shoulder close to the impact direction), which provided an opportunity to better protect the occupant equally between near-side and far-side impacts. The results showed that the suspender 4-point belt did not require air bag changes to help improve occupant protection in oblique crash conditions, and generally provided lower injury measurements than the restraint systems with 3-point belts.

Researchers did not evaluate consumer acceptance or the feasibility for original equipment manufacturers to integrate these prototype systems into a particular vehicle environment.

## 7.2 Chest Deflections of THOR

The THOR has been proved to be a more biofidelic ATD than the HIII ATDs (Parent, Craig, & Moorhouse, 2017). However, the suspender 4-point belt poses very different loading path than a typical 3-point belt. The suspender belt loaded the chest mainly through the clavicles, which may have changed the chest deflection patterns. In some of the tests, chest expansion was observed. In other tests, chest deflection in Z-component (vertical direction) was also observed. Biomechanics studies are needed to investigate the biofidelity of THOR chest deflections in these loading conditions.

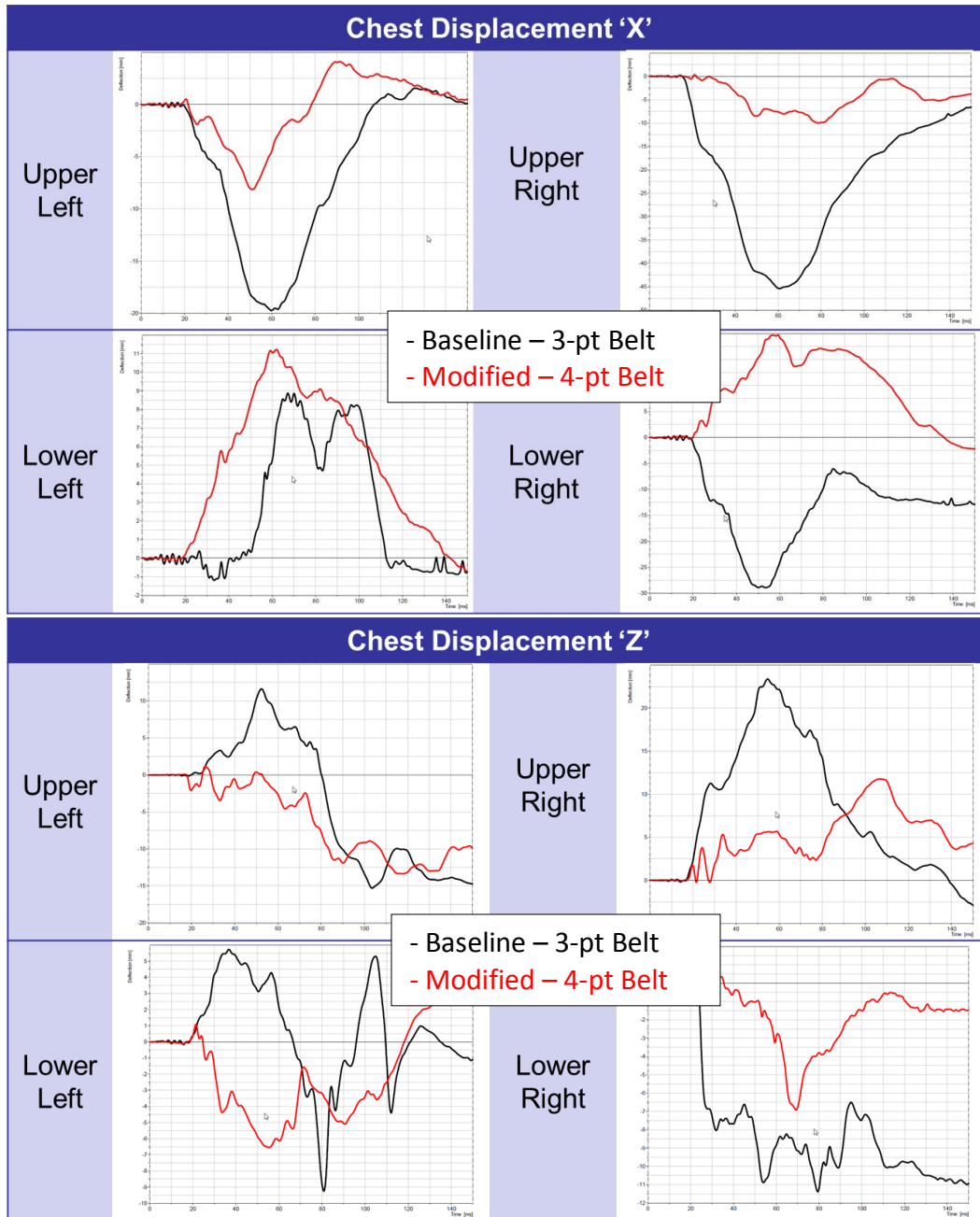


Figure 43: Example of chest deflection with suspender 4-point belt

### 7.3 Abdomen Deflections of THOR

Two THOR dummies were used for different sled tests throughout the study. By compiling all the tests together, it was found that there was a statistically significant difference in the abdomen compression measures between the two THOR dummies (Table 32). The THOR 016 measured much lower abdomen compressions than those measured by THOR 007. Because no specific countermeasures were used to reduce the abdomen compression, we expect that the abdomen measures should be similar between the two THORs. The THOR 007 was used for all the baseline sled tests, and THOR 016 was used for all the final sled tests. Therefore, the reductions in abdomen compressions between the baseline and final sled tests may not be attributed to the restraint systems, but rather the THOR itself.

Table 32: Abdomen compressions between two THORs

ATD Position	Impact Condition	THOR	Mean Abdomen Compression (mm)	S.D. of Abdomen Compression (mm)	P-Value
Driver	Near Side	007	73	3.7	0.001
		016	50	12.2	
	Far Side	007	78	5.2	0.000
		016	46	9.0	
Passenger	Near Side	007	76	7.9	0.000
		016	46	4.6	
	Far Side	007	72	5.7	0.000
		016	42	6.9	

### 7.4 Limitations

In this study, only a single vehicle driver and right front seat passenger compartment based on a compact vehicle was used. Therefore, the findings from this study should not be generalized for all vehicles. Additional simulations could determine whether the compartment size, crash pulse, and crash angle could affect the modified restraint design solutions. Furthermore, air bag sensing system is out of the scope of this study, but the resulted restraint systems from this study may require additional sensors. Active safety sensor could potentially provide additional information to the new restraint systems. Certain provisions in FMVSS may also preclude the implementation of 4-point belt systems, which should be investigated in the future.

## **8 Summary**

This study developed and demonstrated modified, prototype occupant restraint systems for both the driver and front right passenger and evaluated their potential to help reduce injury potential for the 50th percentile male THOR in both left and right oblique frontal crashes. The study was broken down into five tasks, and summary for each task was provided below.

### **8.1 Baseline Tests**

In this study, a surrogate B-segment vehicle was selected as the baseline vehicle to build sled bucks representing driver and front right passenger compartments. A sled test procedure was developed to replicate typical THOR kinematics and injury measures in NHTSA OMDB tests with small/midsize passenger cars. The sled pulse was based on the surrogate B-segment vehicle's resultant deceleration at the vehicle's center of gravity in the NHTSA OMDB test, but with a 20 percent increase in magnitude to help match the general trends in THOR kinematics and injury measures. The driver or passenger sled bucks were set up with an 18° sled angle either to the left or right to mimic left or right oblique impacts.

Overall, the baseline sled tests produced similar THOR kinematics to those in the NHTSA OMDB full vehicle tests. The near-side impacts produced the head rolling off the air bag, which resulted in lateral head rotation, larger BrIC, and potential for head-to-door contact; while the far-side impacts produced torso rolling out of the belt system and head rolling off the air bag, which resulted in lateral head rotation, larger BrIC, and potential for head-to-IP contact. The values and locations of the maximal chest deflections in the sled tests were also consistent to the OMDB full vehicle tests. These sled tests set up the initial benchmark for this study.

### **8.2 Baseline Model Development and Validation**

In this study, a set of baseline MADYMO models were developed with detailed vehicle interior and restraint systems to represent the surrogate B-segment vehicle. These models were validated against the baseline sled tests as well as the FMVSS No. 208 unbelted frontal barrier tests and US-NCAP frontal barrier tests. The model-predicted kinematics and injury measures were quantitatively compared to the testing results. One of the observed limitations of the model was that the THOR model tended to under-estimate the maximal chest deflections in oblique crash conditions, which may have reduced the sensitivity of restraint design parameters on chest deflections using parametric simulations. The HIII 5th female model also tended to over-estimate the maximal chest deflection in frontal crashes, but the predicted values were well below the IARV. This set of models provided a tool for restraint design optimizations in oblique impacts.

### **8.3 Propose Modified Prototype Restraint Systems**

In this study, a wide variety of modified, prototype restraint designs were proposed to help improve occupant protection in OMDB tests. The focus of the near-sided occupant protection was through re-designing curtain air bags, while additional efforts were taken toward far-side occupant protection through re-designing combined seat belt and air bag systems. In total, five seat belt systems (reverse 3-point belt, rerouted 3-point belt, 3-point belt with relocated retractor, X-type 4-point belt, and suspender 4-point belt), four air bag designs (cone DAB, SQS DAB, support bag, and inboard SAB) for the driver, five air bag designs (V64 PAB, V13 PAB, Clapper PAB, Parallel cell PAB, and kickstand PAB), and four curtain air bag designs (three-small chamber CAB, two-medium chamber CAB, Single Large Chamber CAB, and Buckle CAB) for near-side impacts were

proposed. The air bag designs focused on the potential of providing stronger lateral support to the occupant's head; while the seat belt designs focused on engaging the occupant's torso longer and lowering the chest deflections.

#### **8.4 Design Optimizations**

To tune the proposed restraint systems, nearly 100 sled tests and hundreds of MADYMO simulations were conducted to systematically select and tune the proposed prototype seat belt and air bag designs for reduced injury measures in NHTSA OMDB crash conditions. Due to the complicated nature of far-side impacts, both sled tests and computational simulations focused on the far-side oblique impacts.

For both driver and passenger far-side impacts, two types of restraint systems stood out from all the proposed restraint systems. The first one was equipped with a 3-point belt with relocated retractor closer to the THOR shoulder and an additional air bag or air bag features to help prevent the lateral head rotation; and the other was equipped with a suspender 4-point belt with uneven load limiting between two shoulder belts and minimally changed driver or passenger air bags.

For these two selected design systems, several trends shown in the sled tests and parametric simulations are worth noting:

- 1) The relocated retractor for a 3-point belt could help the belt stay on the shoulder longer in a far-side impact, and consequently reduce the occupant rotation and provide the potential of reducing chest deflections by lowering the load limiting on the shoulder.
- 2) Regardless the design configurations, a 3-point belt configuration was not able to improve lateral head rotation and BrIC values in this study without an air bag re-design for a far-side impact. An additional air bag or a new air bag feature that could support the head laterally had the potential to reduce BrIC values in a far-side oblique impact.
- 3) Uneven load limiting at the two shoulders in a suspender 4-point belt helped to control the occupant kinematics. Typically, a higher load limiting should be assigned at the striking side of the shoulder, so that THOR's torso can rotate laterally toward the impact. Such kinematics can reduce the lateral head rotation measurements, and consequently reduce the BrIC value.
- 4) With a suspender 4-point belt, the chest deflections were generally lower than those with 3-point belts, because the belt loadings were mainly transferred through the clavicle, not the ribs.
- 5) With a suspender 4-point belt, only minimal changes in air bag designs were needed to help reduce the occupant's injury measures. Typically, a deeper air bag with higher inflation would be beneficial for reducing HIC and Nij.
- 6) A re-design of curtain air bag can help to prevent head-to-door impacts in near-side oblique impacts. However, the use of a relocated retractor of a 3-point belt and a suspender 4-point belt can reduce the chest deflections.

#### **8.5 Final Sled Tests**

Two modified prototype restraint systems, one with a 3-point belt and relocated retractor, and one with a suspender 4-point belt, were used in the final sled tests. In all four testing conditions (driver near-side, driver far-side, passenger near-side, and passenger far-side), both modified restraint systems reduced the head rotation of THOR and reduced the joint injury probabilities.

In terms of the THOR kinematics, both modified restraint systems limited the lateral head rotations and avoided the potential head-to-interior contacts. Furthermore, there was no shoulder belt rolling off the shoulder, nor head rolling off from the air bag. In terms of the injury measures, the average BrIC and average maximal chest deflection in four baseline sled tests were 1.32 and 51 mm; with the modified system using a 3-point belt, the average BrIC and average maximal chest deflection in the four final sled tests were 0.78, and 40 mm; and with the modified system using a suspender 4-point belt, the average BrIC and average maximal chest deflection in the four final sled tests were 0.70, and 29 mm. The average joint injury probabilities for the baseline restraint, modified restraint with 3-point belt, and modified restraint with suspender 4-point belt were 0.92, 0.51, and 0.38. The two modified prototype systems were also evaluated for FMVSS No. 208 compliance through OOP tests with 6YO and 5th female HIII ATDs and full barrier frontal crash simulations with belted and unbelted 5th female and 50th male HIII ATD models. All the injury measures are below the IARVs.

## References

- 80 FR 78521. (2015, December 16). New Car Assessment Program. Docket No. NHTSA–2015–0119, Federal Register. Vol. 80, No. 241, Page Nos. 78521-78591. Document No. 2015-31323. Available at <https://www.federalregister.gov/documents/2015/12/16/2015-31323/new-car-assessment-program>
- Bai, Z., B. Jiang, et al., (2014). Optimizing the passenger air bag of an adaptive restraint system for multiple size occupants. *Traffic Injury Prevention*, 15(6): 556-563.
- Bean, J. D., C. J. Kahane, C. J., Mynatt, M., Rudd, R. W., Rush, C. J., & Wiacek, C. (2009). *Fatalities in frontal crashes despite seat belts and air bags: Review of all CDS cases; Model and calendar years 2000-2007; 122 fatalities* (Report No. DOT HS 811 202). Washington, DC: National Highway Traffic Safety Administration. Available at <https://crashstats.nhtsa.dot.gov/Api/Public/ViewPublication/811102>
- Bostrom, O., Haland, Y., & Soderstrom, P. (2005). *Seat integrated 3-point belt with reversed geometry and an inboard torso side-support air bag for improved protection in rollover*. 19th International Technical Conference on the Enhanced Safety of Vehicles (ESV), June 6-9, 2005, Washington, DC.
- Brumbelow, M. L. & D. S. Zuby (2009). *Impact and injury patterns in frontal crashes of vehicles with good ratings for frontal crash protection*. 21st International Technical Conference on the Enhanced Safety of Vehicles Conference (ESV), June 15-19, 2009, Stuttgart, Germany.
- Deng, X., S. Potula, S., (2013). Finite element analysis of occupant head injuries: parametric effects of the side curtain air bag deployment interaction with a dummy head in a side impact crash. *Accident Analysis & Prevention*, 55: 232-241.
- El-Jawahri, R. E., Belwafa, J. E., & Cheng, J. C. (2017). U.S. Patent No. 9550465B1. Washington, DC: U.S. Patent and Trademark Office.
- Eppinger, R., Sun, E., Bandak, F., Haffner, M., Khaewpong, N., Maltese, M., ... Saul, R. (1999, November). *Development of improved injury criteria for the assessment of advanced automotive restraint systems–II* (Unnumbered report). Washington, DC: National Highway Traffic Safety Administration. Available at [www.nhtsa.gov/sites/nhtsa.dot.gov/files/rev\\_criteria.pdf](http://www.nhtsa.gov/sites/nhtsa.dot.gov/files/rev_criteria.pdf)
- Hu, J., Klinich, K. D., Manary, M. A., Flannagan, C. A. C., Narayanaswamy, P., Reed, ... Lin, C. H. (2017). Does unbelted safety requirement affect protection for belted occupants? *Traffic Injury Prevention*, 18:sup1, S85-S95, DOI: 10.1080/15389588.2017.1298096
- Hu, J., Klinich, K. D., Reed, M. P., Kokkolaras, M., & Rupp, J. D. (2012). Development and validation of a modified Hybrid-III six-year-old dummy model for simulating submarining in motor-vehicle crashes. *Medical Engineering & Physics*, 34(5): 541-551.
- Hu, J., Reed, M. P., Rupp, J. D., Fischer, K., Lange, P., & Adler, A. (2017). Optimizing seat belt and air bag designs for rear seat occupant protection in frontal crashes. *Stapp Car Crash Journal*, 61: 67-100. Available at [http://mreed.umtri.umich.edu/mreed/pubs/Hu\\_2017\\_Stapp\\_Rear\\_Seat.pdf](http://mreed.umtri.umich.edu/mreed/pubs/Hu_2017_Stapp_Rear_Seat.pdf)

- Hu, J., Rupp, J., Reed, M. P., Kurt, F., Lange, P., & Adler, A. (2015). *Rear seat restraint optimization considering the needs from a diverse population* (Report No. UMTRI-2015-15). Ann Arbor, MI: University of Michigan Transportation Research Institute.
- Hu, J., J. Wu, Klinich, K. D., Reed, M. P., Rupp, J. D., & Cao, L. (2013). Optimizing the rear seat environment for older children, adults, and infants. *Traffic Injury Prevention, 14* Suppl: S13-22. doi: 10.1080/15389588.2013.796043
- Hu, J., J. Wu, Reed, M. P., Klinich, K. D., & Cao, L. (2013). Rear seat restraint system optimization for older children in frontal crashes. *Traffic Injury Prevention, 14*(6): 614-622.
- Ito, D., Yokoi, Y., & Mizuno, K. (2015). Crash pulse optimization for occupant protection at various impact velocities. *Traffic Injury Prevention, 16*: 260-267.
- Jindal, P. K., & Midoun, D. E. (2016). U.S. Patent No. 9499118B2. Washington, DC: U.S. Patent and Trademark Office.
- Kahane, C. (1996, August). *Fatality reduction by air bags: Analysis of accident data through early 1996*. (Report No. DOT HS 808 470). Washington, DC: National Highway Traffic Safety Administration. Available at <https://crashstats.nhtsa.dot.gov/Api/Public/ViewPublication/808470>
- Kahane, C. (2000, December). *Fatality reduction by safety belts for front-seat occupants of cars and light trucks* (Report No. DOT HS 809 199). Washington, DC: National Highway Traffic Safety Administration. Available at <https://crashstats.nhtsa.dot.gov/Api/Public/ViewPublication/809199>
- Kruse, D., M. Himilainen, et al., (2017). Frontal air bag systems for oblique crash protection, U.S. Patent No. 20170072897A1. Washington, DC: U.S. Patent and Trademark Office.
- NHTSA (1999). *Effectiveness of occupant protection systems and their use, Fourth Report to Congress* (Report No. DOT HS 808 919, unnumbered on report cover) Washington, DC: National Highway Traffic Safety Administration. Available at <https://crashstats.nhtsa.dot.gov/Api/Public/ViewPublication/808919>
- NHTSA (2001, November). *Effectiveness of occupant protection systems and their use; Fifth/Sixth Report to Congress* (Report No. DOT HS 809 442). Washington, DC: National Highway Traffic Safety Administration. Available at <https://crashstats.nhtsa.dot.gov/Api/Public/Publication/809442>
- NHTSA (2015). *Seat and Dummy Driver Positioning for the THOR 50th Male Dummy* (Unnumbered test procedure). Washington, DC: National Highway Traffic Safety Administration. Available at [www.nhtsa.gov/DOT/NHTSA/NVS/Crashworthiness/Small%20Overlap%20and%20Oblique%20Research/THOR%20Driver%20Seating%20Procedure%20Draft\\_July%2022%202015.pdf](http://www.nhtsa.gov/DOT/NHTSA/NVS/Crashworthiness/Small%20Overlap%20and%20Oblique%20Research/THOR%20Driver%20Seating%20Procedure%20Draft_July%2022%202015.pdf).
- Parent, D., M. Craig, & Moorhouse, K. (2017). Biofidelity Evaluation of the THOR and Hybrid III 50(th) Percentile Male Frontal Impact Anthropomorphic Test Devices. *Stapp Car Crash Journal, 61*: 227-276.

- Rouhana, S. W., Bedewi, P. G., Kankanala, S. V., Prasad, P., Zwolinski, J. J., Meduvsky, A. G., ... & Schneider, L. (2003). Biomechanics of 4-point seat belt systems in frontal impacts. *Stapp Car Crash Journal*, 47: 367-399.
- Rouhana, S. W., Kankanala, S. V., Prasad, P., Rupp, J. D., Jeffreys, T. A., & Schneider, L. (2006). Biomechanics of 4-point seat belt systems in farside impacts. *Stapp Car Crash Journal*, 50: 267-298.
- Rudd, R. W., Bean, J., Cuentas, C., Kahane, C. J., Mynatt, M., & Wiacek, C. (2009). *A study of the factors affecting fatalities of air bag and belt-restrained occupants in frontal crashes*. 21st International Technical Conference on the Enhanced Safety of Vehicles Conference (ESV), June 15-19, 2009, Stuttgart, Germany.
- Rudd, R. W., M. Scarboro, & Saunders, J. (2011). *Injury analysis of real-world small overlap and oblique frontal crashes*. 22nd International Technical Conference on the Enhanced Safety of Vehicles (ESV), June 13-16, 2011, Washington, DC.
- Saunders, J., & Parent, D. (2014). Update on NHTSA's oblique research program (PowerPoint presentation). SAE 2014 Government/Industry Meeting, January 22-24, Washington, DC.
- Takhounts, E. G., Craig, M. J., Moorhouse, K., McFadden, J., & Hasija, V. (2013). Development of brain injury criteria (BrIC). *Stapp Car Crash Journal*, 57: 243-266.
- Wu, J., J. Hu, Reed, M., Klinich, K., & Cao, L. (2012). 10.1080/13588265.2012.703474. (2012). Development and Validation of a Parametric Child Anthropomorphic Test Device Model Representing 6- to 12-Year-Old Children. *International Journal of Crashworthiness* 17(6): 606-620. 10.1080/13588265.2012.703474.
- Zhang, X., & Zhou, Q. (2016). An energy-absorbing sliding seat for reducing neck injury risks in rear impact - Analysis for prototype built. *Traffic Injury Prevention*, 17(3): 313-319.

## Appendix A: Summary of NHTSA Oblique Crash Test Results

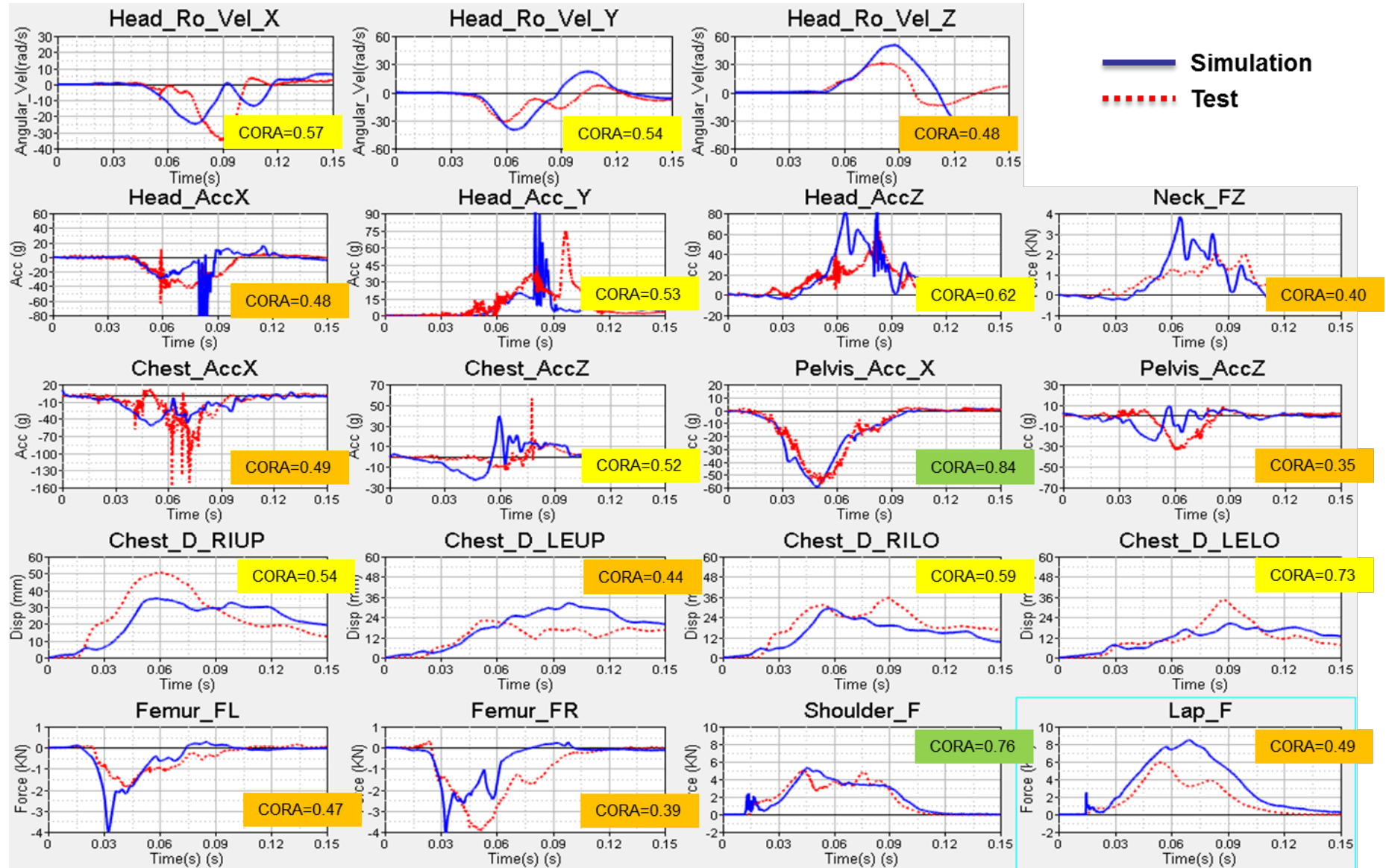
Test #	Vehicle	Impact Vehicle	Velocity	Overlap	Impact Angle	Driver																Passenger							
						Dummy	Head				Upper Neck		Chest		Femur		Dummy	Head				Upper Neck		Chest		Femur			
							HIC	BriC	P AIS 3+	Nij	Ax Tens (N)	Ax Comp (N)	Acc (G)	Comp (mm)	Left (N)	Right (N)		HIC	BriC	P AIS 3+	Nij	Ax Tens (N)	Ax Comp (N)	Acc (G)	Comp (mm)	Left (N)	Right (N)		
9043	2015 Honda Fit	MDB	90 kph	35%	15 deg	THOR	264	1.10	0.74	0.4	2254	217	N/A	52	3533	3615	THOR	908	2.23	1.00	0.6	2845	209	44	56	2824	3861		
9042	2014 Honda Accord	MDB	90 kph	35%	-15 deg	THOR	416	1.78	1.00	0.6	2503	148	N/A	44	5137	5207	THOR	189	0.94	0.58	0.3	1620	18	N/A	58	3916	4801		
8999	2014 Mazda3	MDB	90 kph	35%	-15 deg	THOR	747	1.48	0.95	0.5	2549	492	N/A	41	2106	2987	THOR	356	0.83	0.45	0.4	2140	21	N/A	56	2069	1836		
8998	2014 Mazda CX5	MDB	90 kph	35%	-15 deg	THOR	452	1.31	0.89	0.5	2897	30	N/A	43	859	2733	THOR	247	0.81	0.44	0.4	2225	72	N/A	44	3520	2255		
8789	2014 Honda Accord	MDB	90 kph	35%	15 deg	THOR	185	0.61	0.23	0.3	1540	46	40	49	3373	2000	THOR	935	1.46	0.95	0.4	2097	223	32	39	5192	5513		
8788	2014 Mazda CR-X	MDB	90 kph	35%	15 deg	THOR	218	0.68	0.30	0.3	1968	75	N/A	44	2918	1592	THOR	113	0.91	0.55	0.2	1390	34	N/A	33	3311	1527		
8787	2014 Mazda3	MDB	90 kph	35%	15 deg	THOR	267	1.19	0.82	0.3	1886	284	N/A	41	2401	2078	THOR	806	1.12	0.76	0.3	1655	777	N/A	38	5487	1878		
8488	2012 Volvo S60	MDB	90 kph	35%	15 deg	THOR	151	1.10	0.74	0.3	1820	94	N/A	37	3574	8080	THOR	223	1.46	0.95	0.2	1104	434	N/A	31	5641	1372		
8478	2014 Subaru Forester	MDB	90 kph	35%	15 deg	THOR	192	0.82	0.44	0.3	2031	189	N/A	49	2697	2594	THOR	199	1.08	0.73	0.3	1078	117	N/A	35	4021	3397		
8477	2013 Honda Civic	MDB	90 kph	35%	15 deg	THOR	201	0.85	0.48	0.3	1810	118	N/A	43	4290	3451	THOR	272	2.81	1.00	0.4	1750	2264	N/A	42	5613	6467		
8476	2013 Dodge Dart	MDB	90 kph	35%	15 deg	THOR	313	0.73	0.35	0.4	1056	1077	N/A	49	3859	4120	THOR	113	2.21	1.00	0.3	957	1297	N/A	35	4360	2238		
8475	2013 Volvo XC60	MDB	90 kph	35%	15 deg	THOR	140	1.40	0.93	0.3	1833	91	N/A	46	2476	7696	THOR	466	1.60	0.98	0.3	1191	322	N/A	42	4013	1869		
8383	2013 Hyundai Elantra	MDB	90 kph	35%	15 deg	Modified 50% Male	194	N/A	N/A	0.5	1772	120	50	37	1587	12617	Modified 50% Male	270	N/A	N/A	0.3	1496	39	42	21	4933	588		
8382	2013 Hyundai Elantra	MDB	90 kph	35%	15 deg	THOR	173	N/A	N/A	0.5	2031	136	51	36	2035	14418	THOR	222	N/A	N/A	0.3	1486	39	38	21	3769	1002		
8381	2013 Hyundai Elantra	MDB	90 kph	35%	15 deg	THOR	416	1.14	0.78	0.4	2676	398	48	48	4907	4841	THOR	464	1.33	0.90	0.3	1485	438	36	38	3936	202		
8099	2012 Chevy Silverado	MDB	90 kph	35%	15 deg	THOR	500	1.13	0.77	0.22	1382	495	29	35	5970	8687	THOR	56	1.36	0.92	0.18	930	224	25	29	4301	4054		
8097	2012 Honda Odyssey	MDB	90 kph	35%	15 deg	THOR	96	0.66	0.28	0.24	1537	134	35	40	3271	2898	THOR	622	1.24	0.85	0.34	1978	212	22	39	4256	4297		
8096	2012 Honda CR-V	MDB	90 kph	35%	15 deg	THOR	207	1.03	0.68	0.33	1696	93	45	42	7536	5048	THOR	899	1.49	0.96	0.42	2194	345	29	34	4254	4826		
8089	2013 Hyundai Elantra	MDB	90 kph	35%	15 deg	THOR	344	1.13	0.77	0.32	2047	487	46	53	4196	6202	THOR	951	1.59	0.98	0.44	1471	752	35	39	4784	417		
8088	2012 Toyota Camry	MDB	90 kph	35%	15 deg	THOR	827	0.80	0.42	0.27	1597	149	35	47	3725	4718	THOR	306	1.53	0.97	0.27	1432	1168	26	34	3983	3359		
8087	2012 Ford Taurus	MDB	90 kph	35%	15 deg	THOR	584	1.41	0.94	0.32	2009	722	48	45	2689	4069	THOR	157	1.27	0.87	0.34	1207	42	40	32	2468	3415		
8086	2013 Nissan Versa	MDB	90 kph	35%	-15 deg	THOR	645	1.00	0.65	0.06	20	24	52	40	4783	4445	THOR	824	1.01	0.66	0.45	2489	739	44	42	3865	5880		
8085	2012 Toyota Camry	MDB	90 kph	35%	-15 deg	THOR	104	1.44	0.95	1.00	6676	838	30	36	2124	2757	THOR	355	1.29	0.88	0.44	1222	1584	42	42	3090	3211		
8084	2013 Nissan Versa	MDB	90 kph	35%	15 deg	THOR	137	0.89	0.52	0.29	1841	80	43	36	6185	5898	THOR	543	1.91	1.00	0.63	2531	146	46	41	3270	4126		

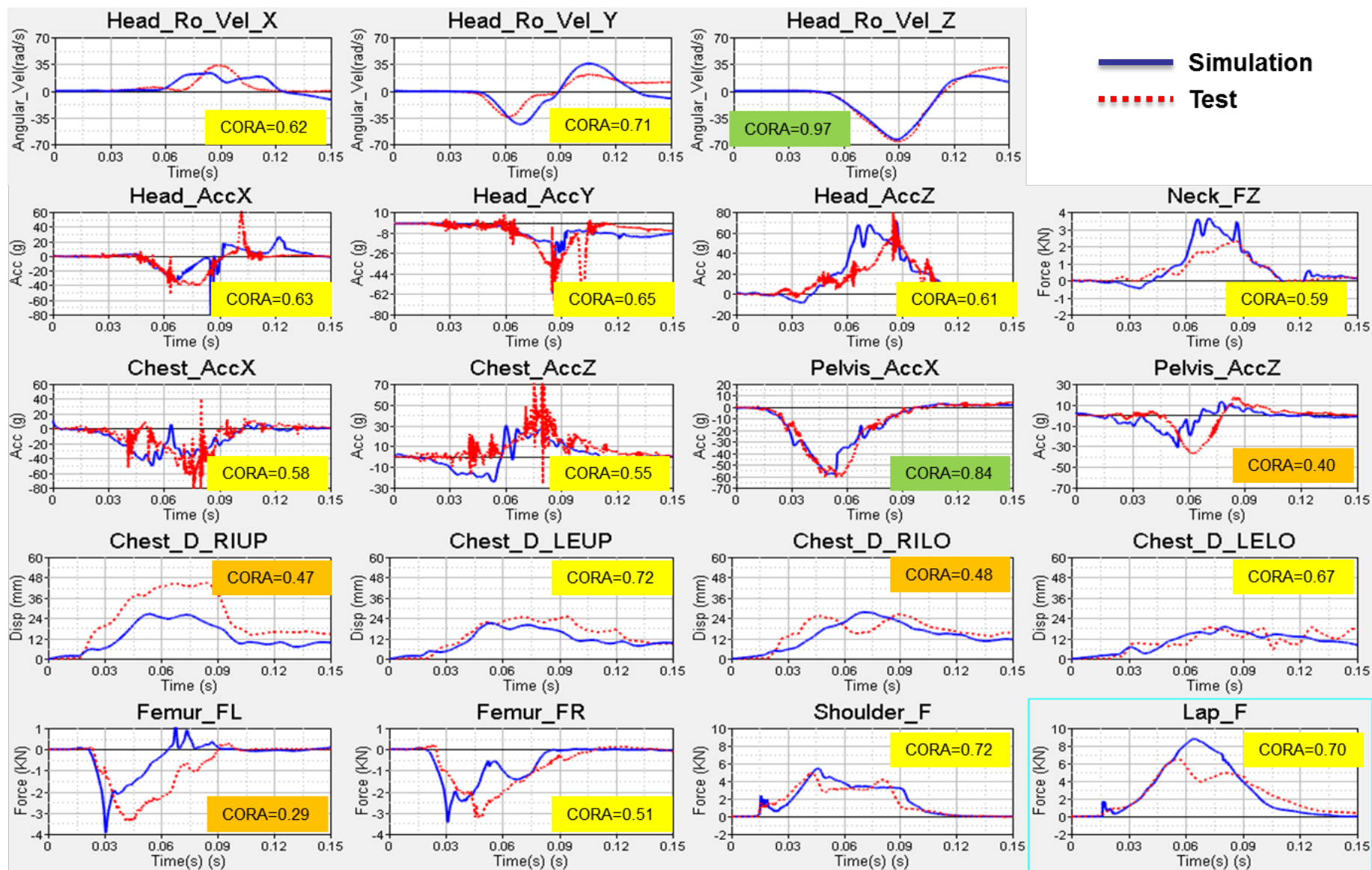
Test #	Vehicle	Impact Vehicle	Velocity	Overlap	Impact Angle	Driver																Rear Seat							
						Dummy	Head				Upper Neck		Chest		Femur		Dummy	Head				Upper Neck		Chest		Femur			
							HIC	BriC	P AIS 3+	Nij	Ax Tens (N)	Ax Comp (N)	Acc (G)	Comp (mm)	Left (N)	Right (N)		HIC	BriC	P AIS 3+	Nij	Ax Tens (N)	Ax Comp (N)	Acc (G)	Comp (mm)	Left (N)	Right (N)		
7852	2011 Chevy Cruze	MDB	90 kph	35%	15 deg	THOR	219	0.95	0.59	0.28	1378	508	43	36	2000	2494	HII 5th	590	1.36	0.92	0.92	2262	68	52	31	285	493		
7851	2011 Chevy Cruze	MDB	90 kph	35%	15 deg	THOR	195	0.90	0.54	0.24	1372	573	55	36	2373	3669	HII 5th	558	1.03	0.68	0.99	2199	86	42	33	329	312		
7476	2011 Ford Explorer	MDB	90 kph	35%	15 deg	THOR	703	1.45	0.95	1.11	6913	6694	41	55	3214	2689	HII 5th	105	0.85	0.48	0.62	1308	405	41	24	3560	3620		
7467	2011 Buick Lacrosse	MDB	90 kph	35%	15 deg	THOR	118	3.47	1.00	1.14	7292	5827	42	46	6985	3579	HII 5th	436	1.24	0.85	0.96	2407	218	52	33	2214	2379		
7458	2011 Smart Fortwo	MDB	90 kph	35%	15 deg	THOR	366	2.82	1.00	1.12	5233	7206	57	47	9106	8576													
7457	2011 Dodge Ram	MDB	90 kph	35%	15 deg	THOR	456	2.12	1.00	1.03	6080	6220	32	36	4800	3448	HII 5th	196	1.44	0.95	0.72	1604	360	34	31	2753	1738		
7441	2011 Toyota Yaris	MDB	90 kph	35%	15 deg	THOR	1564	2.62	1.00	0.38	2149	384	54	55	4351	6221	HII 5th	1088	2.38	1.00	1.36	4912	524	71	32	3349	2516		
7433	2010 Toyota Yaris	MDB	90 kph	35%	15 deg	THOR	263	109.29	1.00	0.40	2262	255	66	43	5211	6650	HII 5th	559	0.82	0.44	0.97	3222	20	57	48	2868	3008		
7431	2011 Chevy Cruze	MDB	90 kph	35%	15 deg	THOR	176	0.94	0.58	0.25	1423	606	35	42	2950	2932	HII 5th	475	25.67	1.00	0.92	2180	62	53	31	1777	1362		
7429	2007 Ford 500	MDB	90 kph	35%	15 deg	THOR	2506	1.28	0.88	0.49	3097	321	44	37	5283	4277	HII 5th	610	1.11	0.75	0.95	3396	1131	53	43	144	2723		
7428	2011 Ford Fiesta	MDB	90 kph	35%	15 deg	THOR	145	1.52	0.97	2.36	1815	199	45	46	1969	2675	HII 5th	872	1.53	1.00	1.32	4702	140	68	45	2347	1845		
7366	2007 Ford Taurus	MDB	90 kph	35%	15 deg	THOR	290	0.83	0.45	0.38	2311	336	49	36	3538	7555	HII 5th	475	1.46	0.95	0.94	3177	1137	36	35	1140	1131		

## Appendix B: Time Histories and CORA Ratings for Baseline Model Validations

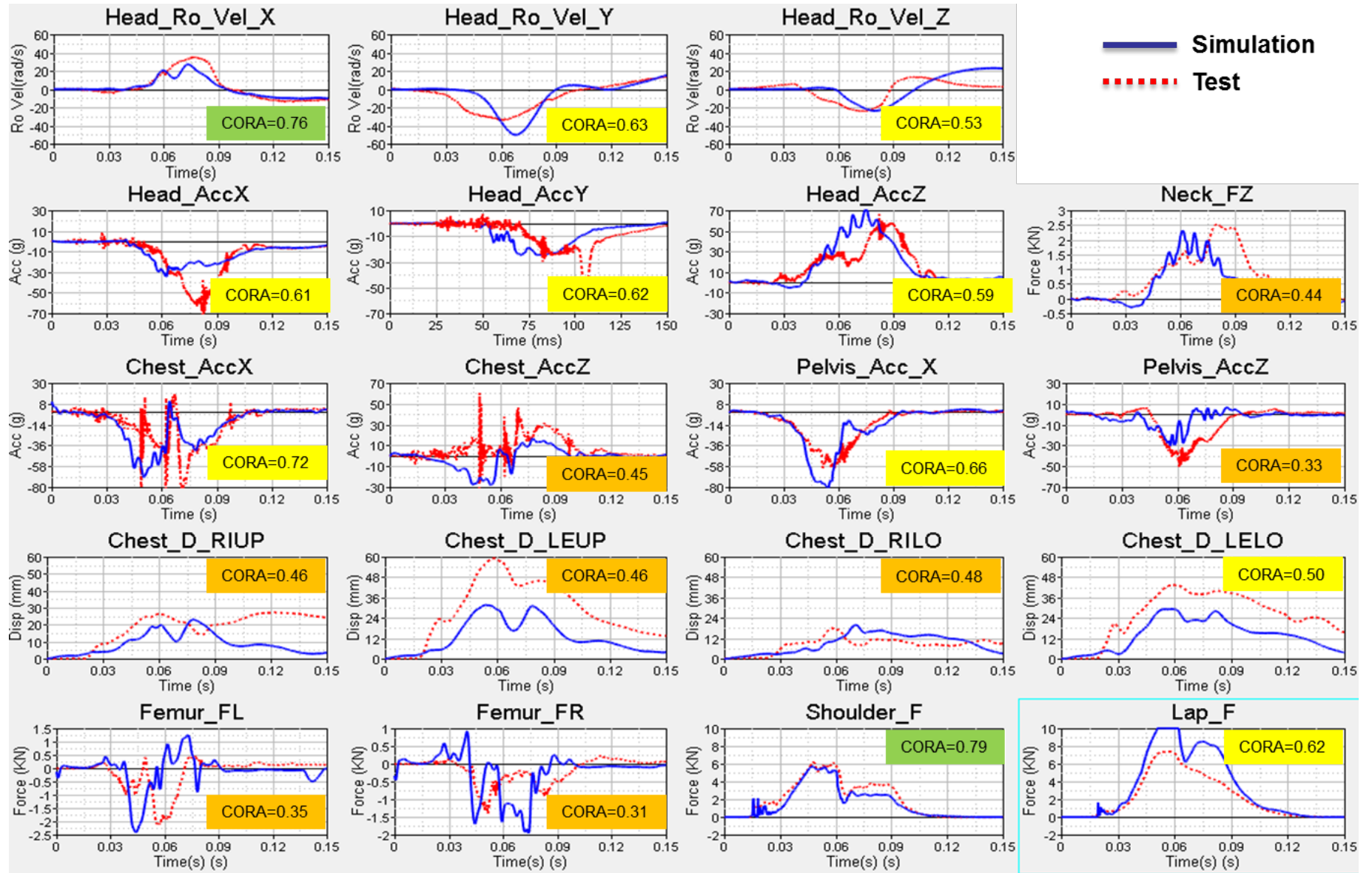
### Driver near-side baseline oblique test



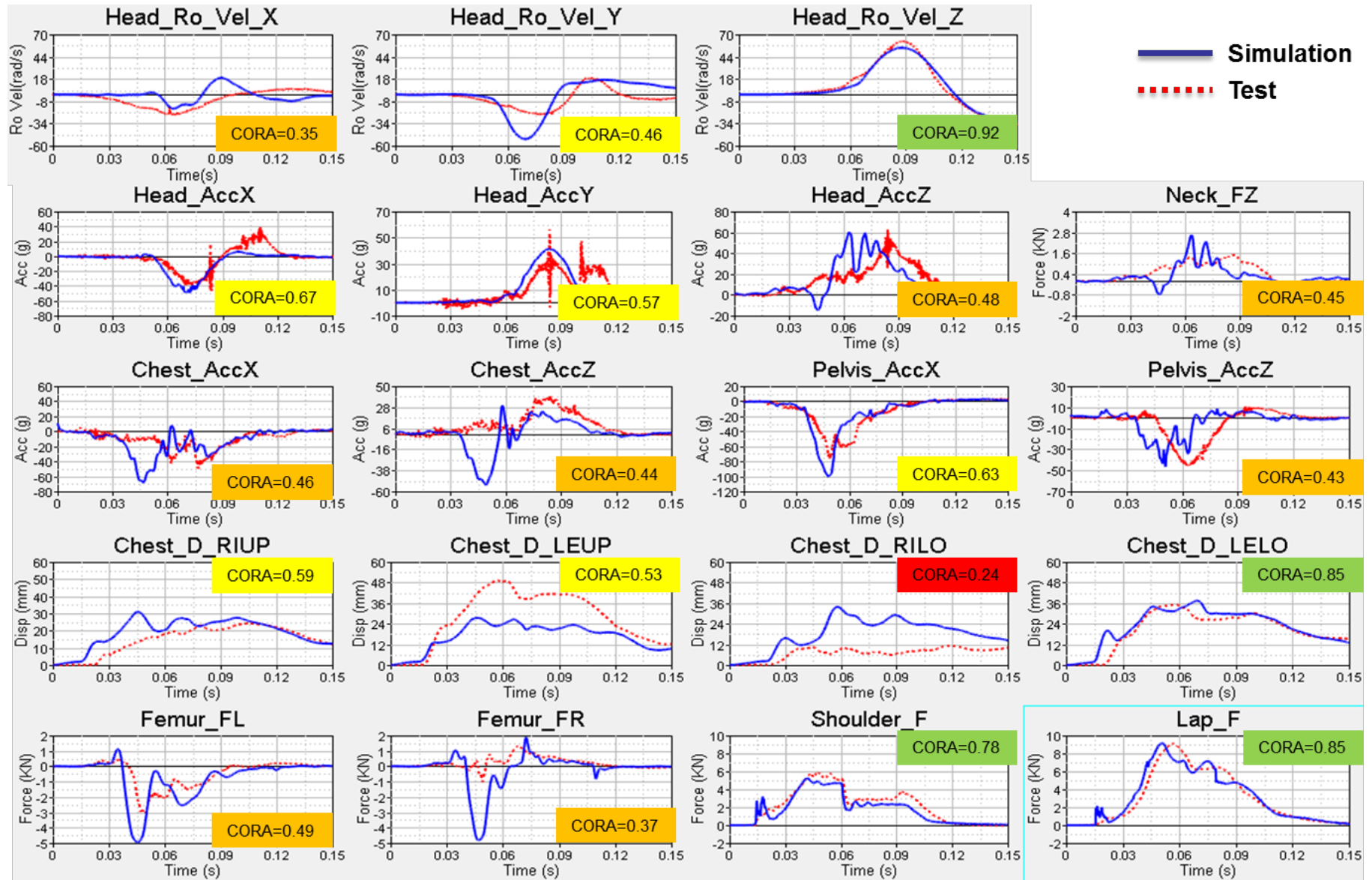
### Driver far-side baseline oblique test



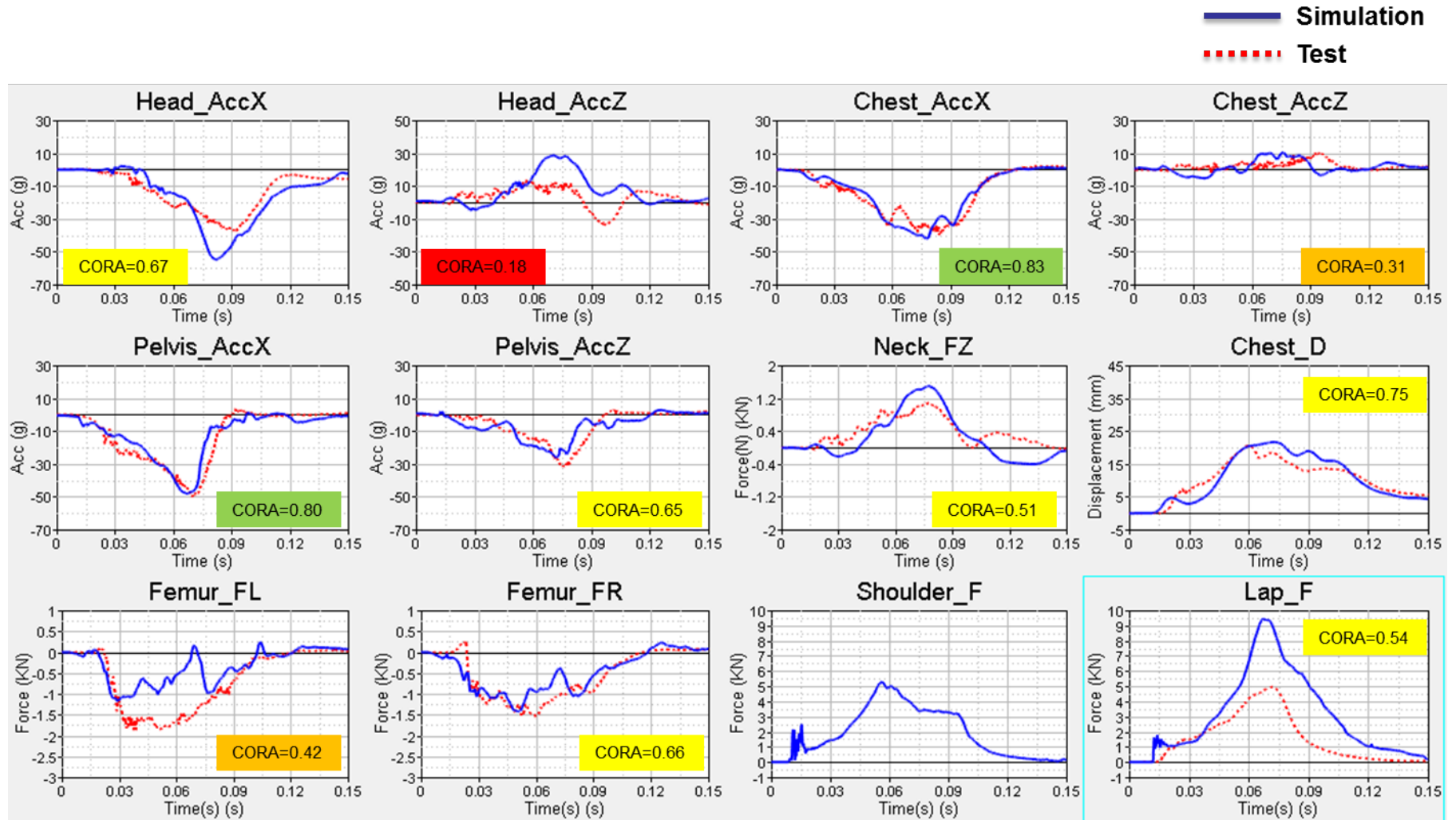
### Passenger near-side baseline oblique test



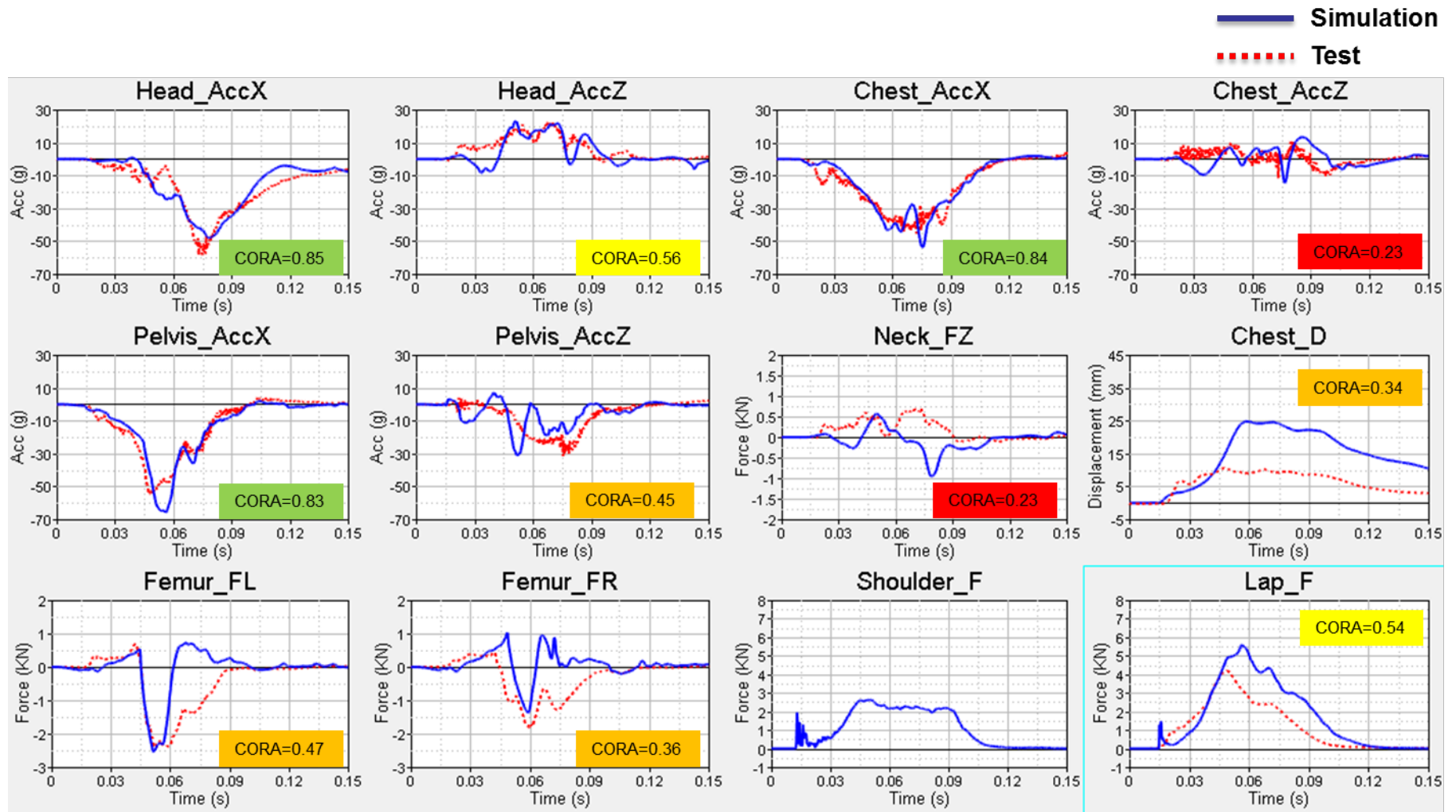
### Passenger far-side baseline oblique test



Belted HIII 50th male ATD on the driver side in a 56 km/h (35 mph) frontal full barrier test

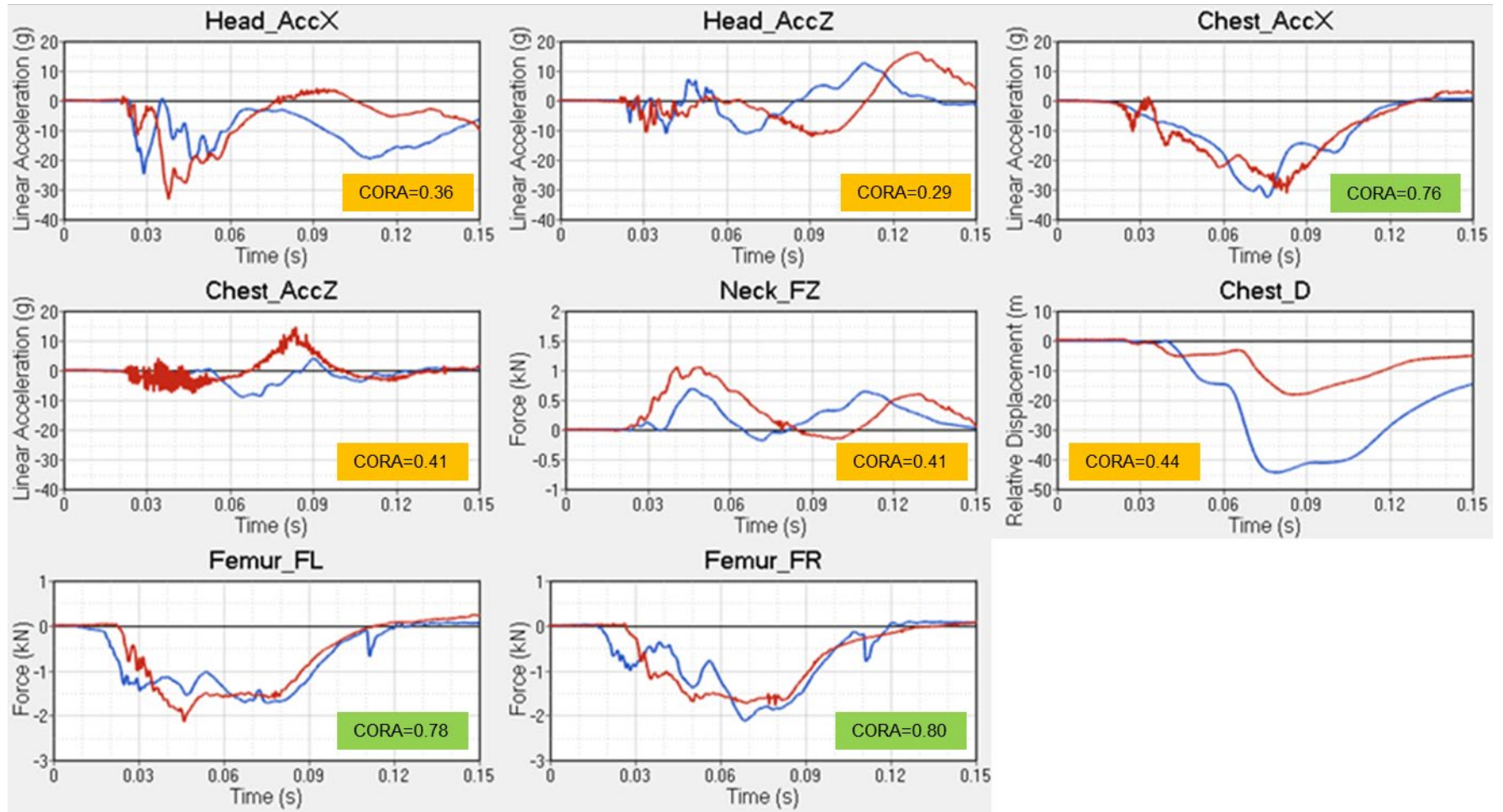


Belted HIII 5th female ATD on the passenger side in a 56 km/h (35 mph) frontal full barrier test



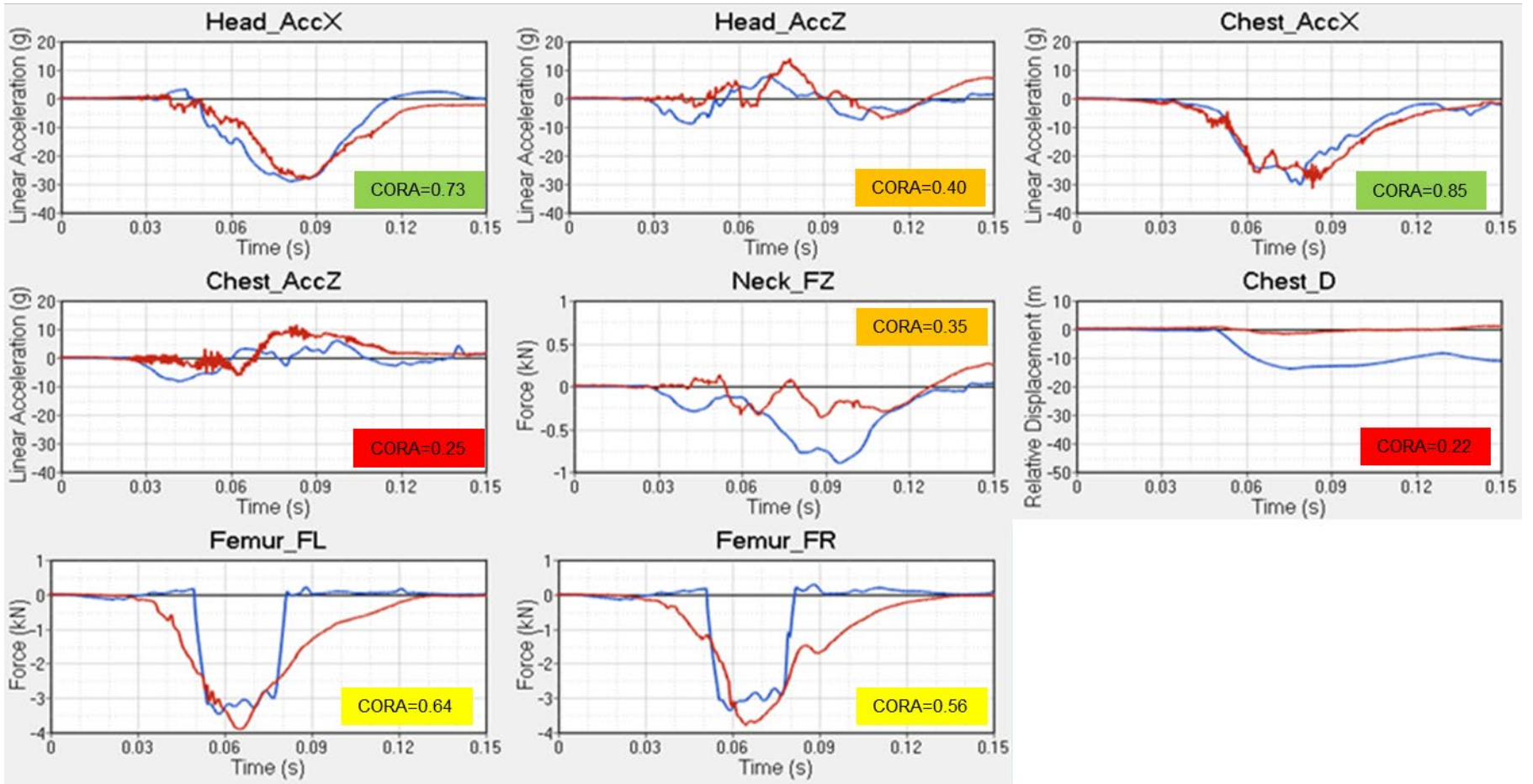
# Unbelted HIII 5th female ATD on the driver side in a 40 km/h (25 mph) frontal full barrier test

— Simulation  
- - - Test



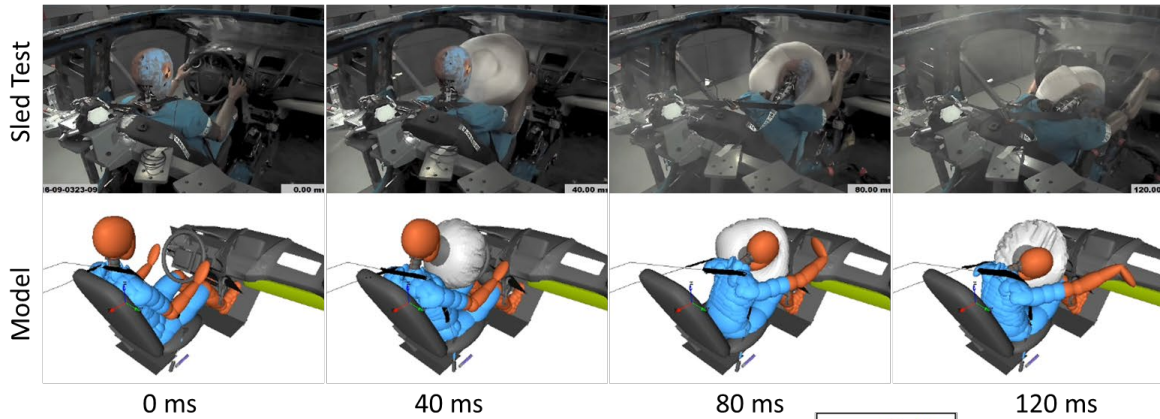
Unbelted HIII 5th female ATD on the driver side in a 40 km/h (25 mph) frontal full barrier test

— Simulation  
 ..... Test

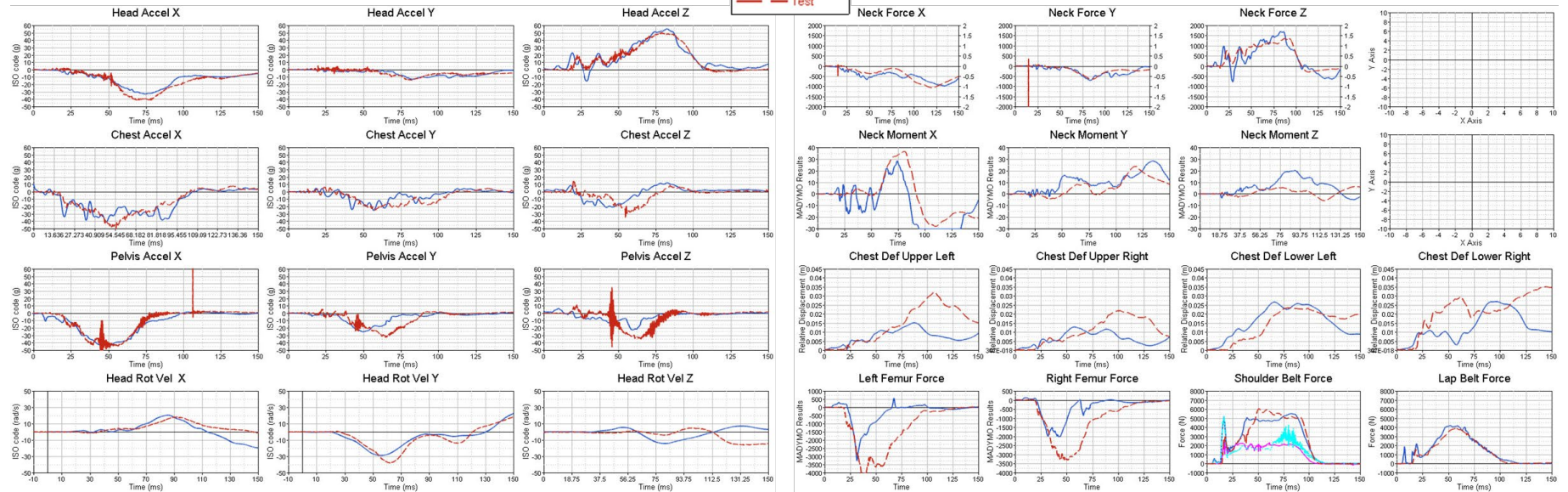


# Appendix C: Examples of Model Validations Against Sled Tests With Modified Restraints

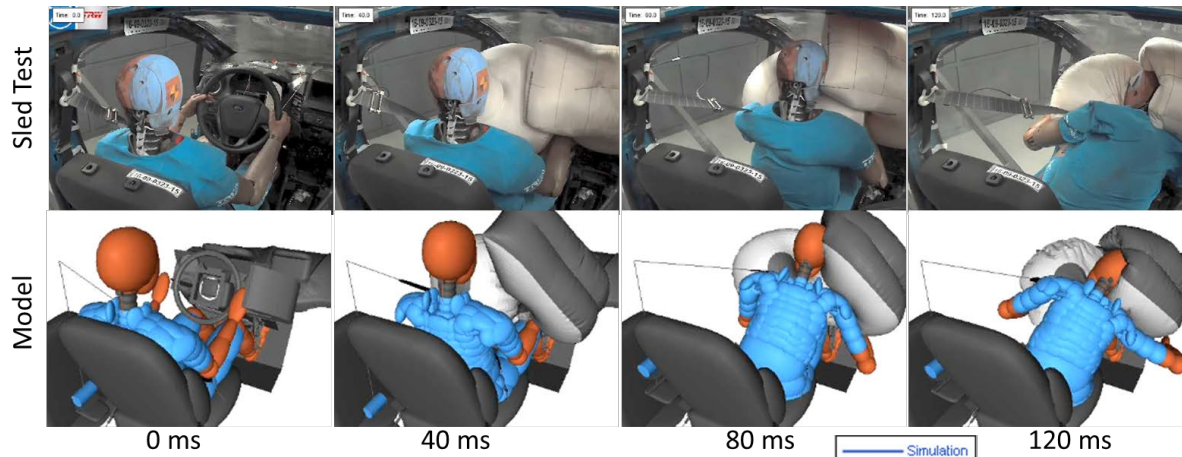
## Driver far-side impact with a suspender 4-point belt and the baseline DAB



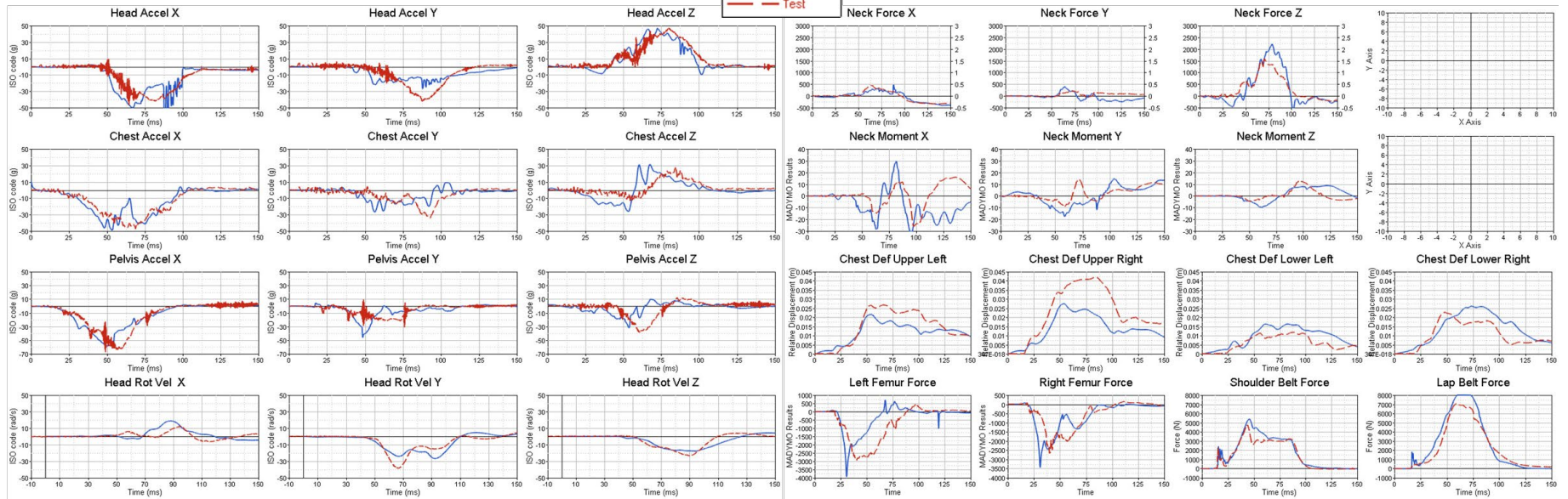
Injury Value	Unit	Simulation	Test
HIC15	-	438	451
BrIC	-	0.68	0.81
Neck T	N	1700	3187
Neck C	N	785	1345
NIJ	-	0.87	0.65
Chest D	mm	27	35
Left Femur F	N	3272	4570
Right Femur F	N	2026	3290



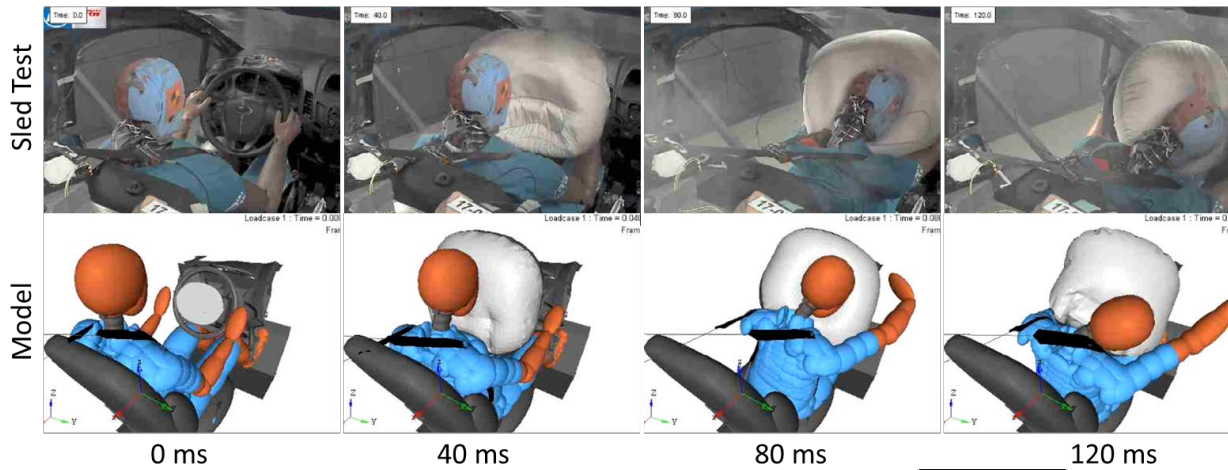
## Driver far-side impact with the baseline 3-point belt, baseline DAB, and the support bag



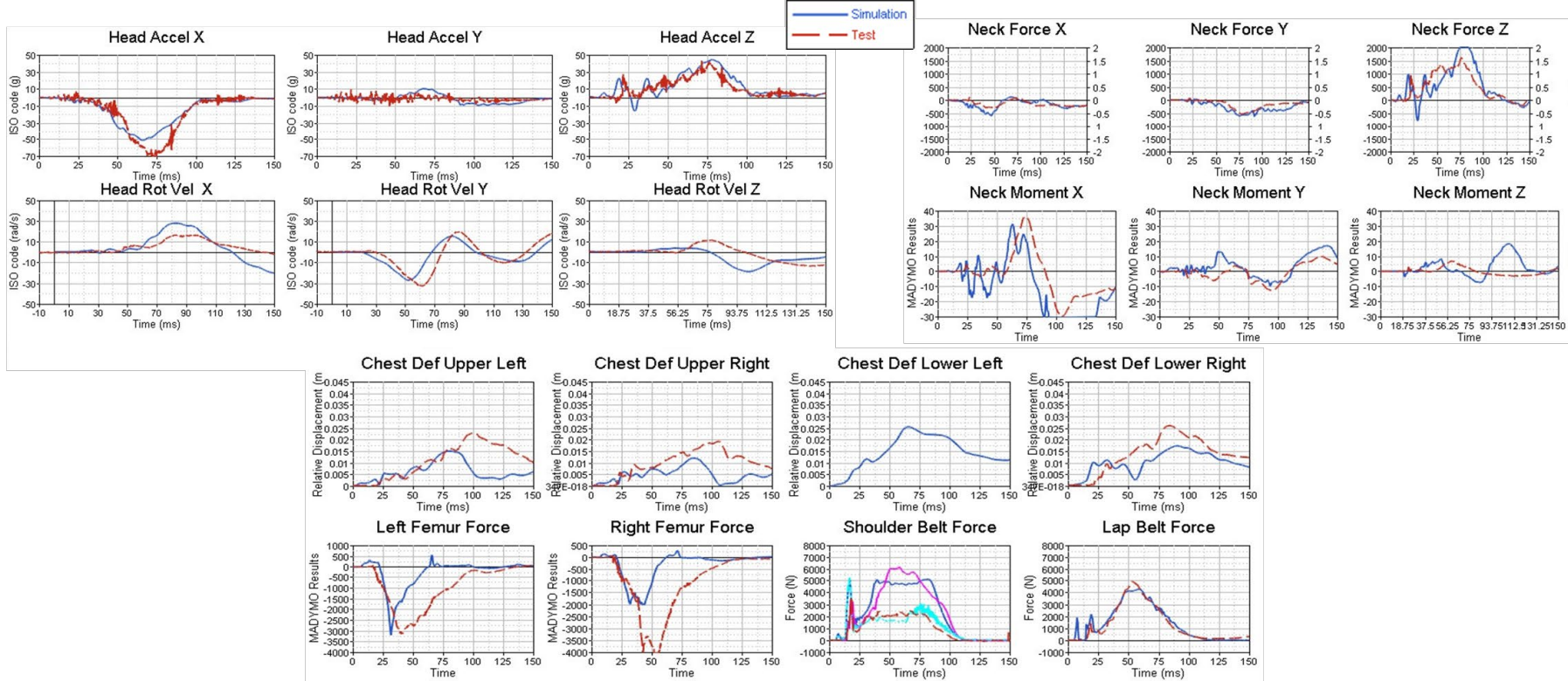
Injury Value	Unit	Simulation	Test
HIC15	-	434	513
BrlC	-	0.69	0.88
Neck T	N	2222	2611
Neck C	N	604	826
NIJ	-	0.96	0.91
Chest D	mm	28	42
Left Femur F	N	3941	2930
Right Femur F	N	3442	2660



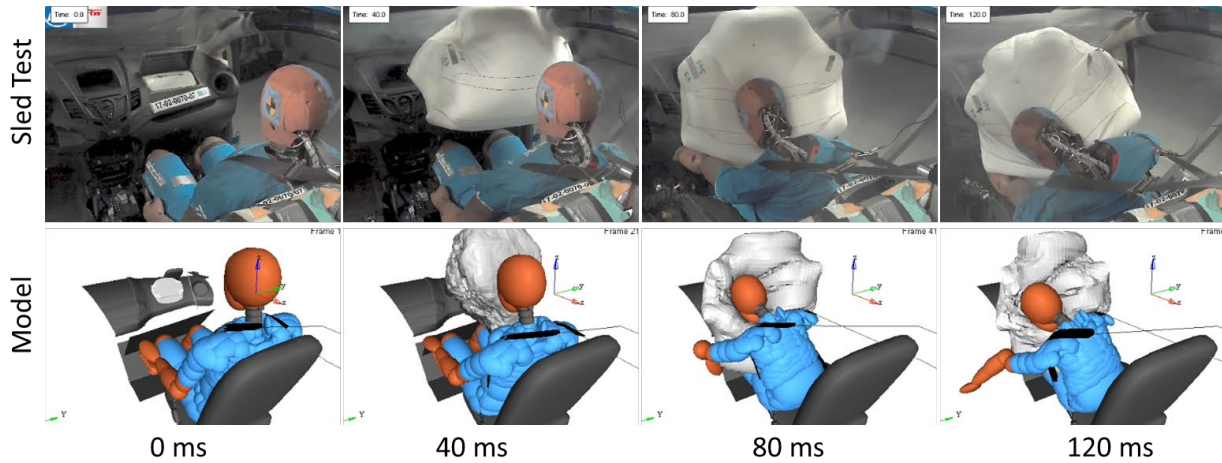
## Driver far-side impact with a suspender 4-point belt and a SQS DAB



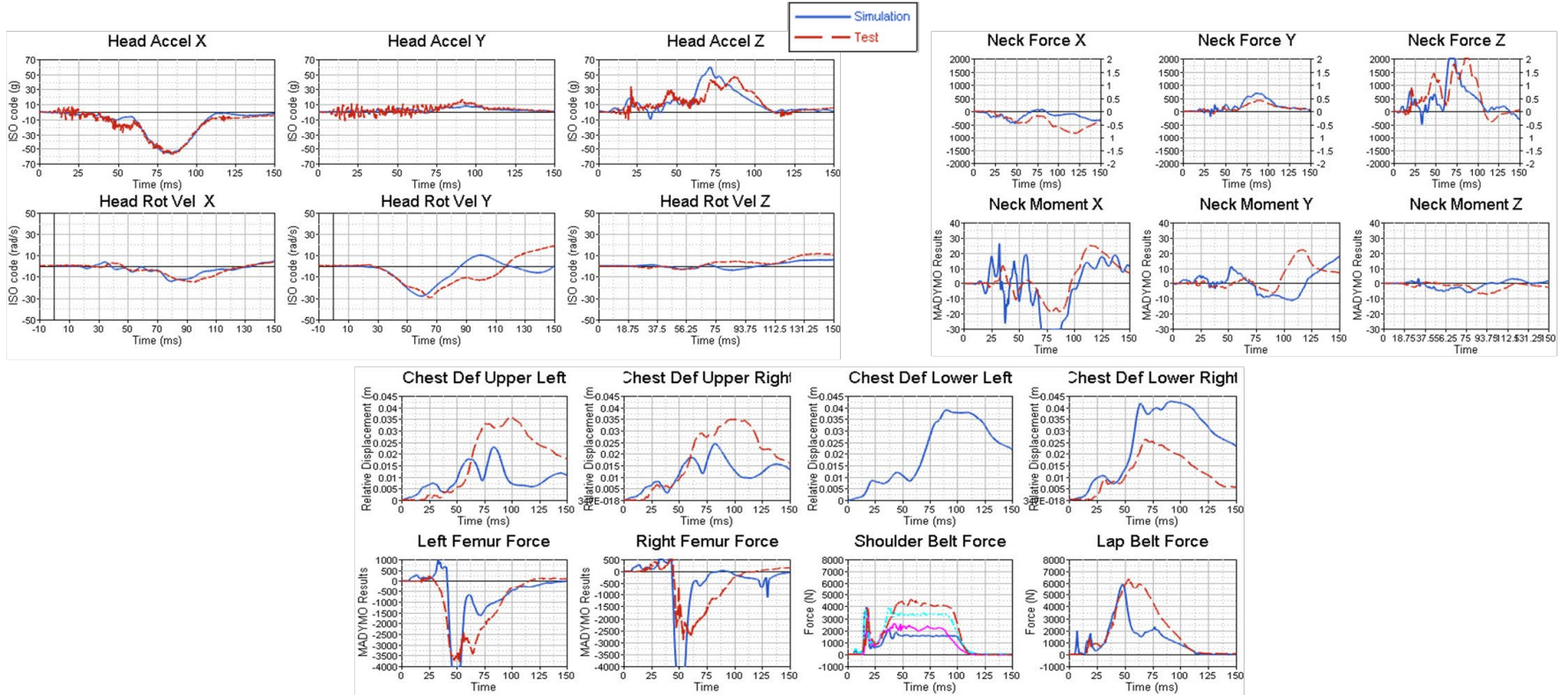
Injury Value	Unit	Simulation	Test
HIC15	-	428	688
BrlC	-	0.78	0.70
Neck T	N	2370	1620
Neck C	N	792	210
NIJ	-	0.99	0.75
Chest D	mm	26	26
Left Femur F	N	3208	3130
Right Femur F	N	2019	4290



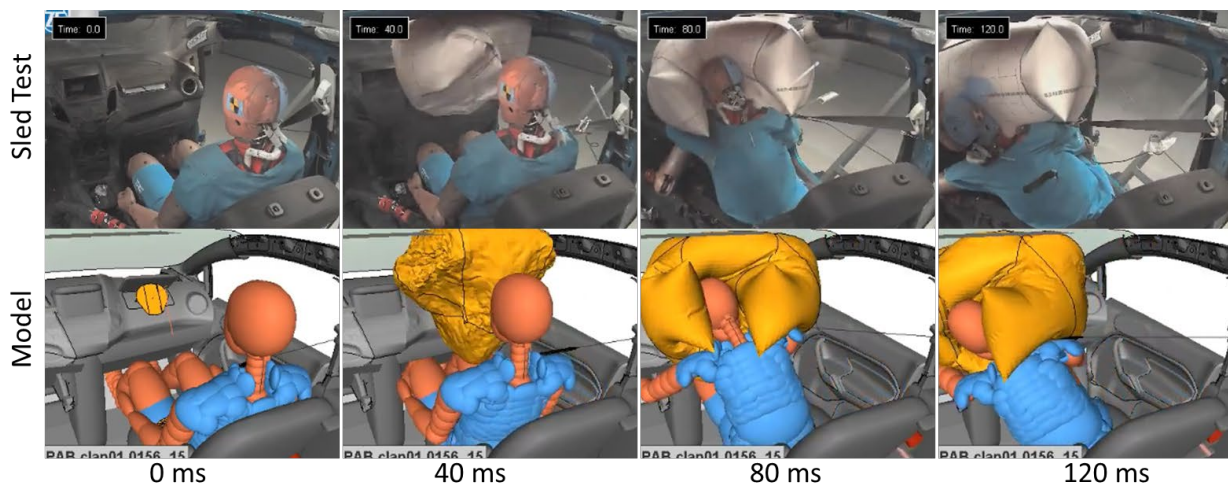
## Passenger far-side impact with a suspender 4-point belt and V13 PAB



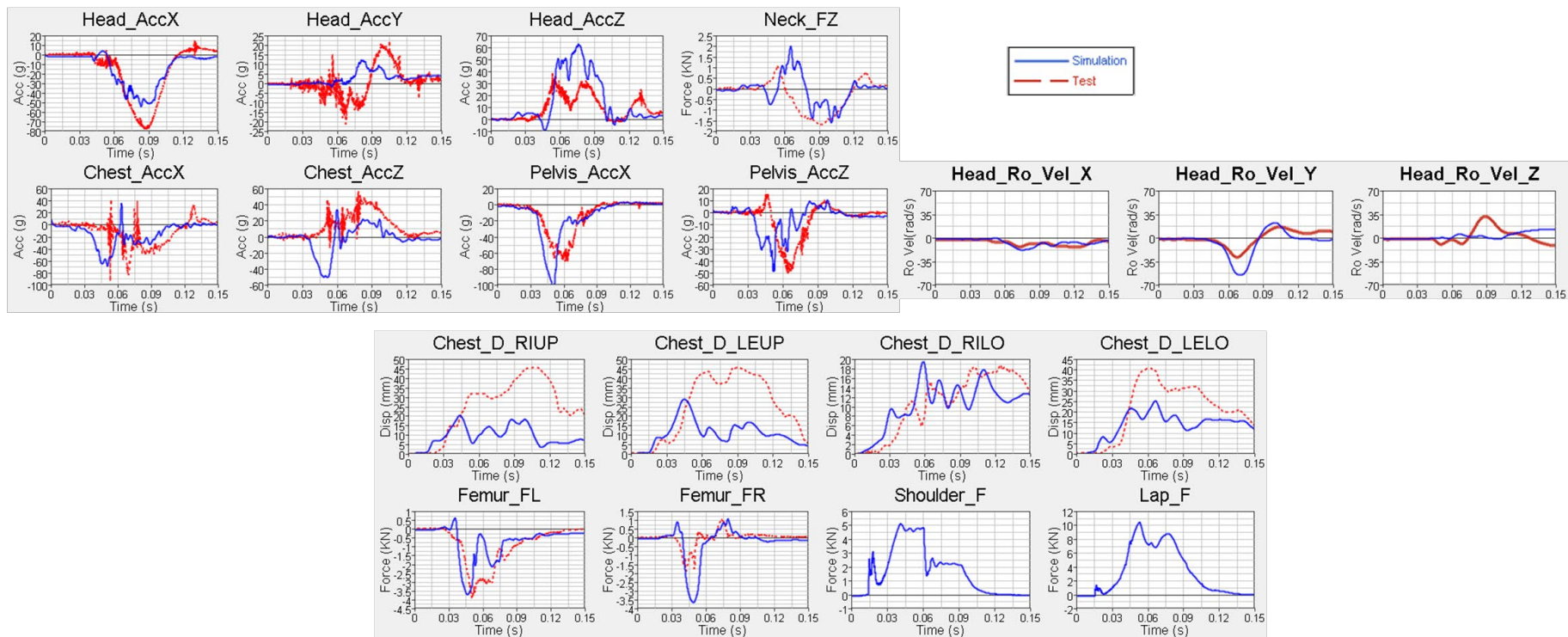
Injury Value	Unit	Simulation	Test
HIC15	-	586	548
BrlC	-	0.56	0.64
Neck T	N	2367	2140
Neck C	N	496	400
NIJ	-	0.95	0.92
Chest D	mm	43	36
Left Femur F	N	5085	3689
Right Femur F	N	4984	4134



## Passenger far-side impact with the baseline 3-point belt and a Clapper PAB



Injury Value	Unit	Simulation	Test
HIC15	-	614	799
BrIC	-	1.04	0.94
Neck T	N	2050	1060
Neck C	N	1560	1710
NIJ	-	1.00	0.59
Chest D	mm	30	44
Left Femur F	N	3640	3980
Right Femur F	N	3580	1900



DOT HS 812 814  
October 2019



U.S. Department  
of Transportation  
**National Highway  
Traffic Safety  
Administration**

